INFORMATION TO USERS

This manuscript has been reproduced from the microfilm master. UMI films the text directly from the original or copy submitted. Thus, some thesis and dissertation copies are in typewriter face, while others may be from any type of computer printer.

The quality of this reproduction is dependent upon the quality of the copy submitted. Broken or indistinct print, colored or poor quality illustrations and photographs, print bleedthrough, substandard margins, and improper alignment can adversely affect reproduction.

In the unlikely event that the author did not send UMI a complete manuscript and there are missing pages, these will be noted. Also, if unauthorized copyright material had to be removed, a note will indicate the deletion.

Oversize materials (e.g., maps, drawings, charts) are reproduced by sectioning the original, beginning at the upper left-hand corner and continuing from left to right in equal sections with small overlaps.

Photographs included in the original manuscript have been reproduced xerographically in this copy. Higher quality 6" x 9" black and white photographic prints are available for any photographs or illustrations appearing in this copy for an additional charge. Contact UMI directly to order.

Bell & Howell Information and Learning
300 North Zeeb Road, Ann Arbor, MI 48106-1346 USA
800-521-0600

NEURONAL CONNECTIVITY IN THE LARVAL VISUAL SYSTEM OF *DROSOPHILA MELANOGASTER*: CELLULAR AND MOLECULAR ANALYSES

By

Mahua Mukhopadhyay

A Thesis

Submitted to the School of Graduate Studies

In Partial Fulfilment of the Requirements

For the Degree

Doctor of Philosophy

McMaster University

Development of neuronal connectivity in the nervous system of *Drososphila melanogaster*

DOCTOR OF PHYLOSOPHY (1999) (Biology)

McMASTER UNIVERSITY HAMILTON, ONTARIO

TITLE: NEURONAL CONNECTIVITY IN THE LARVAL VISUAL SYSTEM OF *DROSOPHILA MELANOGASTER*: CELLULAR AND MOLECULAR ANALYSES.

AUTHOR: Mahua Mukhopadhyay

SUPERVISOR: Dr. A. R. Campos

NUMBER OF PAGES: xiv, 200

Abstract

In this study the *Drosophila melanogaster* larval visual system development was used as a model to identify cellular interactions and uncover molecular mechanisms that govern the formation of precise neuronal pathways during nervous system development.

The first part of this study demonstrates that the outgrowth of two serotonergic processes and their contact with the larval optic nerve at the larval visual center are dependent on the proper development of larval optic nerve (LON).

The second part of this study reports identification of molecular interactions that may be important for larval visual system development. A tissue-specific autoregulatory activity of a putative transcription factor DISCONNECTED (DISCO) has been shown to be important for proper larval visual system connectivity formation. To understand the molecular mechanisms that govern *disco* function in the visual system, two new proteins (DIP1 and DIP2; DISCO-interacting proteins 1 and 2) and a previously known protein that interact with DISCO in yeast and *in vitro* were identified. These proteins also show overlapping mRNA expression patterns with DISCO during embryogenesis.

This study has also led to the identification of a putative activation domain in the DISCO protein. Furthermore, the results of this study suggest a possible protein-binding function of the second zinc-finger domain of DISCO.

The *dip1* gene encodes a protein with two putative dsRNA-binding motifs. An unusual repeated element is present in the 3′ untranslated region of *dip1* cDNAs. Northern analysis revealed expression of three different size transcripts of the gene during embryogenesis. The genetic location of the *dip1* gene is similar to that of a gene called *flamenco*.

The *dip2* gene located at the polytene chromosome band 61B, codes for a highly conserved protein with presently unknown function. The amino acid sequence and mRNA expression pattern of the *Drosophila* DIP2 protein are very similar to its mouse homolog.

This study contributes towards understanding the cellular and molecular mechanisms of neuronal connectivity formation.

ACKNOWLEDGMENT

I would like to sincerely express my gratitude and appreciation to my supervisor Dr. Ana Campos for giving me the opportunity to pursue my graduate career under her excellent guidance and for her continual support in all respects. I would also like to acknowledge the valuable guidance and suggestions provided by the members of my supervisory committee Dr. Colin Nurse and Dr. Corrinne Lobe and other faculty members in the department, Dr. Roger Jacobs in particular. My special thanks go to Dr. Richard Morton for his inspiration, continuous guidance and friendly support. I thank Dr. Rama Singh, Dr. Turlough Finan, Dr. Herb Schellhorn and Dr. David Andrews for letting me use their laboratory resources during the course of my graduate research.

Many thanks goes to my colleagues Dorothy Desousa and Balaji Iyengar for their support and long hours of valuable discussions that helped me in my graduate work and beyond. I would like to thank Peter Pelka for helping me in my work and also for taking future responsibilities of the project. My thanks goes to other past and present members of the laboratory, including Macarena Busto and Marta Boszo. I would like to extend special thanks to my longstanding friend of all time Dr. Aloke Sil (PennState University) for continual technical advice. I am also thankful to Dr. Ralph Voegel, a former postdoctoral fellow of the department for continual technical assistance. A very special thanks goes to Marg Briggs and Pat Hayward of the Biology Department office for all the support and help during the past five years. I greatly acknowledge

McMaster University for the Centennial Scholarship that allowed me to initiate my graduate work as a foreign student.

I would like to thank my dear husband Suman Mukhopadhyay for his continued support, encouragement and loving care at times of difficulty. Special thanks goes to my brother and my sister for their love and support. Most importantly, I would like to thank my parents for their care and sacrifice in an effort to build a better future for me. This thesis is dedicated in the memory of my late father Samaresh Biswas, who will continue to inspire my thoughts and work for the rest of my life.

TABLE OF CONTENTS:

List of Tables:

List of Illustrations:

Chapter 1: Introduction

Introduction:

The complex organization found in a functional nervous system requires that axons establish their correct pathways and find their appropriate targets during development. Precise neuronal connections in the nervous system occur in two steps: In the first step various molecular guidance cues guide a neuron to its target region which is initially broadly defined. The second step includes an exact point-to-point matching between each axon and the specific target neuron. The first step i.e. axon outgrowth, pathfinding and target selection do not require action potentials and synaptic transmission. However, the second step i.e., refinement and remodeling of synaptic connections almost always require neuronal activity (reviewed by Goodman and Shatz, 1993).

General strategies for neuronal pathway formation and cellular guidance

To make precise connections with their targets, axons need to grow long distances, as long as several centimeters or more than a thousand times the diameter of the cell body. To simplify this task the journey is fragmented into shorter steps where intermediate targets provide critical guidance cues directing growth cones to the next stage of the neurons trajectory. The intermediate targets are often provided by smaller, isolated groups of transient neurons, called 'guidepost cells'. In the absence of the 'guidepost cells' the earliest pioneer growth cones often make pathfinding errors (Klose and Bentley, 1989). Later

navigating neurons may be guided to and from choice points by selective fasciculation on earlier-developing axons (reviewed by Goodman *et al.*, 1984).

Studies with vertebrate and invertebrate systems established that pioneer neurons play an important role in neuronal pathway formation (e.g. McConnell *et al.*, 1989; Klose and Bentley, 1989). These neurons establish initial scaffolds of axon tracts that act as substrates for directed migration of later developing neuron growth cones. For example, the first neurons which differentiate in grasshopper limb, the sibling afferent Ti1 neurons, send out axons along a defined pathway, and later developing sensory neurons follow the pathway pioneered by the Ti1 neurons (Bate, 1976). Along the pathway at three locations, the pioneer axons contact specific cells (Fe1, Tr1 and the pair of Cx1 cells) which are likely to act as intermediate targets and guidance cues. The route taken by the pioneer axons always passes over the so called "guidepost" cells, which are immature neurons. Transient gap junctions between the pioneer fibres and the guidepost cells have also been reported. Ablation of the Cx1 cells with UV results in failure of the pioneer growth cones to leave the trochauter/coxa boundary and to grow proximally to the CNS (Bentley and Caudy, 1983).

Cells with characteristics of guidepost cells are likely to act as intermediate targets in the vertebrate nervous system as well. A set of early generated and transient neurons in the cortex, the 'subplate cells', may be involved in guiding the thalamic fibres toward and into their cortical target area. Ablation of the subplate neurons, by kainate injection, leads to a failure of thalamic fibres to recognize their normal cortical target areas (Ghosh *et al.*, 1990). Thus subplate

cells may provide critical guidance cues which help thalamic axons to locate and recognize their correct target.

In vitro assays and *in vivo* perturbation studies have led to the proposal that selective fasciculation is an important determinant of precise neuronal connectivity (Letourneau, 1975; Raper *et al.*, 1984; Bastiani *et al.*, 1986). After pioneer neurons establish the first scaffold of different pathways, follower axons must choose which fascicles will bring them to their correct targets. Reaching a distant target may require a series of navigational choices, each followed by a period of fasciculation along a new pathway. The ordered neuronal pattern in the insect nervous system arises from the ability of individual central nervous system (CNS) neuron growth cones to discriminate between fascicles and make selective choices during outgrowth (Goodman *et al.*, 1984). For example, in the grasshopper embryo, the growth cone of the aCC neuron selectively fasciculates with three U axons in the U fascicle and that of pCC neurons fasciculate with MP1 and dMP2 axons in the MP1 fascicle (Bastani *et al.*, 1986; Du Lac *et al.*, 1986). When the pioneer neurons (U axons, MP1 and dMP2) of these two pathways are selectively ablated, the follower growth cones (aCC and pCC respectively) stall and do not show affinity for any other neighboring axons. This data supports the "labeled pathway" hypothesis (Raper *et al.*, 1984) which proposes that CNS pathways are selectively labeled with guidance molecules that allow axon growth cones to select and fasciculate with appropriate axon fascicles.

Monoclonal antibody screens in the developing insect nervous system and other studies in both invertebrate and vertebrate system led to the identification of molecules selectively expressed on subset of developing axon pathways (e.g.,

Bastiani *et al.*, 1987; Grenningloh *et al.*, 1991; Hynes, 1992). These studies have shown that axonal fasciculation and defasciculation are controlled by adhesion mechanisms mediated by surface glycoproteins. Genetic analyses has revealed the *in vivo* functional significance of at least one of these cell adhesion molecules (Fasciclin II in *Drosophila*) in selectively labeling a subset of CNS axon pathways (Grenningloh *et al.*, 1991).

In vertebrate systems the 'Labeled Pathway' hypothesis may explain the ability of axons from chick motor neurons to select appropriate nerve routes and plexuses (Lance-Jones and Landmesser, 1981). This general principle may even apply to development of the mammalian cerebral cortex. In this system, early developing axons from cortical subplate cells pioneer the pathway from the cortex to the thalamus and other subcortical targets (McConnell *et al.*, 1989). Later, follower axons from cortical neurons associate with these subplate fibres and may be guided along these pathways to their appropriate targets.

Non-neuronal cells have also been implicated in providing guidance cues to axon tracts. For instance, the role of glial cells in growth cone guidance has been recognized in both insects and vertebrates. In vertebrates glial cells appear, prior to neurite outgrowth, along the pathways that axons will subsequently follow. This observation led to the 'blueprint hypothesis' (Singer et al., 1979) which suggests that the paths recognized by growth cones are formed by glial cells before axon outgrowth. This hypothesis is supported by experiments in which this preformed pathway was physically ablated, leading to a disruption of the axon tract (Silver et al., 1982).

The initial evidence suggesting the role of glial cells as guidposts in insects was provided by experiments in grasshopper in which one glial cell type, the segment boundary cell (SBC) was ablated using a laser beam (Bastiani and Goodman, 1986). In this organism, the U axons, which pioneer the intersegmental nerve, contact the SBC prior to exiting the CNS. The growth cone of the aCC motor neurons follow the U axons while exiting the ventral nerve cord in the intersegmental nerve. After ablation of the SBC, both the U and aCC axons fail to exit the CNS.

Studies on the development of chick motor neuron projections to limb muscles have indicated that mesenchyme and connective tissue can directly or indirectly pattern nerve pathways in the nerve plexus region and in the limb (Lance-Jones and Dias, 1991; Tosney and Landmesser, 1984). In addition, somatic tissue can also specify axonal pathways (e.g., Oakley and Tosney, 1993; Keynes and Stern, 1984), as demonstrated by the fact that axons from spinal motor neurons project their axons only through the rostral half of each somite. Following rotation of the paraxial mesoderm such that the rostrocaudal polarity of the somites was reversed, there was a corresponding reversal of the pattern of outgrowth of motor axons (Keynes and Stern, 1984).

Molecular mechanisms of axon guidance and families of axon guidance molecules

At least four axon guidance mechanisms have been recognized; (1) short-range attractive or permissive cues, (2) short range repulsive cues, (3) long range attractive cues and (4) long-range repulsive guidance cues (Reviewed by

Goodman and Shatz, 1993; Keynes and Cook, 1995; Goodman, 1996). The short range cues are provided by non diffusible cell surface molecules and extracellular matrix molecules which either permit axon growth through selective adhesion or inhibit or repel axons on contact (e.g. Luo and Raper, 1994; Jessell, 1988). In contrast, long range cues are provided by diffusible molecules (Cajal, 1892; Tessier-Lavigne *et al.*, 1988; Colamarino and Tessier-Lavigne, 1995; Ebens *et al.*, 1996). Diffusible cues form gradients that originate from distant tissues and specify the direction of axonal growth (reviewed by Tessier-Lavigne, 1992). Although these definitions imply distinct mechanisms, in reality, the differences between these mechanisms are often blurred. For example, a secreted molecule in certain contexts can become immobilized by binding to cell suface or extracellular matrix and thus act as a short range signaling cue (e.g. Baier and Bonhoeffer, 1992). The importance of a balance between positive and negative cues in axon pathfinding have been recognized in both vertebrate and invertebrate systems (reviewed by Tessier-Lavigne and Goodman, 1996). The integration of multiple and often opposing molecular interactions at each site along the axon's trajectory, specially at choice points, help to fine tune the directional response of its growth cones.

In recent years substantial progress have been made in the isolation of molecules involved in axon guidance. The molecular characterization of the guidance cues shows that they belong to different families which provide axon guidance in both vertebrates and invertebrates, supporting the view that both the molecules and the mechanisms of growth cone guidance are conserved phylogenetically (Hynes and Lander 1992, ; Goodman, 1994).

In the context of molecules that behave as short range cues, attention has focused on neural cell adhesion molecules of the immunoglobulin (Ig) superfamily (Reviewed by Walsh and Doherty, 1997). The Eph family of receptor tyrosine kinases have gained attention in recent years for their role in axon navigation, particularly in the context of target recognition (e.g. Callahan *et al.*, 1995; Cheng *et al.*, 1995 ; Xu *et al.*, 1996) .

The gene families which were originally identified on the basis of their role in long-range signaling are the netrin and semaphorin gene families. Interestingly, the first chemoattractant to be isolated, netrin-1, displays sequence similarity with the extracellular matrix protein laminin (Serafini *et al.*, 1994). Similarly, the semaphorin family contains both cell surface and diffusible members (Kolodkin *et al.*, 1993). Thus these families are implicated in both long- and short-range signaling. In addition, netrins are bifunctional, attractive to some axons and repulsive to others (reviewed by Culotti and Kolodkin, 1996). Thus individual molecules or families of molecules do not always fit into any one mechanistic category. Furthermore, how one axon will behave towards a guidance cue presumably depends on the receptors expressed by its growth cones (Colamarino and Tessier-Lavigne, 1995; Wehrle and Chiquet, 1990; Mukhopadhyay *et al.*, 1994; Nose *et al.*, 1994).

The netrins are homologs of the *C. elegans* UNC-6 protein, which plays a role in circumferential guidance (Hedgecock *et al.*, 1990; Ishii *et al*, 1992; Serafini *et al.*, 1994). *In vitro* experiments have shown that the floor plate at the ventral midline of the developing mammalian spinal cord provides chemotrophic guidance signals for the growth cones of commissural neurons whose axons

extend towards the floor plate (Tessier-Lavigne *et al*, 1988; Placzek *et al*, 1990). When a dorsal spinal cord explant is placed within a few hundred microns of a floor plate explant in a collagen gel matrix, commissural growth cones turn and extend towards the floor plate from a distance. Two vertebrate netrins were isolated and identified as the chemoattractants that emanate from the floor plate cells and guide the spinal commissural axons (Serafini et al, 1994; Kennedy et al, 1994). Experimental analysis suggests that vertebarte netrins and nematode UNC-6 are bifunctional molecules that can act both as chemoattractants and chemorepellents. These molecules secreted by ventral cells appear to attract some growth cones toward the ventral midline but to repel other growth cones dorsally from the ventral midline. While netrin 1 attracts commissural growth cones towards the ventral midline, it repels subpopulations of dorsally-projecting hindbrain motor axons including the trochlear motor axons (Colamarino and Tessier-Lavigne, 1995; Varela-Echavarria *et al.*, 1997).

UNC-40 and UNC-5 are receptors for nematode UNC-6 that mediate chemoattractant and chemorepellent effects of UNC-6 respectively (Hedgecock *et al.*, 1990). Based on DNA sequence similarity two vertebrate netrin chemoattractant receptors (DCC and neogenin) have been identified (Keino-Masu *et al.*, 1996). These receptors are members of immunoglobulin superfamily. Functional evidence for the role of DCC came from *in vitro* experiment in which it was demonstrated that the floor plate dependent outgrowth of commissural axons can be blocked by administering antibodies raised against the extracellular domain of DCC (Keino-Masu *et al.*, 1996).

The Semaphorins (Sema) are a family of cell surface and secreted proteins that in general function as chemorepellents or inhibitors of axon pathfinding, branching or targeting (reviewed by Goodman, 1996). The first identified member of the family, Semaphorin-1, (Kolodkin *et al.*, 1992), is a transmembrane protein. Sema 1 is expressed on subsets of fasciculating axons in the developing CNS and on stripes of epithelial cells of the developing limb bud of grasshopper. Antibody blocking experiments in the limb bud show that Sema 1 inhibits branching and prevents steering of identified growth cones. In contrast to Sema I, Sema II and III and several other members of the family lack a transmembrane domain and are secreted. A member of the Semaphorin family, Collapsin (a homolog of human Sema III), was identified in chicken on the basis of its ability to cause the collapse of sensory growth cones in vitro (Luo *et al.*, 1993).

Extracellular matrix molecules (ECM) such as collagen, fibronectin and laminin bind cell surface receptors that may be integrins or immunoglobulin superfamily members. Laminin is known to promote axon outgrowth *in vitro* (Gunderson, 1987) and is present in some axonal pathways, notably in that of the optic tract (Cohen *et al.*, 1987). ECM molecules may have positive or negative effects on axon outgrowth. For example, tenascin-C has both axon outgrowth promoting and anti-adhesive domains (Gotz *et al.*, 1996). It has been suggested that the function of ECM molecules is regulated by binding to proteoglycans. For example, tenascin binds to glypican, laminin to dystroglycan and so on (Vaughan, *et al.*, 1994; Gullberg and Ekblom, 1995).

Cell adhesion molecules (CAMs) are an important class of axon guidance molecules. These are expressed on the cell surface and fall into several structural

classes, most notably the immunoglobulin superfamily, the cadherins and the integrins. Integrins are transmembrane proteins that bind ligands that are components of extracellular matrix, such as laminin, fibronectin, vitronectin, thrombospondin-1 and others (Clark and Brugge, 1995). For example, integrin mediates the thrombospondin-1 promoted outgrowth of sympathetic neurons from the central and peripheral nervous system. Cadherins are transmembrane glycoproteins that constitute the calcium-dependent adhesion system, in which molecules on adjacent cells bind homophilically (Takeichi, 1991). The neural-cadherins are implicated in the guidance of retinal axon outgrowth *in vivo* (Riehl *et al.*, 1996). The CAMs of the immunoglobulin superfamily include neural CAM (NCAM), L1/NgCAM, NrCAM and TAG-1/axonin-1. NCAM is the first identified CAM. It constitutes the calcium-independent adhesion system (Cunningham *et al.*, 1987).

Elegant studies on the role of immunoglobulin superfamily members have examined pathfinding of chick commissural interneurons across the floor plate (Stoeckli and Landmesser, 1995) and axon pathfinding in the muscle target area of the chick limb bud (Tang *et al*, 1992, 1994). During their growth accross the floor plate the commissural axons express NgCAM and axonin-1, while the floor plate expresses NrCAM. Perturbation of axonin-1 function by injecting anti-axonin antibody caused axonal defasciculation of commissural neurons and many axons failed to cross the floor plate, and turned instead along ipsilateral floor plate border (Stoeckli and Landmesser , 1995). Injection of anti-NrCAM also resulted in a similar commissural axon phenotype suggesting that interaction between axonin-1 on growth cones and NrCAM on floor plate cells is

involved in the entry of commissural axons into the floor plate (Stoeckli and Landmesser, 1995).

The navigation of motor axons from the neural tube into the periphery has proved an interesting system for studying the function of cell adhesion and other molecules in axon guidance. The initial growth of motor axons through the anterior sclerotome was proposed to be due to repulsive interactions between peanut agglutinnin binding protein and T-cadherin, expressed on the posterior sclerotome and motor axons respectively (reviewed by Keynes *et al.*, 1991). Polysialic acid (PSA) associated with NCAM is involved in modulating interactions between axons (Tang *et al.*, 1994). PSA expresses at low level in regions were motor axons are tightly fasciculated before reaching the plexus (the region where motor axons rearrange before entering the limb bud of chick embryo), and at higher level in regions of defasciculation. Specific removal of PSA by application of the enzyme endoN resulted in motor axon projection errors and increased fasciculation in the plexus region (Tang et al., 1992, 1994). The effect of endoN on axon pathfinding was reversed by treatment with antibodies against L1, implicating that PSA induces inhibition of L1-mediated fasciculation, which in turn facilitates normal motor axon guidance (Tang et al., 1994). Such balance of interactions mediated by NCAM and L1 is also involved in regulating patterns of nerve branching to fast and slow regions of embryonic muscle (Landmesser et al., 1988).

A variety of receptor protein tyrosine kinases (RPTKs) including fibroblast growth factor receptors, and the Trk family of neurotrophin receptors have been implicated in the regulation of axon outgrowth, target invasion, and axonal

branching (reviewed by Basilici and Moscatelli, 1992; McFarlane *et al.*, 1995; Barbacid, 1995). The largest subfamily of RPTKs in vertebrates is the Eph family, with at least 14 distinct members, and 8 ligands , now termed the 'Ephrins' (reviewed by Gale and Yancopoulos, 1997). Ephrins are all membrane-anchored via either a phospholipid anchor or a transmembrane domain. Many of the Eph receptors and ligands are expressed in the developing nervous system. Several of the lipid-anchored Eph ligands have been implicated as contact repellents that regulate axon fasciculation (Callahan *et al.*, 1995; Tessier-Lavigne, 1995) and retinotectal topographic map formation (e.g. RAGS and Elf-1; Cheng *et al.*, 1995; Drescher *et al.*, 1995).

Although much progress has been made in identifying and elucidating the properties of the different types and families of molecules that influence the direction of axon outgrowth, it is largely unknown how axon growth cones interpret these signals. This is primarily due to the fact that the molecular identity of the receptors that mediate growth cone responses to guidance cues are still unknown, with the exception of the Eph receptor tyrosine kinases. It is generally thought that receptor-ligand interactions on the surface result in activation of intracellular signaling pathways that induce changes in the cytoskeletal organization in the growth cone, leading to neurite extension in the proper direction. Little is known about the second messengers involved in the intracellular signaling pathway. Calcium has been implicated in the regulation of a wide range of growth cone behaviors (Kater and Mills, 1991; Cypher and Letourneau, 1992). Most $Ca2^{+}$ signaling is transduced by calmodulin (CaM). In *Drosophila* embryos, a selective disruption of calcium-CaM function in a specific

subset of growth cones was achieved through tissue specific expression of CaM antagonists. This disruption resulted in dosage-dependent stalls in extension and errors in axon guidance (VanBerkum and Goodman, 1995). The results of this study demonstrated an *in vivo* function for calcium-CaM signaling in growth cone guidance.

It has been shown that CAMs stimulate neurite outgrowth by activating fibroblast growth factor receptors (FGFR; reviewed by Doherty and Walsh, 1996). Activated FGFR triggers a presently unknown second messenger system involving tyrosine phosphorylation and increased calcium influx into neurons. This presumably leads to the activation of calcium-calmodulin dependent protein kinase, which may in turn be responsible for the phosphorylation of proteins required for axon motility. The intracellular proteins which are strongly implicated in the regulation of cytoskeletal rearrangement are the Rho family of small GTP-binding proteins, which includes Rho, Rac and Cdc42 (Nobes and Hall, 1995).

Transcription factors and neuronal connectivity

A number of transcription factors have been identified that regulate specific pathway selections by navigating axons in the developing nervous system. This is achieved through temporal and spatial regulation of expression of external guidance cues and molecules that allow a growing axon to respond appropriately to the cues it encounters (Lundgren, *et al.*, 1995; Mastick, *et al.*, 1997; Retaux and Harris, 1996; Bossing, *et al.*, 1996; Ginger, *et al.*, 1994).

Axon outgrowth occurs following final cell division. Thus, a transcription factor expressed solely in postmitotic neurons is more likely to be involved in pathfinding decisions of a neuron than those expressed earlier in neural cell lineages. These factors either control expression of receptors, or intracellular signaling components that are activated by the external guidance cues. Examples of such regulatory factors include the family of LIM domain containing proteins that carry a homeodomain and a cysteine-histidine rich LIM domain (Tsuchida, *et al.*, 1994; Tokumoto, *et al.*, 1995; Lundgren, *et al.*, 1995). Examples of transcription factors that are implicated in the regulation of expression of external guidance cues include Pax-6 (Mastick, *et al.*, 1997), *engrailed* (*en*; Retaux and Harris, 1996), and others (Bossing, *et al.*, 1996).

The family of LIM domain proteins have generated much interest as possible regulators of axon pathfinding because of a close correlation seen between the expression pattern of family members and the projection phenotype of motor neurons in the spinal cord of chick and zebrafish (Tsuchida, *et al.*, 1994; Tokumoto, *et al.*, 1995). The role of a LIM homeobox gene called *apeterous* (*ap*) in axon pathfinding has been examined in *Drosophila* (Lundgren, *et al.*, 1995). *ap* is expressed in a subset of interneurons that normally choose a single projection pathway in the ventral nerve cord. These neurons send out axons that grow towards the midline, but prior to reaching the midline the axons fasciculate with each other and extend anteriorly in the ipsilateral connective. In the absence of *ap* function, these axons fail to fasciculate normally and extend along the appropriate pathway. This specific mutant phenotype together with a restricted pattern of expression of the *ap* gene seen in the postmitotic interneurons, led

investigators to propose a direct role of *ap* in regulating the expression of cell surface molecules that mediate recognition events necessary for the formation of the *ap* fascicle (Lundgren *et al.*, 1995).

In the mouse CNS, the LIM and homeodomain containing protein Pax-6 regulates the formation of the first prosencephalic tract called tpoc (Mastick, *et al.*, 1997). Tpoc originates as axons projecting caudally from a cluster of neurons located at the base of the optic stalk. In wild-type embryos, the developing tract comes in close contact with a superficial patch of *Pax-6* expressing neurons. In *Pax-6* mutants, the projections of the tract forming axons are disrupted in the region where these axons contact the *Pax-6* expressing neurons. The differentiation of the *Pax-6* expressing neurons is not affected in the mutant. These observations suggest a role for *Pax-6* in providing local positional information for proper guidance of axons that form the first prosencephalic tract.

The *en* gene codes for a homeodomain containing transcription factor. A gradient of *en* expression is seen in the mesencephalon that correlates with the topographic projections of optic axons (Retaux and Harris, 1996). A role for *en* in guiding optic axons has been demonstrated through various manipulations of the *en* gradient that lead to the disruption in the formation of retinotectal topographic map. Interestingly, the guidance function of *en* appears to be mediated by several candidate cell surface molecules, notably the Eph ligands that are upregulated by *en* (Logan, *et al.*, 1996).

Another transcription factor that regulates both axon growth and guidance is *longitudinals lacking* (*lola*; Ginger, *et al.*, 1994). The *lola* gene is a member of the *tramtrack* family of proteins with two zinc finger domains.

Mutations in the *lola* gene leads to fused commissures in *Drosophila*. Two different isoforms of *lola* have been shown to be expressed in two different cell-types, the navigating axons and the tissue (midline glia) that provides guidance cues to these axons. Identifying the mechanistic difference in the mode of action of the two isoforms of *lola* will thus be important in understanding the difference between the two pathways regulating axon growth and guidance.

It is likely that in the near future the role of previously known transcription factors as regulators of neuronal pathway formation will emerge along with the identification of new transcription factors. Spatial and temporal control of the activity of these regulators along with characterization of their targets will provide valuable information on axon growth and guidance.

Genetic analysis of growth cone guidance:

The fact that the behavior of growth cones can be influenced by both attractive and repulsive factors, either by contact-mediated or diffusible mechanisms, is well established from *in-vitro* studies (reviewed by Goodman, 1996). An understanding at the molecular level of how these different forces are coordinated *in-vivo* to establish the stereotypical patterns of synaptic connections of a complex nervous system remains, however, largely elusive. A powerful approach to studying this problem is to use genetics to identify genes necessary for *in vivo* axon guidance. Two methods of genetic analysis can be used to identify and study *in vivo* function of molecules that control growth cone guidance. One approach is the so called reverse genetic approach which has been used in a variety of organisms to test the function of previously identified

molecules through disruption of gene function or misexpression studies. The other approach is the classical genetic approach, in which a large-scale mutagenesis in performed. Mutations that result in defects in axonal projections may define genes involved in establishing neuronal connectivity in the intact organism. By doing large-scale systematic screens it is theoretically possible to identify all genes involved in a given developmental pathway. The proteins identified in this fashion could function in any step in the process (i. e., regulators, signals, receptors, effectors). An innovative classical genetic approach is an interactive genetic screen in which one begins with a mutation in a particular gene that creates a sensitized background (using either partial loss-of-function or gain-of-function mutants) and then screens for mutations in other genes that either enhance of suppress this phenotype. Such screens can be used to identify upstream and downstream components in a genetic pathway (e. g. Simon *et al.*, 1991). Until recently classical genetic approaches were restricted to invertebrate systems, most notably the nematode and *Drosophila*. However, large-scale mutant screens have now been conducted in the lower vertebrate Zebrafish. Using anatomical probes to search for defects in the retinotectal projection, a number of interesting mutants have been identified (reviewed by Kuwada, 1995).

Genetic analysis in *Drosophila*:

There are a number of reasons for using *Drosophila* as a model system to unravel complex biological processes. The most compelling is the power of the genetic approach. This is best exemplified in the genetic screen of Nusslein-Volhard and

Wieschaus (1980) from over a decade ago, which revolutionized our understanding of early embryonic pattern formation.

Behavioral assays have been used in *Drosophila* identifying mutations that disrupt axon pathfinding and cellular connectivity in the nervous system. Two such screens were based on the jumping behavior of flies in response to light-off stimulus (Thomas and Wyman, 1984) and grooming behavior (Phillis *et al.*, 1993). The screen for jumpless mutants led to the identification of two mutants (*bendless* and *passover*) that disrupt connectivity between an identified paired neuron (GF neuron) and a specific jump muscle motoneuron (the TTMmn, tergotrochauteral jump muscle motor neuron).

The *bendless* gene, that encodes a ubiquitine conjugating enzyme, is required for normal pathfinding/target recognition by the GF axons; while, the *passover* gene is required for function and maintenance of synaptic connections between GF and TTMmn neurons (Thomas and Wyman, 1984). The *passover* gene encodes a transmembrane protein similar to the *Drosophila ogre* and *C. elegans* Unc-7 proteins (Krishnan *et al.*, 1993). Unc-7 is also required for proper neuronal connectivity in *C. elegans* (Starich, *et al.*, 1993). Later studies have shown that the *passover* gene is also necessary for gap junction communication between neurons of the *Drosophila* giant fibre system (Crompton *et al*, 1992; Krishnan *et al*, 1993), the group of eight neurons that relay excitation from the eyes to the muscles of the thorax.

Using anatomical probes, three large-scale histological screens have been conducted in *Drosophila* to identify molecules required for axon guidance and neuronal connectivity. These screens were aimed at studying CNS axon

pathways (Seeger *et al.*, 1993), neuromuscular connectivity (Van Vactor *et al.*, 1993) and retinotopic connectivity (Martin *et al.*, 1995).

The midline of bilaterally symmetric CNS from arthropods to vertebrates represents a boundary that has major influences on growth cone behavior. A systematic genetic screen using a general CNS axon marker (MAb BP102) was conducted to identify mutations that affect CNS patterning in *Drosophila* (Seeger *et al.*, 1993). Two mutations, *commissureless* (*comm*) and *roundabout* (*robo*), were isolated that severely affected axonal growth across midline. Mutations in the *comm* gene resulted in absence of nearly all CNS axon commissures. Axons that normally project across the midline, such as RP1 and SP1 (two identified commissural neurons), failed to do so in these mutant embryos. Instead these neurons sent ipsilateral projections which are normal in all respects except for being on the wrong side of the embryo. The *comm* mutant does not cause abnormality in the midline structure or disrupt any other axon pathway that may be important for commissural axons outgrowth towards the midline. This suggests that the *comm* gene is a good candidate to act either as a signal or a receptor that guide axon growth cones towards the midline.

Mutations in the gene *roundabout* (*robo*) lead to a phenotype opposite to that of *comm*. In *robo* mutant embryos, axons that are close to the midline, but do not normally cross it, are inappropriately attracted towards the midline and their contralateral homologues on the other side. On the basis of this mutant phenotype a role of *robo* in directly or indirectly generating repulsive cues at the midline for the ipsilaterally projecting neurons has been proposed. Furthermore, the observation that the *comm* phenotype is suppressed in *comm-robo* double

mutant suggests that these two systems do not act independently. Instead, there may be a balance between attractive and repulsive cues that affect growth cone behaviour in the midline (Seeger, *et al.*, 1993).

Mutations in two other genes (*fasciclin I* and *abelson*) isolated in the same screen led to the identification of two redundant pathways that attract commissural axons outgrowth towards midline (Elikins, *et al*, 1990). Mutation in either gene does not reveal any obvious commissural axon pathfinding defect; however, a phenotype similar to that of *comm* mutant is seen when both genes are mutated simultaneously.

The ability of motoneurons to find and recognize their appropriate muscle targets has long been an excellent model system for studying axon pathfinding and target recognition. Using an antibody probe that identifies motoneuron growth cones and axons (MAb 1D4), a screen of the second chromosome for mutations that disrupt motoneuron pathfinding and target recognition was conducted (VanVactor *et al.*, 1993). The screen led to the identification of several genes that are necessary for motoneurons to navigate past particular choice points in the pathfinding process, e. g. *beaten path, stranded* and *short stop*. In addition, two genes (*walkabout* and *clueless*) required for target recognition by a group of motoneurons, have also been identified in this screen.

In the retinal connectivity screen (Martin *et al.*, 1995), a *lacZ* reporter gene (*glass-lacZ*) specific for photoreceptor neurons was used to identify mutations affecting retinal axon outgrowth, retinotopy and target recognition. The screen led to the identification of four genes that play direct roles in neuronal connectivity. These include genes regulating axonal outgrowth (e.g. *eddy*), target

recognition (e.g. *limbo* and *nonstop*) and retinotopy (e.g. *limbo*). Some of these genes appear to encode components of the growth cone itself (*limbo* and *diva*), while others may act as extracellular cues for growth cone guidance (*eddy* and *nonstop*).

Reverse genetics has provided a complementary approach in *Drosophila* to identify guidance molecules. In the past, several molecules implicated in growth cone guidance have been identified in *Drosophila* based on their pattern of expression (using MAb or enhancer trap screens), or sequence similarity to known guidance molecules (e.g., Grenningloh *et al.*, 1991; Nose *et al.*, 1992; Klambt *et al.*, 1991). The specific function of these molecules was subsequently studied using a reverse genetic approach. For example, three receptor-like tyrosine phosphatases that are expressed in the embryonic CNS have been cloned based on sequence similarity to vertebrate proteins (Nose *et a*l., 1992, Chiba *et al.*, 1995, Matthes, *et al.*, 1995). These proteins (connectin, fasciclin III and semaphorin II) are expressed by subsets of muscles during the establishment of neuromuscular connections. These proteins contain immunoglobulin-like domains and fibronectin typeIII repeats in the extracellular domain, protein motifs often associated with recognition/adhesion proteins. Additionally, the obvious signaling potential of the cytoplasmic tyrosine phosphatase domain of these proteins, raise intriguing questions about the function of these proteins during growth cone guidance. Ectopic expression studies showed that all three proteins can function in growth cone guidance: connectin as a bifunctional signal (Nose *et al.*, 1994), fasciclin as an attractive signal (Chiba *et al.*, 1995) and semaphorin as an inhibitory signal (Matthes *et al.*, 1995).

Genetic analysis in zebrafish:

Until recently, large-scale genetic screens have not been practical in vertebrates. Unfortunately, applying reverse genetics to study just the molecules which have already been identified limits the extent of the investigation. Additionally, when functions of multiple proteins overlap in guidance of a particular axon pathway, knock out of a gene corresponding to one of these proteins with overlapping function might not lead to an obvious pathfinding phenotype, even though the gene might be expected to play a role in axon guidance. By employing forward genetics in zebrafish it has become possible to overcome these problems and to analyze *in vivo* axon guidance systematically in a vertebrate system for the first time.

The convergence of biochemical approaches in vertebrates and genetic approaches in invertebrates has shown that some axon-guidance mechanisms are conserved to a remarkable degree (Goodman, 1994). At the same time, given the complexity of the vertebrate CNS, it seems likely that evolution has provided vertebrates with novel guidance mechanisms or has used conserved guidance cues in novel pathways. Thus it is important to study axon guidance systematically in vertebrates as has been done in invertebrates. The refinement of zebrafish as a genetic system (Mullins *et al.*, 1994; Grunwald and Streisinger, 1992) has made it possible to apply a systematic genetic approach to the study of axon guidance in vertebrates.

A mutant screen was performed on zebrafish larvae in search for defects in axon projections between the eye and its main target in the brain, the optic

tectum (Baier *et al.*, 1996; Trowe *et al.*, 1996; Karlstrom *et al.*, 1996). In addition to finding several genes specifically involved in retinotectal topography, a large number of genes were found that affect axon guidance more generally. Four classes of mutants were identified in this screen. In one class of pathfinding mutants, retinal axons fail to cross the ventral midline of the brain. These neurons connect to the ipsilateral rather than contralateral tectal lobe. Five of these mutations (*chameleon, detour, iguana, umleitung* and *you-too*) affect differentiation of midline structures. These mutants demonstrate the importance of midline cells in retinal axon guidance. Another class of mutations that affect the ability of retinal axons to turn toward the contralateral tectal lobe after they reach the midline include *bashful, grumpy* and *sleepy*. In these mutants, after axons cross the midline they often turn anteriorly and grow along the margin of the telencephalon.

Three mutations that affect sorting of retinal axons in the optic tract were identified. These are *boxer, dackel* and *pinscher*. In these mutants, dorsal axons grow through both dorsal and ventral nerve bundles instead of selectively using the ventral bunch and arrive at the dorsal side of the tectum. These axons then traverse the tectum to find their correct ventral targets. Further molecular analysis of these genes will elucidate the process of fibre sorting, a phenomenon that is poorly understood.

Four mutations, *nevermind, who-cares, gnarled* and *macho* affecting the mapping of the retinal fibres have also been identified in this screen. The first two affect the retinal axons mapping along the dorsoventral axis, while *gnarled*

(*gna*) and *macho* (*mao*) affect it along the anterior-posterior axis. In *gna* and *mao* Nasodorsal axons defasciculate and terminate too soon in the anterior tectum.

A general finding of the screen in zebrafish is that most of the retinotectal mutants show other developmental defects. This indicates that molecular mechanisms used for axon guidance are also used in other developmental processes. In addition, genes absolutely necessary for early development can not be found in the screen. Affected embryos do not develop to a stage where axon guidance could be assayed. A genetic screen designed to find conditional, temperature-sensitive mutations may provide an alternative way to find more of the genes involved in axon guidance.

Organization and neuronal connectivity pattern in the *Drosophila* visual system

The *Drosophila* visual system offers an excellent model for the investigation of neuronal patterning. The advantages include, relative simplicity, availability of numerous molecular markers which can be used to identify and analyse individual neurons (Bellen *et al.*, 1989; Bier *etal.*, 1989; Wilson *et al.*, 1989; Zipursky *et al.*, 1984), availability of behavioral tests (phototaxis and optomotor behavior), opportunity for genetic analysis and most importantly, the remarkable similarity in the mechanism of neuronal growth cone guidance in insect and mammals (Harrelson and Goodman, 1988; Klose and Bentley, 1989; McConnell *et al.*, 1989).

Drosophila displays two distinct visual systems during larval and adult stages. The adult visual system consists of compound eyes and the optic lobes,

the portion of the visual system that receives and processes visual information from the eyes (reviewed by Wolff and Ready, 1993; Meinertzhagen and Hanson, 1993). The compound eyes are composed of approximately 800 ommatidia, each containing eight photoreceptor cells. The photoreceptor cells differentiate from the eye imaginal disc during third instar larval stage (Ready *et al.*, 1976). These cells send their axons to the optic lobe primordium through a specialized epithelium tube called optic stalk. Retinotopy is seen in the adult visual system, i.e., retinal axons send their axons to the corresponding positions in the brain. An examination of photoreceptor projections in mutants containing fewer number of these cells and in mosaic animals containing patches of wild-type axons in a mutant background, has shown that each photoreceptor axon is independently guided to its target cell (Kunes *et al.*, 1993). These findings suggest a model similar to Sperry's chemoaffinity hypothesis where positional guidance and recognition cues label pathways and synaptic targets (Sperry, 1963).

All three components of the *Drosophila* visual system; the adult eye, larval eye and the optic lobe originates from a small region of the procephalic lobe (embryonic head; Green *et al.*, 1993). The optic lobe and the larval photoreceptor cells arise from within a coherent region of the posterior head ectoderm, while the eye imaginal disc develops from two pouches of the anterior ectoderm. Each primordium of adult optic lobes develops from a mass of tissue that invaginates from the posterior portion of the procephalic lobe during stage 12 of embryogenesis. The optic lobes form in direct contact to the developing larval brain and by late embryogenesis this tissue completely incorporates into the

brain hemispheres. The optic lobe primordium remains undifferentiated until larval stage, when it resumes mitosis and differentiates to form the optic ganglia (Meinertzhagen, 1973; White and Kankel, 1978).

Although the tissue origin for the eye imaginal disc and the optic lobe primordium are different from each other, the two tissues interact extensively during development. The differentiation of the first order interneurons of the first ganglion layer (lamina) of the optic lobe is dependent on photoreceptor axon innervation (reviewed by Meinertzhagen and Hanson, 1993). However, the dependence of the second order neurons in the second optic ganglion (medulla) upon retinal innervation is less extensive. Retrograde interaction, that is, the dependence of photoreceptor integrity on connection of these cells with their synaptic partners of lamina ganglionaris has also been shown to be a characteristic of insect visual system development (Campos *et al.*, 1992).

In comparison to the adult visual system, the larval visual system is extremely simple, consisting of two bilateral clusters of 12 photoreceptor cells. These cells extend their axons in a fascicle (the Bolwig's nerve; Bolwig, 1946) towards the larval visual system target area located within the anlage of the adult optic lobes (Green *et al.*, 1993). The Bolwig's organ develops at the ventral tip of the invaginating optic lobe primordium. These cells send short axonal projections that contact the cells of the neighboring optic lobe invagination (Steller *et al.*, 1987; Schmucker *et al.*, 1992; Green *et al.*, 1993). At stages 15-16, during head involution, the larval photoreceptor cells begin to migrate out of the head epidermis by delamination. While these cells migrate anteriorly their axons retain connection with the optic lobe primordium (Green *et al.*, 1993). During

this period the Bolwig's nerve which is formed from fasciculation of the 12 photoreceptor axons undergo extensive elongation. Later in embryogenesis, the Bolwig's nerve terminal extends deeper into the brain, past the optic lobe primordium and terminates at the posterior margin of the optic lobe primordium (Green *et al.*, 1993; Campos *et al.*, 1995). The cells in the invaginating optic lobe primordia that contact the larval optic nerve act as intermediate targets for the larval photoreceptor cells, analogous to the guidepost cells discussed earlier (Campos et al., 1995).

Some of the cell types that are contacted by the larval optic nerve during larval visual system development have been identified, among the most interesting are the three optic lobe pioneer cells (OLPs; Tix *et al.*, 1989; Campos *et al.*, 1995). Two of these cells that originate from the optic lobe primordium itself are called the corner OLPs. The one that originates from outside this region is called the central OLP. This cell is contacted by the LON in the final stage of nerve pathway formation. The axon of this cell extends towards the central brain into the larval optic neuropil before it contacts the LON (Campos *et al.*, 1995). The LON and the axons from the two corner OLPs fasciculate with the central OLP axon and together project towards the central brain. Thus the central OLP is thought to pioneer the route taken by the LON toward the central brain. On the other hand the corner OLP cells that contact the LON at initial stages of development before invagination of the optic lobe primordium are thought to act as intermediate targets for the LON and are thus analogous to the guidepost cells discussed earlier (Campos *et al.*, 1995). The OLP cells are also incorporated into

the adult optic lobe and are thought to play a role in organizing the adult visual system as well (Fischbach and Technau, 1987).

The *Drosophila disconnected* gene and its role in the establishment of neuronal connections in the visual system

The *disconnected* (*disco*) gene codes for a putative transcription factor with two C2H2 type zinc finger motifs (Heilig *et al.*, 1991). The zinc finger proteins represent a major group of transcription factors that play an important role in many aspects of eukaryotic gene regulation. Proteins of this family contain tandem repeats of 30 amino acids zinc finger motifs enriched in Cysteine and /or Histidine residues (reviewed by Berg, 1990).

The importance of the zinc finger domains in *disco* function was demonstrated by the fact that mutations in the conserved Cysteine residues of either zinc finger motif result in a visual system phenotype similar to that seen in mutants in which the *disco* gene is deleted (Heilig *et al.*, 1991). Since two zinc finger domains are sufficient for sequence specific DNA binding activity (Keller and Maniatis, 1992), it is hypothesized that *disco* is a DNA binding protein. Nuclear localization of the DISCO protein and an autoregulatory activity of *disco* demonstrated in the cells of the optic lobe primordium support this hypothesis. A high affinity DNA binding site has also been identified in genomic DNA, 2.5 kb upstream of the *disco* transcription start site in an *in vivo* electrophoretic mobility shift assay (Kevin Lee, Ph. D. thesis, 1993).

disco gene function is required for proper neuronal connectivity formation in both larval and adult visual system of *Drosophila*. Mutations in the *disco* gene

cause failure of the larval and adult photoreceptor axons to make proper connections with their target cells (Figure 1; Steller, *et al.*, 1987). In the majority of the adult *disco* mutant flies the compound eyes fail to innervate the brain and show a significant reduction in the volume of the optic lobes. This phenotype is referred to as the unconnected phenotype (Steller *et al.*, 1987). In other adult mutant flies, the retinal innervation of the optic ganglia occurs, but the optic ganglia in these mutants are roughly normal in size although still grossly disorganized. This phenotype is called the connected phenotype. Since retinal innervation is required for proper development of the optic ganglia, the reduced optic ganglia in the unconnected *disco* mutant is at least partly due to the lack of retinal innervation. The presence or absence of retinal innervation again depends on presence or absence of the optic stalk, the tube that connects the eye disc to the optic lobe and through which retinal axons enter the optic lobe area of the brain. Individual mutant larvae can lack just one or both optic stalks.

The *disco* gene is expressed in several of the different cell types contacted by the larval optic nerve including a group of glial cells distributed along the LON and the OLP cells (Lee *et al.*, 1991; Campos *et al.*, 1995). Interestingly, mutation in *disco* leads to failure in the differentiation of corner OLP cells and mislocation of the glial cells (Campos *et al.*, 1995). Thus, loss of *disco* function leads to defects in cellular interactions between the LON and the cells it contacts during pathway formation. The absence of *disco* expression in the photoreceptor cells at least during axon outgrowth indicates that the effect of a *disco* mutation on the LON phenotype is nonautonomous. The *disco* gene function is required at least in the OLPs or LON glial cells for proper LON connectivity. It may regulate

cellular guidance cues and recognition cues that are specific to the development of the larval optic nerve pathway and connectivity.

Questions and aims of this thesis

The goal of the work presented in this thesis is to study some of the cellular and molecular mechanisms underlying nervous system development. To that end I focused on the development of neuronal pathways in a simple model system, the larval visual system of *Drosophila melanogaster*. The simplicity of the larval visual system makes is amenable to cellular biological studies, and the classical genetic approaches that are uniquely applicable to *Drosophila* research together with a recent advent in molecular biological tools made the visual system of *Drosophila* an attractive model system for neurobiological studies.

The first part of my thesis described identification and characterization of specific cellular interactions at the larval optic center of *Drosophila*. The outcome of this study may suggest that changes in behavior of an organism that occur as a function of normal development require establishment of new neuronal connections. The second part of my thesis addressed the role of the *disconnected* gene in establishing proper neuronal connections in the visual system of *Drosophila*. The tissue specific autoregulatory activity of *disco* in the cells of the optic lobe primordium, and the differential effect of *disco* mutations on the *disco* expressing cells contacted by the LON, reveal the importance of tissue specific *disco* function in establishing proper LON connectivity. Therefore, identification of tissue specific factors regulating *disco* function will provide us with valuable

information on the role of the *disco* gene in *Drosophila* visual system development. In this part of my thesis, I used the yeast interaction trap approach to identify DISCO interacting proteins.

Chapter 2 of this thesis describes the identification of a serotonergic neuronal process and the influence of the LON on the outgrowth and establishment of arborization from the newly identified process at the larval optic center. This study led to the speculation that the establishment of connections between the LON and the serotonin process modulates larval photoresponse.

Chapter 3 describes the identification of three *Drosophila* proteins (DISCO-interacting proteins DIP1, DIP2 and DIP3) that interact with DISCO in yeast interaction trap and *in vitro* binding assays. Among these two are newly identified proteins, one of which contains two putative double stranded RNA-binding domains (DIP1) and the other is a highly conserved protein (DIP2) of unknown function. The known DISCO interacting protein (DIP3) is the putative ATPase component of the 26S proteasome. Expression of the DIP1 and DIP2 proteins partially overlap with that of *disco*, and therefore, these are good candidates to act as components of *disco* mediated pathway that reulate larval visual system connectivity formation.

Northern analysis and analysis of *dip1* cDNAs isolated from various cDNA libraries indicate expression of three alternatively spliced forms of the *dip1* mRNA. Repetitive sequences in the 3' untranslated region of these transcripts may confer translational regulation and therefore may suggest a less extensive expression pattern of the DIP1 protein than its mRNA. Based on the

chromosomal location and the deficiency map of the *dip1* gene, a putative mutant (*flamenco, flam*) for this gene has been identified. The physiological role of the gene affected in *flam* mutant is presently unknown; however, the effect of the hypomorphic mutant allele on the expression and mobilization of a retroviral element in *Drosophila* ovary might support a RNA binding activity of the gene.

The human and *C. elegans* homologs of the *dip2* gene have been cloned in the corresponding genome projects. The work presented in this thesis describes the isolation of the *Drosophila* and mouse homologs of this gene. The putative DIP2 protein lacks any known functional domain. Although no functional analysis has yet been done on any *dip2* homologs, nervous system specific expression of the *Drosophila* and the mouse homologs during embryogenesis suggest an important role for *dip2* in nervous system development.

References:

Bacilico, C. and Moscatelli, D. (1992). The EGF family of growth factors and oncogenes. Adv. Cancer res. **59**: 115-165.

Baier, H. and Bonhoeffer, F. (1992). Axon guidance by gradients of a target-derived component. Science **255**: 472-475.

Baier, H., Klostermann, S., Trowe, T., Karlstrom, R. O., Nusslein-Volhard, C. and Bonhoeffer, F. (1996). Getetic dissection of the retinotectal projection. Development **123**: 415-425.

Barbacid, M. (1995). Neurotrophic factors and their receptors. Curr. Opin. Cell Biol. 7: 148-155.

Bastiani, M. J. and Goodman, C. S. 1986. Guidance of neuronal growth cones in the grasshopper embryo. III. Recognition of specific glial pathways. J. Neurosci. **6**: 3542-3551.

Bastiani, M. J., Harrelson, A. L., Snow, P. M. and Goodman, C. S. 1987. Expression of fasciclin I and II glycoproteins on subsets of axon pathways during neuronal development in the grasshopper. Cell **48**: 745-755.

Bate, C. M. 1976. Pioneer neurons in an insect embryo. Nature **260**: 54-56.

Bellen, H. J., O'Kane, C. J., Wilson, C., Grossniklaus, U., Pearson, R. K. and Gehring, W. J. 1989. P-element-mediated enhancer detection: a versatile method to study development in *Drosophila*. Genes. Dev. **3**: 1288-1300.

Bentley, D. and Caudy, M. 1983. Pioneer axons loose directed growth after selective killing of guidepost cells. Nature **304**: 62-65.

Berg, J. M. 1990. Zinc finger domain: hypothesis and current knowledge. Ann. Rev. Biophys. Biophysical Chem. **19**: 405-421.

Bier, E., Vaessin, H., Shepherd, S., Lee, K., McCall, K., Barbel., S., Ackerman, L., Carretto, R., Uemura, T., Grell, E., Jan, L. Y. and Yan, Y. N. (1989). Searching for pattern and mutation in the *Drosophila* genome with a P-*lacZ* vector. Genes Dev. **3**: 1273-1287.

Bolwig, N. (1946). Senses and sense organs of the anterior end of the house fly larva. Vidensk. Medd. Fra. Dansk. Naturh. Foren. **109**: 80-212.

Bossing, T., Technau, G. M. and Doe, C. Q. (1996). *huckebein* is required for glial development and axon pathfinding in the neuroblast 1-1 and neuroblast 2-2 lineages in the *Drosophila* central nervous system. Mech. Dev. **55**: 53-64.

Callahan, C. A., Muralidhar, M. G., Lundgreen, S. E., Scully, A. L. and Thomas, J. B. 1995. Control of neuronal pathway selection by a *Drosophila* receptor protein-tyrosine kinase family member. Nature **376**: 171-174.

Campos, A. R., Fischbach, K. F. and Steller, H. 1992. Survival of photoreceptor neurons in the compound eye of *Drosophila* depends on connections with optic ganglia. Development **114**: 355-366.

Campos, A. R., Lee, K. J. and Steller, H. 1995. Establishment of neuronal connectivity during development of the *Drosophila* larval visual system. J. Neurobiol. **28**: 313-329.

Cheng, H. -J., Nakamoto, M., Bergemann, A. D. and Flanagan, J. G. (1995). Complementary gradients in expression and binding of ELF-1 and Mek 4 in development of the topographic retinotectal projection map. Cell **82**: 371-381.

Chiba, A., Snow, P., Keshishian, H. and Hotta, Y. (1995). Fasciclin III as a synaptic target recognition molecule in *Drosophila*. Nature **374**: 166-168.

Clark, E. A. and Brugge, J. S. (1995). Integrins and signal transduction pathways: the road taken. Science **268**: 233-239.

Cohen, J., Burne, J. F., McKinlay, C. and Winter, J. (1987). The role of laminin/fibronectin receptor complex in the outgrowth of retinal ganglion cell axons. Dev. Biol. **122**: 407-418.

Colamarino, S. A. and Tessier-Lavigne, M. 1995. The axonal chemoattractant netrin-1 is also a chemorepellent for trochlea motor axons. Cell **81**: 621-629.

Crompton, D. E., Griffin, A., Davies, J. A. and Miklos, G. L. 1992. Analysis of a cDNA from the neurologically active locus *shaking-B* (*passover*) of *Drosophila melanogaster*. Gene **122**: 385-386.

Culotti, J. G. and Kolodkin, A. L. (1996). Functions of netrins and semaphorins in axon guidance. Curr. Opin. Neurobiol. **6**: 81-88.

Cunningham, B. A., Hemperly, J. J., Murray, B. A., Prediger, E. A., Brackenbury, R. and Edelman, G. M. 1987. Neural cell adhesion molecule: structure, immunoglobulin-like domains, cell surface modulations and alternative RNA splicing. Science **236**: 799-806.

Cypher, C. and Letourneau, P. C. 1992. Growth cone motility. Curr. Opin. Cell. Biol. **4**: 4-7.

Doherty, P. and Walsh, F. S. 1996. CAM-FGF receptor interactions: a model for axonal growth. Mol. Cell. Neurosci. **8**: 99-111.

Drescher, U., Kremoser, C., Handwerker, C., Loschinger, J., Noda, M. and Bonhoeffer, F. 1995. In vitro guidance of retinal ganglion cell axons by RAGS, a 25 KDa tectal protein related to ligands for Eph-receptor tyrosine kinases. Cell **82**: 359-370.

Ebens, A., Brose, K., Leonardo, E. D., Hanson, M. G. Jr., Bladt, F., Birchmeier, C., Barres, B. A. and Tessier-Lavigne, M. (1996). Hepatocyte growth factor/Scatter factor is an axonal chemoattractant and a neurotrophic factor for spinal motor neurons. Neuron **17**: 1157-1172.

Elkins, T., Zinn, K., McAllister, L., Hoffmann, F. M. ang Goodman, C. S. (1990). Genetic analysis of a Drosophila neural cell adhesion molecule: interaction of fasciclin 1 and abelson tyrosine kinase mutations. Cell **60**: 565-575.

Fischbach, K. F. and Technau, G. (1987). Mutant analysis of optic lobe development in *Drosophila*. In *New Frontiers in Brain Research*, Proceedings of the 15th Gottingen Neurobiology Conference (ed. N. Elsner and Crentzfeld, O.) pp. 35. George Thieme Verlag, Stuttgart.

Gale, N. W. and Yancopoulos, G. D. (1997). Ephrins and their receptors: a repulsive topic. Cell tissue res. **290**: 227-241.

Ghosh, A., Antonini, A., McConnell, S. K. and Schatz, C. J. 1990. Requirement for subplate neurons in the formation of thalamocortical connections. Nature **347**: 179-181.

Ginger, E., Tietje, K., Jan, L. Y. and Jan, Y. N. (1994). *lola* encodes a putative transcription factor required for axon growth and guidance in *Drosophila*. Development **120**: 1385-1389.

Goodman, C. S. Bastiani, M. J., Doe, C. Q., Lac, S. D., Helfand, S. L., Kuwada, J. Y. and Thomas, J. B. (1984). Cell recognition during neuronal development. Science **225**: 1271-1279.

Goodman, C. S. and Shatz, C. J. (1993). Developmental mechanisms that generate precise patterns of neuronal connectivity. Cell **72**: 77-98.

Goodman, C. S. (1994). The likeness of being: phylogenetically conserved molecular mechanisms of growth cone guidance. Cell **78**, 353-356.

Goodman, C. S. (1996). Mechanisms and molecules that control growth cone guidance. Ann. Rev. Neurosci. **19**: 341-377.

Gotz, B., Scholze, A., Clement, A., Joester, A., Schutte, K., Wigger, F., Frank, R., Spiess, E., Ekblom, P. and Faissner, A. Tenascin-C contains distinct adhesive, anti-adhesive, and neurite outgrowth promoting sites for neurons. J. Cell. Biol. **132**: 681-697.

Green, P., Hartenstein, A. Y and Hartenstein, V. 1993. The embryonic development of the *Drosophila* visual system. Cell Tissue Res. **273**: 583-598.

Grenningloh, G., Rehm, E. J. and Goodman, C. S. 1991. Genetic analysis of growth cone guidance in *Drosophila*: fasciclin II functions as a neuronal recognition molecule. Cell **67**: 45-57.

Grunwald, D. J. and Streisinger, G. (1992). Induction of recessive lethal and specific locus mutations in zebrafish with ethylnitrosourea. Genet. Res. **59**: 103-116.

Gullberg, G. and Ekblom, P. (1995). Extracellular matrix and its receptors during developemnt. Int. J. Dev. Biol. **39**: 845-854.

Gunderson, R. W. (1987). Response of sensory neurites and growth cones to patterned substrata of laminin and fibronectin *in vitro*. Dev. Biol. **121**: 423-431.

Harrelson, A. L. and Goodman, C. S. 1988. Growth cone guidance in insects: fasciclin II is a member of the immunoglobulin superfamily. Science **242**: 700-708.

Hedgecock, E. M., Culotti, J. G. and Hall, D. H. 1990. The *unc-5*, *unc-6* and *unc-40* genes guide circumferential migration of pioneer axons and mesodermal cells on the epidermis in *C. elegans*. Neuron **4**: 61-85.

Heilig, J. S., Freeman, M., Laverty, T., Lee, K. J., Campos, A. R., Rubin, G. M. and Steller, H. 1991. Isolation and characterization of the *disconnected* gene of *Drosophila melanogaster*. EMBO J. **10**: 809-815.

Hynes, R. O. and Lander, A. D. 1992 . Contact and adhesive specificities in the associations, migrations and targetting of cells and axons. Cell **68**: 303-322.

Ishii, N., Wadsworth, W. G., Stern, B. D., Culotti, J. G. and Hedgecock, E. M. 1992. UNC-6, a laminin-related protein, guides cell and pioneer axon migrations in *C. elegans*. Neuron **9**: 873-881.

Jessell, T. M. (1988). Adhesion molecules and the hierarchy of neural development. Neuron **1**: 3-13.

Karlstrom, R. O., Trowe, T., Klosterman, S., Baier, H., *et al.* (1996). Zebrafish mutations affecting retinotectal axon pathfinding. Development **123**: 427-438.

Kater, S. B. and Mills, L. R. (1991). Regulation of growth cone behavior by calcium. J. Neurosci. **11**: 891-899.

Keino-Masu, K., Masu, M., Hink, L., Leonardo, E. D., Chan, S. S. Y., Culotti, G. and Tessier-Lavigne, M. (1996). Deleted in colorectal cancer (DCC) encodes a netrin receptor. Cell **87**: 175-185.

Keller, A. D. and Maniatis, T. (1992). Only two of the five zinc fingers of the eukaryotic transcriptional repressor PRD1-BF1 are required for sequence-specific DNA binding. Mol. Cell. Biol. **12**: 1940-1949.

Kennedy, T. E., Serafini, T., de la Torre, J. R. and Tessier-Lavigne, M. (1994). Netrins are diffusible chemotrophic factors for commissural axons in the embryonic spinal cord. Cell **78**: 425-435.

Keynes, R. and Stern, C. (1984). Segmentation in the vertebrate nervous system. Nature **310**: 786-789.

Keynes, R. J., Jaques, K. F. and Cook, G. M.W. (1991). Axon repulsion during peripheral nerve segmentation. Development(suppl.) **2**: 131-139.

Keynes, R. J. and Cook, G. M. W. (1995). Axon guidance molecules. Cell **83**: 161-169.

Klose, M. and Bentley, D. (1989). Transient pioneer neurons are essential for formation of an embryonic peripheral nerve. Science **245**: 982-984.

Kolodkin, A. L., Matthes, D. J., O'Conner, T. P., Patel, N. H., Admon, A., Bentley, D. and Goodman, C. S. (1992). Fasciclin IV: sequence, expression and function during growth cone guidance in the grasshopper embryo. Neuron **9**: 831-845.

Klambt, C., Jacobs, J. R. and Goodman, C. S. (1991). The midline of the *Drosophila* central nervous system: a model for the genetic analysis of cell fate, cell migration, and growth cone guidance. Cell **64**: 801-815.

Kolodkin, A. L., Matthes, D. J. and Goodman, C. S. 1993. The semaphorin genes encode a family of transmembrane and secreted growth cone guidance molecules. Cell **75**: 1389-1399.

Krishnan, S. N., Frei, E., Swain, G. P. and Wyman, R. J. (1993). *Passover*: a gene required for synaptic connectivity in the giant fibre system of *Drosophila*. Cell **73**: 967-977.

Kunes, S., Wilson, C. and Steller, H. (1993). Independent guidance of retinal axons in the developing visual system of *Drosophila*. J. Neurosci. **13**: 752-767.

Kuwada, J. Y. 1995. Development of the zebrafish nervous system: genetic analysis and manipulation. Curr. Opin. neurobiol. 5: 50-54.

Lance-Jones, C. and Landmesser, L. (1981). Pathway selection by embryonic chick motoneurons in an experimentally altered environment. Proc. R. Soc. Lon. (Biol.) **214**: 19-52.

Lance-Jones, C. and Dias, M. (1991). The influence of presumptive limb connective tissue on motoneuron axon guidance. Dev. Biol. **143**: 93-110.

Landmesser, L., Dahm, L., Schultz, K. and Rutishauser, U. (1988). Distinct roles for adhesion molecules during innervation of embryonic chick muscle. Dev. Biol. **130**: 645-670.

Lee, K. J., Freeman, M. amd Steller, H. (1991). Expression of the *disconnected* gene during development of *Drosophila melanogaster*. EMBO J. **10**: 817-826.

Letourneau, P. C. (1975). Cell-to-substrate adhesion and guidance of axonal elongation. Dev. Biol. **44**: 92-101.

Logan, C., Wizenmann, A., Drescher, U., Monschou, B., Bonhoeffer, F. and Lumsden, A. (1996). Rostral optic tectum acquires caudal characteristics following ectopic Engrailed expression. Curr. Biol. **6**: 1006-1014.

Lundgren, S. E., Callahan, C. A., Thor, S. and Thomas, J. B. (1995). Control of neuronal pathway selection by the *Drosophila* LIM homeodomain gene *apterous*. Development **121**: 1769-1773.

Luo, Y., Raible, D. and Raper, J. A. (1993). Collapsin: a protein in brain that induces the collapse and paralysis of neuronal growth cones. Cell **75**: 217-227.

Luo, Y. and Raper, J. A. (1994). Inhibitory factors controlling growth cone motility and guidance. Curr. Opin. Neurobiol. **4**: 648-654.

Martin, K. A., Poeck, B., Roth, H., Ebens, A. J., Balard, L. and Zipursky, S. L. (1995). Mutations disrupting neuronal connectivity in the *Drosophila* visual system. Neuron **14**: 229-240.

Mastick, G. S., Davis, N. M., Andrews, G. L. and Easter, Jr. S. S. (1997). *Pax-6* functions in boundary formation and axon guidance in the embryonic mouse forebrain. Development **124**: 1985-1997.

Matthes, D. J., Sink, H., Kolodkin, A. K. and Goodman, C. S. (1995). Semaphorin II can function as a selective inhibitor of specific synaptic arborizations. Cell **81**: 631-539.

McConnell, S. K., Ghosh, A. and Schatz, C. J. (1989). Subplate neurons pioneer the first axon pathway from the cerebral cortex. Science **245**: 978-982.

McFarlane, S., McNeill, L. and Holt, C. E. (1995). FGF signaling and target recognition in the developing *Xenopus* visual system. Neuron **15**: 1017-1028.
Meinertzhagen, I. A. 1973. Development of the compound eye and optic lobe of insects. In Developmental Neurobiology of Arthropods. D. Young, eds. (Cambridge University Press), pp. 51-104.

Meinertzhagen, I. A. and Hanson, T. E. (1993). " The development of the optic lobe". In The Development of Drosophila melanogaster. (ed. Bate, M. and Aries, A. M.) pp: 1363. Cold Spring Harbor, NY.

Mullins, M. C., et al (1994). Large-scale mutagenesis in the zebrafish: in search of genes controlling development in a vertebrate. Curr. Biol. **4**: 189-202.

Mukhopadhyay, G., Doherty, P, Walsh, F. S., Crocker, P. R. and Filbin, M. T. (1994). A novel role for myelin-associated glycoprotein as an inhibitor of axonal regeneration. Neuron **13** 757-767.

Nobes, C. D. and Hall, A. (1995). Rho, Rac and Cdc-42 GTPases regulate the assembly of multimolecular focal complexes associated with actin stress fibres, lamellipodia and filopodia. Cell **81**: 53-62.

Nose, A., Mahajan, V. B. and Goodman, C. S. (1992). Connectin: a homophilic cell adhesion molecule expressed on a subset of muscles and the motoneurons that innervate them in *Drosophila*. Cell **70**: 553-567.

Nose, A., Takeichi, M. and Goodman, C. S. (1994). Ectopic expression of connectin reveals a repulsive function during growth cone guidance and synapse formation. Neuron **13**: 525-539.

Nusslein-Volhard, C. and Wieschaus, E. (1980). Mutations affecting segment number and polarity in *Drosophila*. Nature **287**: 795-801.

Oakley, R. A. and Tosney, K. 1993. Contact-mediated mechanisms of motor axon segmentation. J. Neurosci. **13**: 3773-3792.

Phillis, R. W., Bramlage, A. T., Wotus, C., Whittaker, A., Gramates, S., et al. (1993). Isolation of mutations affecting neural circuitry required for grooming behavior in *Drosophila melanogaster*. Genetics **133**: 581-592.

Placzek, M., Tessier-Lavigne, M., Jessell, T., Dodd, J. (1990). Orientation of commissural axons *in vitro* in response to a floor plate-derived chemoattractant. Development **110**: 19-30.

Raper, J. A., Bastiani, M. J. and Goodman, C. S. (1984). Pathfinding by neuronal growth cones in grasshopper embryos. IV. The effects of ablating the A and P axons upon the behavior of the G growth cone. J. Neurosci. **4**: 2329-2345.

Ready, D. F., Hanson, T. E. and Benzer, S. (1976). Development of the *Drosophila* retina, a neurocrystalline lattice. Dev. Biol. **53**: 217-240.

Retaux, S, and Harris, W. A. (1996). Engrailed and retinotectal topography. Trends Neurosci. **19**: 542-546.

Riehl, R., Johnson, K., Bradley, R., Grunwald, G. B., Coronel, E., Lilienbaum, A. and Holt, C. E. (1996). Cadherin function is required for axon outgrowth in retinal ganglion cells *in vivo*. Neuron **17**: 837-848.

Schmucker, D., Taubert, H. and Jackle, H. (1992). Formation of the *Drosophila* larval photoreceptor organ and its neuronal differentiation require continuous *kruppel* gene activity. Neuron **9**: 1025-1039.

Seeger, M., Tear, G., Ferres-Marco, D. and Goodman, C. S. (1993). Mutations affecting growth cone guidance in *Drosophila*: genes necessary for guidance towards or away from the midline. Neuron **10**: 409-426.

Serafini, T., Kenneddy, T. E., Galko, M. J., Mirzayan, C., Jessell, T. M. and Tessier-Lavigne, M. (1994). The netrins define a family of axon outgrowth-promoting proteins homologous to *C. elegans* UNC-6. Cell **78**: 409-424.

Silver, J., Lorenz, S. E., Wahlstein, D. and Coughlin, J. (1982). Axonal guidance during development of the great cerebral commissures: descriptive and experimental studies *in vivo* on the role of preformed glial pathways. J. Comp. Neurology **210**: 10-29.

Simon, M. A., Bowtell, D. D., Dodson, G. S., Laverty, T. R. and Rubin, G. M. (1991). Ras1 and a putative guanine nucleotide exchange factor perform crucial steps in signaling by the sevenless tyrosine protein kinase. Cell **67**: 701-716.

Singer, M., Nordlander, R. H. and Egar, M. (1979). Axonal guidance during embryogenesis and regeneration in the spinal cord of the newt: the blueprint hypothesis of neuronal pathway patterning. J. Comp. Neurology **185**: 1-22.

Sperry, R. W. (1963). Chemoaffinity in the orderly growth of nerve fibre patterns and connections. Proc. Natl. Acad. Sci. USA **50**: 703-710.

Starich, T. A., Herman, R. K. and Shaw, J. E. (1993). Molecular and genetic analysis of *unc-7*, a *Caenorhabditis elegans* gene required for coordinated locomotion. Genetics **133**: 527-541.

Steller, H., Fischbach, K. F. and Rubin, G. M. (1987). *disconnected*: A locus required for neuronal pathway formation in visual system of *Drosophila*. Cell **50**: 1139-1153.

Stoeckli, E. T. and Landmesser, L. (1995). Axonin-1, Nr-CAM and Ng-CAM play different roles in the *in vivo* guidance of chick commissural neurons. Neuron **14**: 1165-1179.

Takeichi, M. (1991). Cadherin cell adhesion receptors as a morphogenetic regulator. Science **251**: 1451-1455.

Tang, J., Landmesser, L. and Rutishauser, U. (1992). Polysialic acid influences speciffic pathfinding by avian motoneurons. Neuron **8**: 1031-1044.

Tang, J., Rutishauser, U. and Landmesser, L. (1994). Polysialic acid regulates growth cone behavior during sorting of motoneurons in the plexus region. Neuron **13**: 405-414.

Tessier-Lavigne, M., Placzek, M., Lumsden, A. G. S., Dodd, J., and Jessell, T. M. (1988). Chemotrophic guidance of developing axons in the mammalian CNS. Nature **336**: 775-778.

Tessier-Lavigne, M. (1992). Axon guidance by molecular gradients. Curr. Opin. Neurobiol. **2**: 60-65.

Tessier-Lavigne, M. (1995). Eph receptor tyrosine kinases, axon repulsion and the development of topographic maps. Cell **82**: 345-348.

Tessier-Lavigne, M. and Goodman, C. S. (1996). The molecular biology of axon guidance. Science **274**: 1123-1133.

Thomas, J. B. and Wyman, R. J. 1984. Mutations altering synaptic connectivity between identified neurons in *Drosophila*. J. Neurosci. **4**: 530-538.

Tix, S., Minden, J. S. and Technau, G. M. (1989). Pre-existing neuronal pathways in the developing optic lobes of *Drosophila*. Development **105**: 739-746.

Tokumoto, M., Gong, Z., Tsubokawa, T., Hew, C. L., Uyemura, K., Hotta, Y. and Okamoto, H. (1995). Molecular heterogeneity among primary motoneurons and within myotomes revealed by the differential mRNA expression of novel islet-1 homologs in embryonic zebrafish. Dev. Biol. **171**: 579-589.

Tosney, K. W. and Landmesser, L. T. (1984). Pattern and specificity of axonal outgrowth following varying degrees of chick lib bud ablation. J. Neurosci. **4**: 2518-2527.

Tsuchida, T., Ensini, M., Morton, S. B., Baldassare, M., Edlund, T., Jessell, T. M. and Pfaff, S. L. (1994). Topographic organization of embryonic motor neurons defined by expression of LIM homeobox genes. Cell **79**: 957-970.

Trowe, T., Klostermann, S., Baier, H., Haffter, P., and Nusslein-Volhard, C. (1996). Mutations disrupting the ordering and topographic mapping of axons in the retinotectal projection of the zebrafish, *Danio rerio*. Development **123**: 439-450.

VanBerkum, M. F. A. and Goodman, C. S. (1995). Targeted disruption of calcium-calmodulin signaling in *Drosophila* growth cones leads to stalls in axon extension and errors in axon guidance. Neuron **14**: 43-56.

VanVactor, D., Sink, H., Fambrough, D., Tsoo, R. and Goodman, C. S. (1993). Genes that control neuromuscular specificity in *Drosophila*. Cell **73**: 1137-1153.

Varela-Echavarria, A., Tucker, A., Puschel, A. W. and Guthrie, S. (1997). Motor axon subpopulations respond differentially to the chemorepellents netrin-1 and semaphorin D. Neuron **18**: 193-207.

Vaughan, L., Weber, P., D'Alessandri, L., Zisch, A. H. and Winterhalter, K. H. (1994). Tenascin-contactin/F11 interactions: a clue for a developmental role. Prespect. Dev. Neurobiol. **2**: 43-52.

Walsh, F. S. and Doherty, P. (1997). Neural cell adhesion molecules of the immunoglobulin superfamily: role in axon growth and guidance. Ann. Rev. Cell Dev. Biol. **13**: 425-456.

Wehrle, B. and Chiquet, M. (1990). Tenascin is accumulated along developing peripheral nerves and allows neurite outgrowth in vitro. Development **110**: 401-415.

White, K. and Kankel, D. R. (1978). Patterns of cell division and cell movement in the formation of the imaginal nervous system in *Drosophila melanogaster*. Dev. Biol. **65**: 296-321.

Wilson, C., Pearson, R. K., Bellen, H. J., O'Kane, C. -J., Grosniklaus, U. and Gehring, W. J. (1989). P-element-mediated enhancer detection: an efficient

method for isolating and characterizing developmentally regulated genes in *Drosophila*. Genes. Dev. **3**: 1301-1313.

Wolff, T. and Ready, D. F. (1993). Pattern formation in the *Drosophila* retina. In *"The Development of Drosophila melanogaster"* (M. Bate and A. M. Arias, Eds), pp. 1277-1325. Cold Spring Harbor Laboratory, Cold Spring Harbor, NY.

Xu, Q., Alldus, G., Macdonald, R., Wilkinson, D. J. and Holder, N. (1996). Function of Eph-related kinase rtk1 in patterning of the zebrafish forebrain. Nature **381**: 319-327.

Zipursky, S. L., Venkatesh, T. R, Teplow, D. B. and Benzer, S. (1984). Neuronal development in the *Drosophila* retina: monoclonal antibodies as molecular probes. Cell **36**: 15-26.

Chapter 2: Manucsript

THE LARVAL OPTIC NERVE IS REQUIRED FOR THE DEVELOPMENT OF AN IDENTIFIED SEROTONERGIC ARBORIZATION IN *DROSOPHILA MELANOGASTER.*

Preface

The work presented in this chapter has been published in Developmental Biology, 1995, vol. **169**. p629-643.

DEVELOPMENTAL BIOLOGY 169, 629–643 (1995)

The Larval Optic Nerve Is Required for the Development of an Identified Serotonergic Arborization in *Drosophila melanogaster*

MAHUA MUKHOPADHYAY AND ANA REGINA CAMPOS[1]

Department of Biology, McMaster University, 1280 Main st West, Hamilton, Ontario, Canada, L8S 4K1

Accepted February 22, 1995

The larval visual system in the fruitfly *Drosophila melanogaster* consists of two bilateral clusters of 12 photoreceptor cells. These neurons send their axons in a fascicle, the Bolwig's nerve, toward the target area in the ventral lateral region of the brain hemispheres. We describe the development of a serotonergic arborization originating in the central brain found in the larval optic center in association with the larval optic nerve. This arborization is formed by processes from larval neurons born during embryogenesis. However, these neuronal processes do not reach their final destination, the larval optic center, until late in larval development. Using mutations that disrupt the connectivity and/or development of the larval photoreceptor cells, as well as mosaic analysis, we demonstrate that the innervation of the larval optic center by this serotonergic arborization depends upon contact with the larval optic nerve.

INTRODUCTION

A fundamental aspect of nervous system development is the precise interconnection between different cell types. That precise assembly of a complex network depends not only on the matching of pre- and postsynaptic cell populations but also on the development and maintenance of the appropriate axonal and dendritic arborizations.

The dependence for development and maintenance of neuronal arbors on connections with other neurons is well documented in several different model systems (e.g., Loer and Kristan, 1989; Antonini and Stryker, 1993; Byrd and Burd, 1993). While several molecules required for axonal guidance have been described (reviewed by Goodman and Shatz, 1993), comparatively little is known about the nature of the intercellular signals required for the local induction and maintenance of dendritic and axonal arbors.

[1] To whom correspondence should be addressed. E-mail: camposa@mcmail.cis.mcmaster.ca.

The role of activity of afferent synaptic inputs in the development and remodeling of dendritic arbors has been extensively examined. Neurotransmitters contained in afferent innervation have been shown to regulate dendritic growth (reviewed in Schwartz, 1992). Several reports demonstrate that patterned afferent excitatory activity results in structural changes of the corresponding dendritic arbors (Tieman and Hirsch, 1982 and Katz and Constantine-Paton, 1988). Activation of *N*-methyl-D-aspartate subtype of glutamate receptors is involved in motor neuron dendritic maturation in early postnatal life (Kalb, 1994). Endogeneous electrical activity has also been shown to influence dendritic growth patterns in Purkinje cells in primary dissociated cultures of mouse cerebellum (Schilling *et al.*, 1991).

Cell interactions are also likely to play a role in the development of neuronal arbors. Regulation of axonal and dendritic growth by glial cells has been demonstrated by a variety of coculture experiments (Prochiantz *et al.*, 1990; Rousselet *et al.*, 1990; and Qian *et al.*, 1992). Recently, it has been suggested that glia-mediated dendritic growth is promoted by a diffusible factor (Le Roux and Reh, 1994). Beyond its role in the control of cell number, NGF has also been shown to influence the degree of axonal branching locally both *in vivo* and *in vitro* (Campenot, 1982a; Campenot, 1982b; De Konnick *et al.*, 1993; Van der Zee *et al.*, 1995).

The visual system of the holometabolous insect *Drosophila melanogaster* has been successfully used as a model system for the study of cell interactions during development. *Drosophila* displays two visual systems during its life cycle; the adult and the larval visual system. The adult visual system consists of compound eyes containing photoreceptor neurons that project to the underlying optic lobes (reviewed by Wolff and Ready, 1993, and Meinertzhagen and Hanson, 1993). The larval visual system is considerably less complex, consisting of two bilateral clusters of 12 photoreceptor cells which send their axons in a fascicle (The Bolwig's nerve, Bolwig, 1946) toward the larval visual system target area located within the anlagen of the adult optic lobes

0012-1606/95 $6.00

(Steller *et al.*, 1987; Green *et al.*, 1993; Campos *et al.*, 1995).

Cell interactions have been shown to play a fundamental role in the development of the adult visual system in the fruitfly *Drosophila melanogaster* (reviewed by Meinertzhagen and Hanson, 1993, and Wolff and Ready, 1993). This assertion is well exemplified by reports on the dependence of adult optic lobes on afferent innervation (reviewed by Meinertzhagen and Hanson, 1993, and Power, 1943; Meyerowitz and Kankel, 1978; Fischbach, 1983; Fischbach and Technau, 1984; Hofbauer and Campos-Ortega, 1990; Selleck and Steller, 1991). In particular, the first optic ganglion, the lamina, requires retinal innervation not only for mitosis of the lamina precursor cells but also for proper morphogenesis of the lamina cartridges (Meyerowitz and Kankel, 1978, and Selleck and Steller, 1991). The dependence of the second order neurons in the medulla ganglion upon retinal innervation is less extensive than that found in the lamina ganglion. Several optic lobe neurons are able to survive deafferentation, although they display sprouting and compensatory innervation (Fischbach, 1983; Fischbach and Technau, 1984).

The larval optic nerve is apparently not required for the establishment of the optic stalk nor for the targeting of the retinal projections to the developing optic lobes, the OLPs (Moses *et al.*, 1989; Kunes and Steller, 1991). The connectivity of the larval optic nerve to the optic lobe anlagen, however, may depend upon the presence of the optic lobe pioneer cells (Tix *et al.*, 1989; Campos *et al.*, 1995). The differentiation of OLPs precedes the final step in the establishment of connectivity of the larval optic nerve to the optic lobe primordium and is apparently not dependent upon contact with the larval optic nerve (Campos *et al.*, 1995).

A role for the larval optic nerve in the development of adult optic lobe projections is suggested by the observation that certain identified neurons which project from the central brain toward the lamina (the LBO 5-HT, Nassel, 1987) follow the same pathway pioneered by the larval optic nerve during larval stages. The projections from these serotonergic cells as well as the OLPs occupy the posterior optic tract which contains axons of the lamina and medulla tangential cells (reviewed in Meinertzhagen and Hanson, 1993). Additionally, it is possible that larval retinal innervation is required for the development of the larval visual system target cells, similar to what is observed in the adult visual system. These target cells may in turn be incorporated into the developing adult optic lobes and there participate in the organization of the optic lobes during development.

Here, we report the consequences of deafferentation of the larval optic center. We focus our analysis on the development of an identified serotonergic arborization that projects from the central brain. Using mutant strains that impair the connectivity of the larval optic nerve to the larval neuropil center as well as mosaic analysis, we conclude that neither the cell viability nor the initial outgrowth of this projection depends on the presence of the larval optic nerve. However, the arborization of this projection within the larval optic neuropil requires the presence of the larval optic nerve. Interestingly, this serotonergic process does not contact the larval optic nerve until late in larval development.

MATERIALS AND METHODS

Drosophila Strains and Culture

Flies were grown at 25°C or 19°C in inactivated yeast, sucrose, and agar medium supplemented with fresh active yeast. Ten percent tegosept in ethanol was used to prevent microbial growth. Eggs were collected on molasses-agar egg-collection plates and aged as described by Ashburner (1989).

gl^{esj}. Null mutant allele of the *glass* (*gl*) gene. Expression of the *glass* gene is disrupted by an insertion (>30 kb) in the coding region (Moses *et al.*, 1989).

$disco^{1}$. Ethyl methanesulfonate-induced allele of *disconnected* (*disco*) gene (Fischbach and Heisenberg, 1984). In *$disco^{1}$* a point mutation (cys127 to ser) in the coding region of the *disco* gene resulted in a missense mutation (Heilig *et al.*, 1991). In this mutant, the larval optic nerve cannot establish proper connections with its target cells during embryonic development (Steller *et al.*, 1987).

P[gl^{+}(10 kb Sal), *ry^{+}*]; *gl^{esj}*. The third chromosome is homozygous for the *gl^{esj}* mutation, while the first chromosome is homozygous for a P-element insert carrying a normal *glass* gene and a wild-type *rosy* gene (Moses *et al.*, 1989).

Delta 2-3, gl^{esj}. The third chromosome is homozygous for the *gl^{esj}* mutation and carries the gene for a transposase enzyme which can mobilize P-element inserts. However, the transposable element that carries the transposase gene is stable in this position (Laski *et al.*, 1986; Robertson *et al.*, 1988).

C50.1S1. A *disco*-enhancer trap line, in which expression of a *β-galactosidase* gene is driven by the *disco* promoter. Thus, *β-galactosidase* expression is localized to the *disco* expressing cells and acts as a marker for *disco* expression (Cohen *et al.*, 1991; Heilig *et al.*, 1991, and Lee *et al.*, 1991).

Immunocytochemistry of Larval Brain

Larval brains of different larval stages were dissected in *Drosophila* Ringer's solution and fixed in 4% paraformaldehyde (pH 7.4) for 4 hr or overnight at 4°C.

Fixed brains were washed several times in 0.1 *M* phosphate buffer containing 0.3% Triton X-100 (PBT) and blocked with PBT containing 5% goat serum for an hour at room temperature. Incubation with primary antibody (monoclonal or polyclonal) diluted with PBT containing 5% goat serum was performed overnight at 4°C. After several washes with PBT for 2 hr at room temperature the brains were again blocked with PBT + goat serum and then incubated with secondary antibody for 5 hr at room temperature. This was followed by washing the samples several times in PBT for 2 hr. Enzymatic reactions were carried out for Horseradish peroxidase-conjugated secondary antibodies using diaminobenzidene and hydrogen peroxide as described by Steller *et al.* (1987). In some cases 2.5 m*M* $CoCl_2$ was used to intensify the signal. For fluorescence-tagged secondary antibodies brains were mounted in 70% glycerol containing *p*-phenylenediamine.

The primary antibodies used were rat monoclonal anti-serotonin, clone YC5/45 (Consolazione *et al.*, 1981), a mouse monoclonal anti-CHAOPTIN (24B10, Zipursky *et al.*, 1984), and a mouse monoclonal anti-GLASS (Ellis *et al.*, 1993). The secondary antibodies used were Cy3-conjugated goat anti-rat IgG (Jackson ImmunoResearch Laboratories, Inc.), FITC-conjugated goat anti-mouse IgG (Cappel), and Peroxidase-conjugated goat anti-mouse IgG (Jackson ImmunoResearch Laboratories, Inc.).

The specimens were viewed under Nomarski optics in a Zeiss Axioscope. Confocal microscopy was performed on a Bio-Rad MRC 600 Krypton/Argon laser confocal microscope.

Generation of glass Somatic Mosaics

gl mosaics were created using the same scheme as described by Kunes *et al.* (1993). Somatic loss of a gl^{+} P-element (Moses *et al.*, 1989) in a strain carrying a null mutation in the *gl* gene was induced by somatic expression of the Delta 2-3 transposase (Laski *et al.*, 1986; Robertson *et al.*, 1988). Females homozygous for the null allele gl^{60j} and carrying a wild type *glass* gene in a transposable element inserted in the X chromosome (P[gl^{+}(10 kb Sal), *ry*]; Moses *et al.*, 1989) were crossed to males P[*ry*+, Delta 2-3], gl^{60j}. In the progeny of this cross the constitutive source of the transposase mobilized the P-element carrying the normal *glass* gene in some somatic cells, thereby uncovering the gl^{60j} mutation. Cells which retained the P-element remained wild-type. Excision occurs in 100% of the cases as seen by the presence of mosaic compound eyes in all adult flies.

RESULTS

Serotonin Immunoreactive Processes Are Found Innervating the Larval Optic Neuropil

Little is known about the influence of the larval photoreceptor innervation on the development of the larval visual system neuropil. In this investigation we sought to address this question by examining a newly identified arborization found in intimate association with the termini of the larval photoreceptor axons in the larval visual neuropil of the third instar larvae (Fig. 1). This serotonergic arborization is found in the third instar larval brain, apparently associated with the larval photoreceptor axons (Fig. 1C–1E). It can be easily and reproducibly identified in larval brain whole-mount preparations. It is the only serotonergic process found in the larval optic lobes at this point in development. Additionally it emerges at the same level where the LP1 axons enter the central brain. The LP1 cell bodies are located in a midlateral position at the margin of the optic lobes and can therefore be used as a landmark for the identification of the larval optic center serotonergic innervation (Fig. 1C, empty arrow). Brains from late third instar wandering larvae showed, in addition to the larval optic center serotonergic projection, fibers from the

FIG. 1. Localization of the 5-HT immunoreactive arborization in the third instar larval brain. All photomicrographs depict a horizontal view of the larval brain. (A) A line drawing of a third instar larval brain showing 5-HT immunoreactive neurons and their projections. There are four prominent serotonergic cell clusters in the brain; SP1, SP2, LP1, and IP (Valles and White, 1988). The 5-HT arborization in the larval optic center (arrowhead) is formed by one or two cells of the SP2 cluster. The SP2 cell cluster is located just posterior to the anterior-most cell cluster SP1 and is composed of four cells. It is also the dorsal-most cluster. The LP1 cell cluster is composed of two cells that occupy a midlateral position in the brain. In a horizontal or frontal view of the larval brain the processes of the LP1 cells always cross the arborization forming neuronal processes (arrow) hardly seen under conventional microscopy. The box represents the area of interest depicted in all subsequent figures. (B) A third instar larval brain hemisphere double-labeled with the anti-CHAOPTIN antibody (black/brown) to visualize the photoreceptor axons and an anti-5-HT antibody (brown) seen under Nomarsky optics. The larval optic nerve which traverses the eye disc (ed) and the optic stalk (os) can be seen terminating (open arrow) in the developing optic lobe (ol). The solid arrow points to the thin neuronal process that forms the 5-HT arborization in the larval optic center, shown in A inside the boxed area (solid arrowhead). (C, D, and E) Confocal micrographs of a third instar larval brain double-labeled with anti-5-HT (rhodamine channel seen in red in C and E) and with anti-CHAOPTIN (FITC channel seen in green in D and E) antibodies. (E) Merge of C and D. The 5-HT arborization (arrowhead in C) can be seen overlapping with the LON (arrow in D) in E. The LP1 cluster (empty arrow in C) axons cross the serotonergic processes that arborize in the larval optic neuropil. Scale bar in B, 50 μm and in C, D, and E, 25 μm.

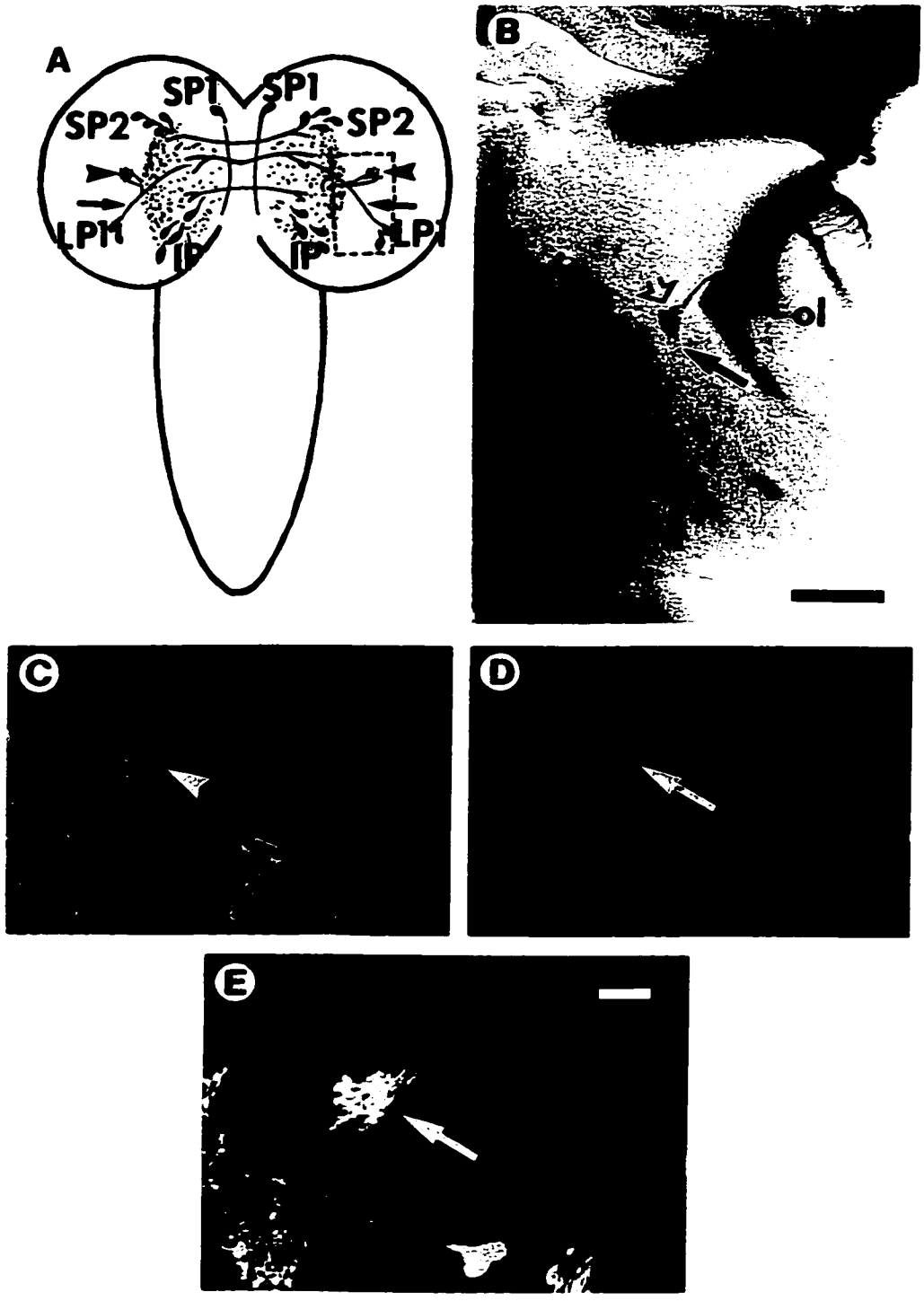
A
SP1
SP1
SP2
SP2
LP1
LP1
B
C
D
E

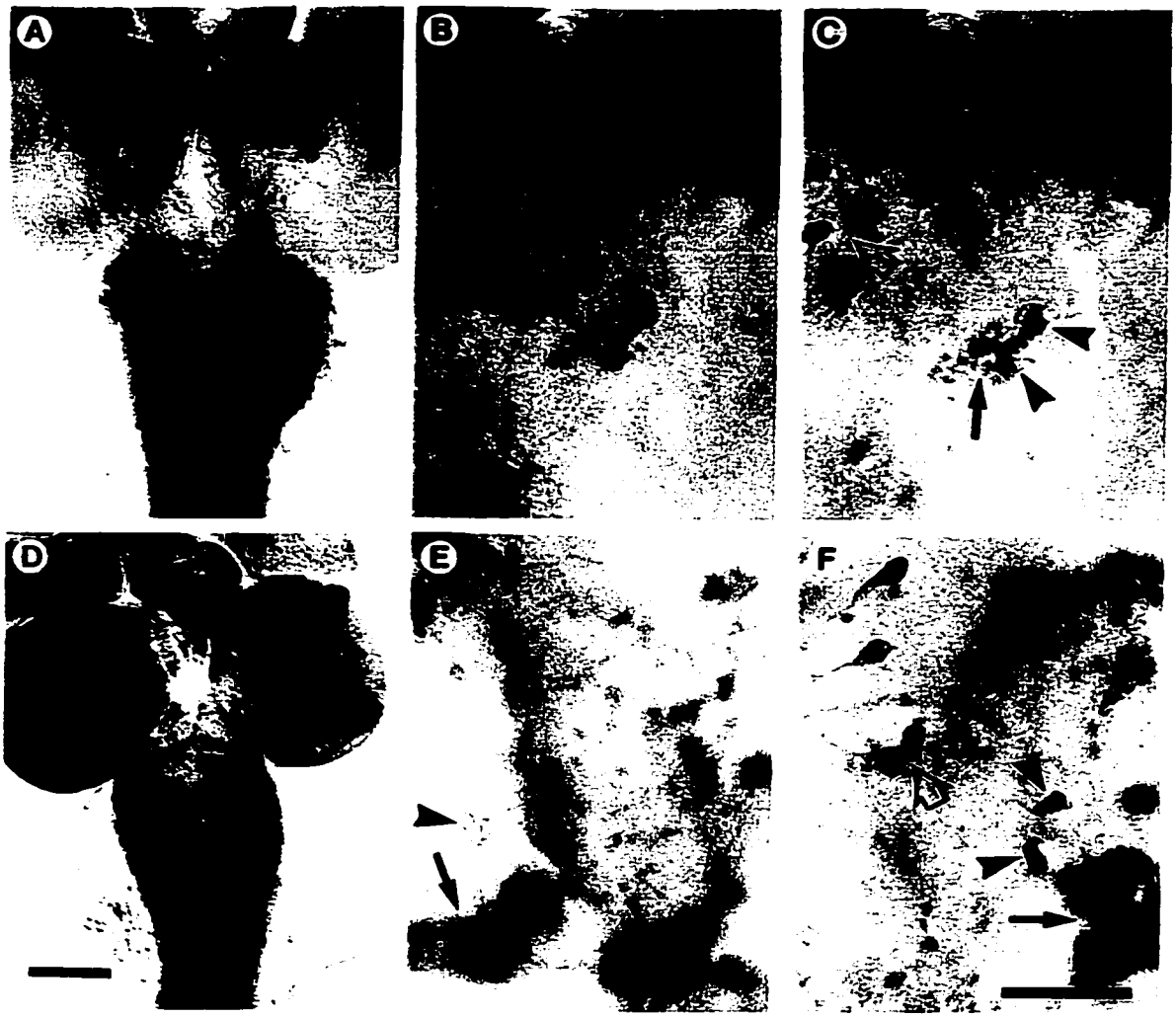

FIG. 4. Expression of the *glass* and the *disco* genes relative to 5-HT expression. (A) Third instar larval brain double-labeled with anti-GLASS (blue-black) and anti-5-HT (brown) antibodies (horizontal view where anterior is up in all panels). (B) Right brain hemisphere of the brain shown in A at higher magnification. The anterior *glass* cell cluster (arrow) is in focus. (C) Same brain hemisphere as in B at a different focal plane. The posterior *glass* cell cluster (arrow) is in focus. The 5-HT expressing LP1 cells (arrowheads) lie very close to the posterior *glass* cell cluster; however, there is no overlap of the two patterns of expression. The SP2 cluster which is involved in the formation of the 5-HT arborization at the larval optic center is shown by an empty arrow. (D) Third instar larval CNS of a *disco*-enhancer trap strain double-labeled with anti-β-galactosidase antibody for the detection of the *disco* gene expression (blue-black) and anti-5-HT antibody (brown). (E) Left brain hemisphere of the CNS shown in D. The *disco* gene is expressed in several scattered cells and in a band of cells (arrow) that wraps around the brain lobe. The 5-HT arborization (arrowhead) at the larval optic center can be seen. (F) Right brain hemisphere of the CNS shown in D. The two 5-HT-expressing LP1 cells (arrowheads) lie very close to the band of *disco*-expressing cells (arrow). However, there is no overlap between *disco* and 5-HT expression. The SP2 cell cluster is surrounded by faint *disco*-expressing cells (empty arrow). Scale bar in A and D, 100 μm. Scale bar in B, C, E, and F, 50 μm.

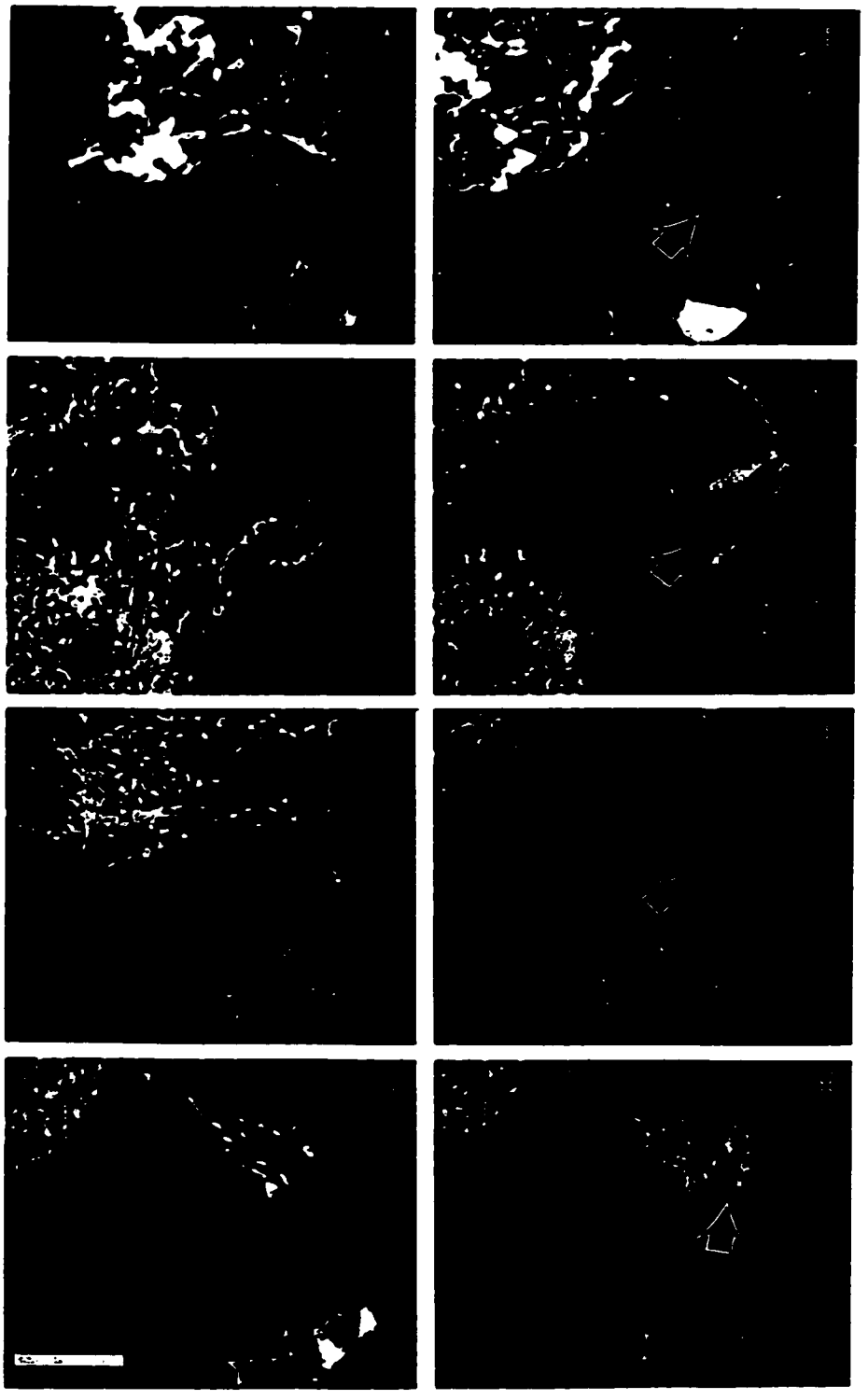

LBO 5-HT neurons described in more detail in the Fleshfly (Nassel *et al.*, 1987) (data not shown).

Observations in earlier stages of larval development (see below) suggest that this arborization is formed by two neuronal processes. However, the level of resolution conferred by the confocal microscope does not allow us to determine if the 5-HT processes innervating the larval optic neuropil in the third instar larval brain correspond to two axons only or to assess the ultra structural nature of the interaction between the larval optic nerve (LON) and the 5-HT arborization. Our observations in whole-mount preparations suggest that this projection is formed by axons of the contralateral SP2 cell cluster located in the central brain dorsal rind, posterior to the SP1 cell (nomenclature according to Valles and White, 1988) (data not shown). Similar processes were also described in the Fleshfly by Nassel *et al.* (1987).

Development of the 5-HT Innervation of the Larval Optic Center

In order to determine the time course of the development of the 5-HT innervation of the larval optic neuropil, double labeling of dissected brains from different larval stages with anti-5-HT antibody and with anti-CHAOPTIN antibody was performed.

5-HT neuronal processes whose position is consistent with those that are later found innervating the larval optic neuropil were first visualized during mid first instar larval stage (Fig. 2A, solid arrow). At this time, only a single neuronal process is seen extending toward the larval optic center. During late first instar larval stage a second neuronal process was often seen joining the first one (Fig. 2C, solid arrow). These processes started branching during early second instar larval stage (Fig. 2E, solid arrow). Up to this time the terminus of the LON can be seen lying ventral to the very tip of the 5-HT projections (Figs. 2B, 2D, and 2F, empty arrow). It was during late second instar larval stage that the 5-HT processes were first seen on the same focal plane of the LON, apparently contacting each other (Figs. 2G and 2H, solid arrow and empty arrow, respectively). These 5-HT processes undergo further branching after the first contact with the LON up to the level seen in the middle third instar stage (Fig. 1C, arrowhead).

Absence of the 5-HT Arborization in Mutants Lacking LON Connection with the Larval Optic Center

In order to determine whether the development of the larval neuropil 5-HT arborization is dependent upon contact with the larval photoreceptor axons, we examined visual system mutants in which the connection of the LON to the target area was either absent or impaired. For this, we chose to examine larval brains of strains carrying mutations in either the *glass* (*gl*) gene or in the *disconnected* (*disco*) gene. In larvae homozygous for the null *glass* gene allele gl^{ea}, only a few loosely clustered photoreceptor cells can be seen without formation of a LON (Moses *et al.*, 1989; Schmucker *et al.*, 1992; Campos *et al.*, 1995). Mutations in the *disco* gene prevent the proper connection of the LON with its target area during embryonic development. In most cases the optic stalk which connects the larval brain to the anlagen of the adult eye is absent in *disco* mutants and the LON does not enter the larval brain (unconnected phenotype, Steller *et al.*, 1987). A few of the *disco* mutant larvae carry normal optic stalk and the LON can be seen projecting to the brain. However, in these animals the LON is still unable to establish proper connections with the target area and is often found in abnormal locations (the connected phenotype, Steller *et al.*, 1987; Campos *et al.*, 1995).

In gl^{ea} mutant larvae no 5-HT immunoreactivity re-

FIG. 2. Development of the larval optic neuropil 5-HT arborization. Dissected larval brains from various developmental stages were double-labeled with anti-5-HT and anti-CHAOPTIN. All confocal micrographs show the boxed area depicted in Fig. 1A. For the efficient visualization of the serotonergic arborization a CY3-conjugated secondary antibody was used while *chaoptin* expression was visualized with a FITC-conjugate secondary antibody. The CY3 fluorochrome provides a much stronger signal than the rhodamine fluorochrome (seen through the rhodamine channel) but it has the disadvantage of substantial bleeding into the FITC channel. Thus images obtained in the FITC channel include both 5-HT and *chaoptin* expression. (A) Mid first instar larval brain (rhodamine channel). Only one neuronal process (arrow) can be seen extending towards the larval optic center. At this focal plane only one LP1 cell and part of the second LP1 cell can be seen (arrowhead). (B) Same specimen as in A (FITC channel) seen at a different focal plane, showing the LON (empty arrow) and the second LP1 cell (arrowhead). At this stage in larval development the 5-HT processes and the LON terminus are located in different levels of the brain. (C) Late first instar larval brain (rhodamine channel). Two separate 5-HT processes are visible directed towards the larval optic neuropil (arrow). (D) Same specimen as in C (FITC channel) but at a different focal plane, showing the LON (empty arrow) and the LP1 cluster (arrowhead). There is no overlap between the 5-HT processes and the LON terminus at this stage in larval development. (E) Early second instar larval brain (rhodamine channel). The 5-HT processes begin branching (arrow). The LP1 cells are indicated by arrowhead. (F) Same specimen as in E (FITC channel) at a focal plane where the LON (empty arrow) can be seen. At this stage in larval development the 5-HT projection and the LON do not overlap; however, they are very close to each other as demonstrated by the presence of the LP1 cells (arrowhead) in both focal planes. (G) Late second instar larval brain (rhodamine channel). The 5-HT processes (arrow) show more extensive branching. Arrowhead points to the LP1 cells. (H) Same specimen as in G (FITC channel) at a focal plane where the LON (empty arrow) can be seen. The LON is first seen overlapping with the 5-HT terminal at this stage in larval development. Scale bar in A–F, 10 μm.

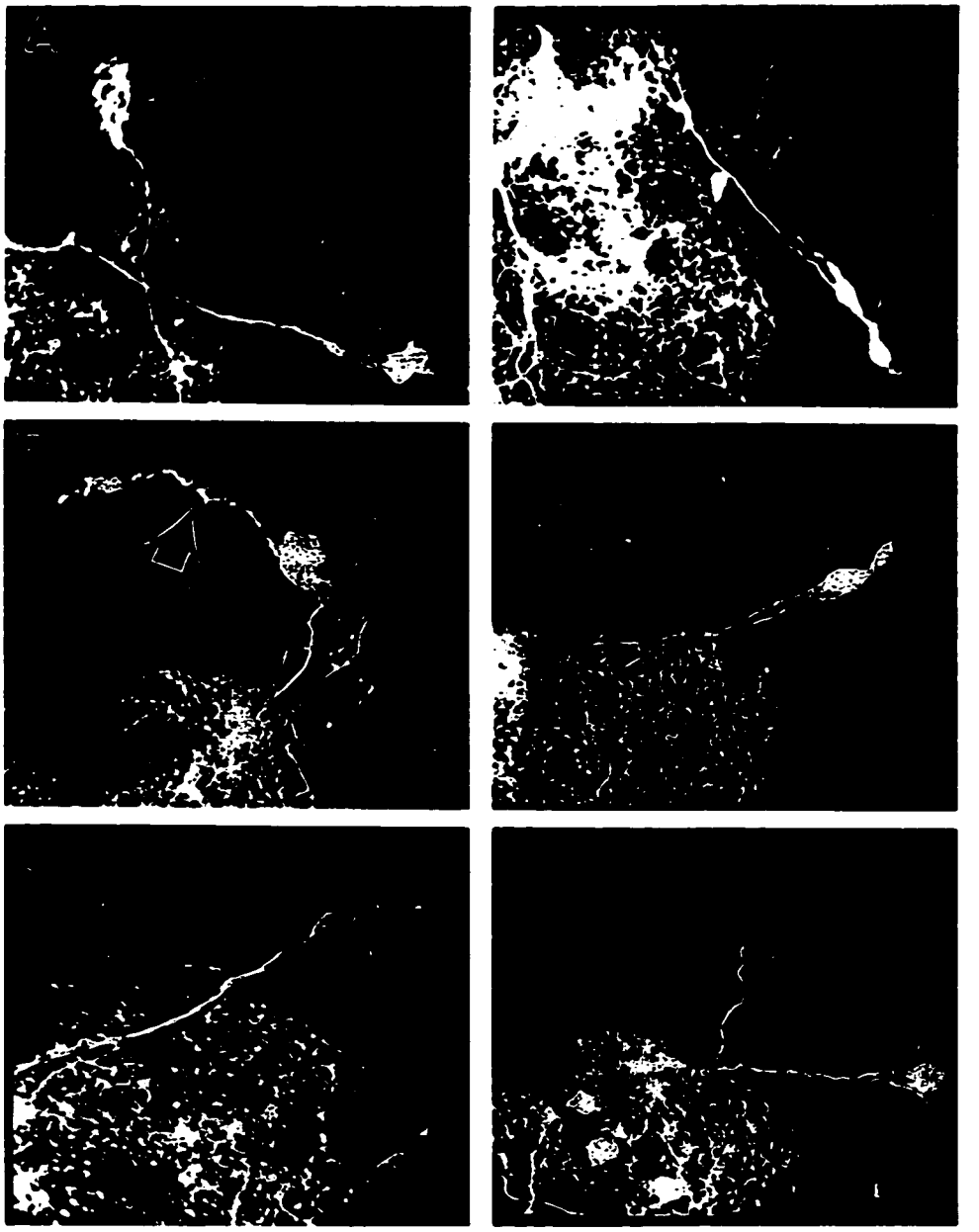

FIG. 3. Absence of the 5-HT arborization in gl^{esg} and *disco*^{l} third instar larval brains. Confocal micrographs of 5-HT expression in third instar larval brains of gl^{esg} and *disco*^{l} mutant strains. In all panels the serotonergic larval optic neuropil arborization is indicated by an arrowhead and the LP1 cell cluster by an arrow. (A) Wild-type. (B) gl^{esg}. Often in gl^{esg} mutants the LP1 cells (arrow) show abnormal neuronal processes (empty arrow) but no clear 5-HT arborization can be detected. (C) gl^{esg}. In a few specimens thin unpatterned 5-HT processes can be seen (arrowhead). Their location is consistent with that of the one described for the serotonergic processes that innervate the larval optic neuropil of wild-type strains. (D) *disco*^{l}. The 5-HT arborization is mostly absent (arrowhead). This is an unconnected *disco*^{l} mutant brain where no adult or larval photoreceptor projection was seen (Steller *et al.*, 1987). (E) *disco*^{l}. Again, in this specimen very thin 5-HT processes (arrowhead) can be seen. In a different focal plane adult and presumably larval photoreceptor axons were seen (connected phenotype, Steller *et al.*, 1987). (F) *disco*^{l}. The two arrows point to the apparent duplication of the LP1 cell cluster. No 5-HT arborization can be seen. Scale bar in A–E, 25 μm.

TABLE 1
MOSAIC ANALYSIS

Total number of brain hemisphe es	Number of brain hemispheres	Anterior *glass* cell cluster	Posterior *glass* cell cluster	Larval optic nerve	5HT arborization
	1	−	−	+	+
	3	−	+	+	+
	9	+/−	+	+	+
771	14	+	−	+	+
	18	+	+/−	+	+
	1	+	+	−	−
	725	+	+	+	+

sembling the arborization seen in wild-type preparations (Fig. 3A, arrowhead) was found in the larval optic center (Figs. 3B and 3C). In a few cases, thin neuronal processes were seen (Fig. 3C, arrowhead). Additionally, the two 5-HT-expressing LP1 cells often displayed abnormal sprouting (Fig. 3B, open arrow).

Examination of *disco*^{l} third instar larval brains showed that regardless of absence or presence of LON, 5-HT immunoreactivity in the larval optic center was always absent (Figs. 3D and 3E, arrowheads). Furthermore, extra 5-HT-expressing cells were often found (Fig. 3F, solid arrows). These cells were seen in the midlateral portion of the brain at the margin of the optic lobes. Their location and their pattern of projection sug-

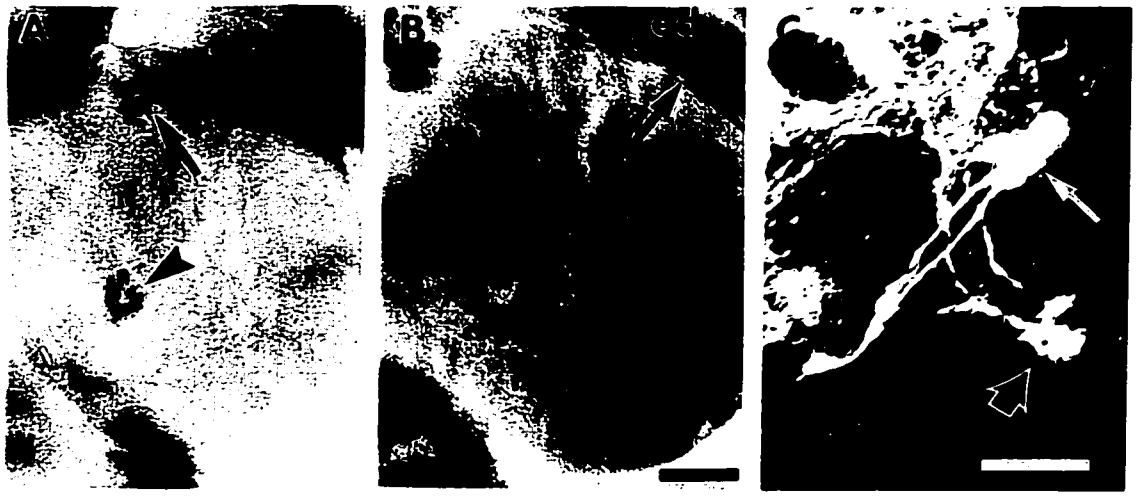

FIG. 5. Mosaic analysis for the gl^{ms9} allele. Putative mosaic larval brains were dissected and labeled with anti-GLASS, anti-5-HT antibodies. The anti-GLASS binding was detected by HRP-conjugated secondary antibodies. $CoCl_2$ was added during the reaction for the detection of *glass* expression. The anti-5-HT antibody was detected using a CY3-conjugated secondary antibody. *glass* were analyzed using Nomarski optics while 5-HT expression was seen under the confocal microscope. The presence of larval visual system was determined by anti-CHAOPTIN antibody detected by a FITC-conjugated secondary antibody (not shown). (A) Wild-type third instar larval brain hemisphere, labeled with anti-GLASS antibody. There are two *glass*-expressing cell clusters: one anterior (arrow) and one posterior (arrowhead). Horizontal view where anterior is up in all panels. (B) One example of a gl^{ms9} mosaic third instar CNS where the left brain hemisphere is completely mutant as seen by the absence of *glass* gene expression in both the anterior and posterior cell clusters. The larval visual system is present as determined by anti-CHAOPTIN expression (data not shown). In the eye disc (ed) the developing adult photoreceptor cells are stained with the anti-GLASS antibody (arrow) demonstrating that (1) this specimen does contain a functional *glass* gene in areas of the nervous system other than the central brain and (2) immunostaining of the GLASS protein was successful in this sample. (C) Same mosaic brain as in B, showing anti-5-HT antibody labeling as seen in the confocal microscope. The 5-HT arborization (empty arrow) is present. Arrow points to the LP1 cells. This brain lobe is positioned on a slightly frontal plane, therefore the orientation of the LP1 cells appears different from the one shown in previous figures. Scale bar in A and B, 50 μm and in C, 25 μm.

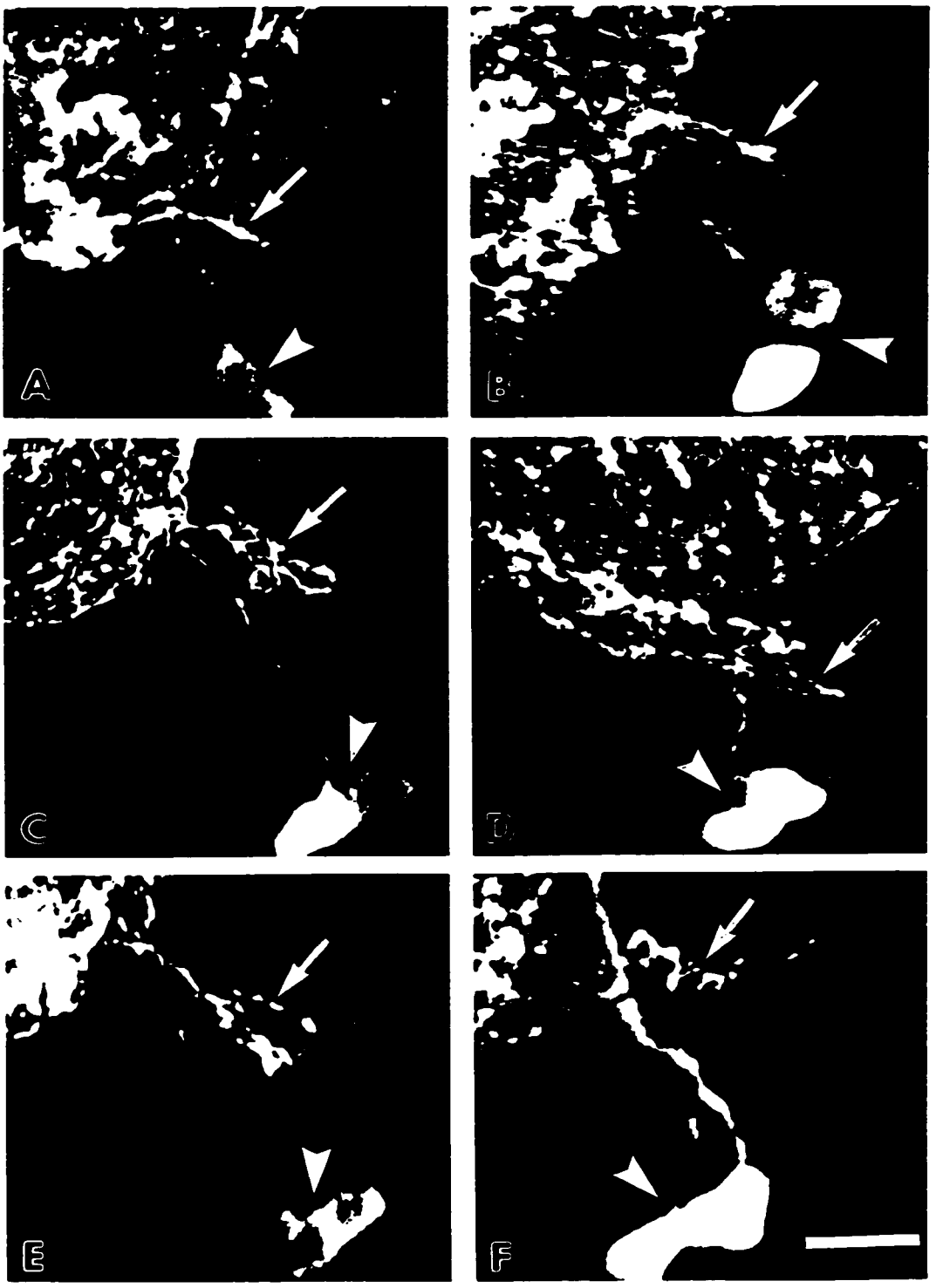
A
B
C
D
E
F

gested that these extra cells in *disco* mutants represented duplication of the LP1 cluster.

In order to determine if the absence of the 5-HT arborization in gl^{60j} and *disco*^{1} mutants is due to the absence of the corresponding neurons, we counted the number of all 5-HT-expressing cells in 24 brain hemispheres of wild-type, gl^{60j}, and *disco*^{1} mutant strains. Except for the LP1 cells all other 5-HT clusters were found in equal numbers in wild-type and in mutant brains, including the SP2 cell cluster presumed to be the corresponding cell bodies for the 5-HT arborization. No difference was found regarding the general morphology or immunoreactivity level of these neurons in either one of the mutant strains. Thus the absence of the 5-HT larval optic neuropil arborization is not accompanied by a decrease in 5-HT positive cells in *disco*^{1} or gl^{60j} mutants.

Expression of the glass and of the disco Gene Relative to 5-HT Expression

The results described above suggest that the presence of the LON connection is required for the proper innervation of the larval optic neuropil by 5-HT fibers originating in the central brain. It is possible, however, that in both mutants the absence of 5-HT immunoreactivity in the larval optic neuropil is due to an autonomous or nonautonomous effect of the mutant gene on the serotonergic cells rather than to the lack of interaction with the LON. In order to begin addressing this question we examined the expression of the *disco* and of the *glass* gene relative to the expression of 5-HT in third instar larval brains.

The *glass* gene is expressed in only two cell clusters in the third instar larval brain in addition to the larval photoreceptor cells (Ellis *et al.*, 1993). In contrast, the *disco* gene is widely expressed in the central nervous system. *disco* expression is particularly extensive in the developing adult optic lobes, in which it is displayed as a solid band of cells that wraps around the brain hemisphere at the level of the optic lobes (Lee *et al.*, 1991).

Double labeling of wild-type third instar larval brain with anti-GLASS and anti-5-HT antibodies showed that the posterior *glass*-expressing cell cluster lies very close to the 5-HT-expressing LP1 cells (Fig. 4C, solid arrow and arrowheads). However, there was no overlap in the expression of *glass* and 5-HT in this or in the other more anterior *glass*-expressing cell cluster (Fig. 4B, solid arrow).

In order to assess *disco* gene expression, the *disco* enhancer-trap line C50 1S1, previously shown to reflect *disco* expression, was used. (Lee *et al.*, 1991). Double labeling with anti-βgal (for *disco* expression) and anti-5-HT antibodies showed that the 5-HT-expressing LP1 cells lie very close to the band of *disco*-expressing cells (Fig. 4F, arrowheads and solid arrow). However, there was no significant overlap between *disco* and 5-HT expression in any part of the brain at that point in development. Given that there is widespread expression of *disco*, some of which is faint, it is possible that some of the 5-HT cells express *disco* at low levels (Fig. 4F, open arrows). Additionally, the *disco* gene expression undergoes complex temporal regulation: the pattern of expression found in the late third instar brain is more widespread than that found in the CNS during embryogenesis (Lee *et al.*, 1991). The expression of the *glass* gene in the third instar, however, reflects the expression described in the late embryo (Ellis *et al.*, 1993).

The absence of overlap between both *glass* and *disco* expression with the 5-HT expression suggests that the absence of the 5-HT arborization in the larval optic center of gl^{60j} and *disco*^{1} mutants is not due to the lack of GLASS protein or abnormal function of the DISCO protein in the 5-HT neurons. However, it is still possible that the *glass* and *disco* genes may have a nonautonomous influence on 5-HT neurons which can lead to absence of the serotonergic innervation of the larval optic neuropil.

Absence of the 5-HT Arborization Is Strictly Correlated with Absence of Larval Optic Nerve Innervation in gl^{60j} Mosaic Larvae

The results described so far suggest that proper innervation of the larval optic neuropil by serotonergic fibers is dependent upon contact with the LON. However, given that both mutations used in this study are likely to affect the central brain (see pattern of expression above), one cannot exclude the possibility of direct or indirect influence of these mutations on the development of the 5-HT arborization.

In order to address this question we decided to concentrate on the mutation in the *glass* gene because of its restricted expression in the central brain (circa 20 cells per brain hemisphere) as opposed to the widespread expression of the *disco* gene throughout the central nervous system, making the latter more likely to display a

FIG. 6. Development of the larval optic neuropil 5-HT arborization in gl^{60j} mutants. (A) Wild-type mid first instar larval brain. (B) gl^{60j} mid first instar larval brain. The 5-HT process (arrow) is very similar to that seen in wild-type. (C) Wild-type early second instar larval brain. (D) gl^{60j} early second instar larval brain. The 5-HT projection (arrow) is not as developed as in wild-type larvae. (E) Wild-type late second instar larval brain. (F) gl^{60j} late second instar larval brain. The 5-HT arborization is distinct from wild-type (arrow). Scale bar in A-H, 10 μm.

pleiotropic phenotype. To that end we examined mosaic larvae lacking *glass* gene expression in one or both *glass*-expressing clusters in the central brain and/or in the larval visual system. These were concomitantly analyzed for the presence of 5-HT immunoreactivity in the larval optic neuropil.

Mosaic animals were generated by somatic excision of a P-element transposon carrying a wild-type copy of the *glass* gene in a gl^{60j} mutant background (Kunes and Steller, 1991). Given that the *glass* mutation employed does not express any detectable protein (Moses *et al.*, 1989), reduction or absence of *glass* expression in the central brain indicated excision of the transposable element carrying the wild-type *glass* gene function and thus a mutant patch. In the case of the larval photoreceptor cells we used the presence of the photoreceptor-specific protein CHAOPTIN (Zipursky *et al.*, 1984) to assess absence or reduction of larval optic nerve which in turn was indicative of mutant patches in the larval photoreceptor cells. Additionally, anti-5-HT antibody was used to determine the presence of 5-HT processes arborizing within the larval optic center.

Table 1 depicts the distribution of mosaic patches and the phenotype of the corresponding 5-HT projection innervating the larval optic center in a total of 771 brain hemispheres. In spite of the low frequency of mosaic patches it is clear that absence of *glass* expression in the central brain cells is not correlated with lack of serotonergic innervation of the larval optic center. Complete absence of *glass* expression in either the anterior or posterior cluster in the presence of the larval optic nerve was not sufficient to affect the serotonergic projection. Absence of the 5-HT arborization was only seen in cases where the larval optic nerve was also absent. An additional 316 brain hemispheres from putative mosaic larvae were double labeled with anti-CHAOPTIN and anti-5-HT antibodies (data not shown). Of these, only two did not show any recognizable 5-HT immunoreactivity within the larval optic center. Both brains lacked innervation by the LON. An example of a larval brain with a normal LON but completely lacking *glass* gene function in the central brain, as seen by the absence of GLASS immunoreactivity in both anterior and posterior clusters, is shown in Fig. 5B. In this brain the 5-HT projections could be easily seen displaying the expected morphology (empty arrow in Fig. 5C). These results demonstrate that the absence of 5-HT arborization in the larval optic neuropil in *glass* mutants is solely due to lack of innervation of the LON and not to lack of gene function in the central brain.

Larval Optic Nerve Interaction Is Required for the Development but Not for the Initial Outgrowth of the 5-HT Projection

The absence of the 5-HT arborization in gl^{60j} mutants could be due to arrest in the initial outgrowth or to disruption in the subsequent development and/or maintenance of the 5-HT neuronal processes. Developmental analysis of gl^{60j} allele (Figs. 6A and 6B, solid arrow) showed that the initial outgrowth of the 5-HT processes during first instar larval stage is similar to that of the wild-type larvae. However, during second instar larval stage, at the time in which the first contact with the LON is made, the 5-HT arborization of gl^{60j} mutant larvae was significantly different from that of wild-type (Fig. 6F, solid arrow). These results suggest that the role of the LON is in the development of the 5-HT arborization and not in the initial outgrowth of the arborization forming processes, however, we cannot exclude a possible role for the LON in the maintenance of the 5-HT arborization later in larval development.

DISCUSSION

In this study, the role of the larval optic nerve on the development of the larval visual system neuropil was examined. We focused our investigation on the fate of newly described serotonergic arborization that innervates the larval optic center whose cell bodies are located in the central brain. We examined the consequences of absence of contact with the LON in the development of this arborization and the viability of the corresponding cell bodies. To that end two mutations that disrupt connectivity in the larval visual system were used: $glass^{60j}$(gl^{60j}) and $disconnected^{1}$($disco^{1}$). In gl^{60j} mutant flies the larval photoreceptors do not differentiate appropriately, resulting in absence of the LON (Moses *et al.*, 1989). In flies carrying mutations in the *disco* gene the LON fails to maintain stable connections with the optic lobe primordium (Steller *et al.*, 1987). In larvae mutant for either one of these genes the arborization of 5-HT processes could not be seen. No apparent effect on the viability of the cell bodies could be detected.

Developmental studies in gl^{60j} mutant larvae showed that the arborization of the 5-HT processes in the larval optic center, but not the initial outgrowth of these processes, is disrupted. The direct influence of the LON on the 5-HT arborization was further confirmed by mosaic analysis of the gl^{60j} mutation. Our results demonstrated that, although a *glass*-expressing cell cluster lies very close to the 5-HT arborization, lack of *glass* gene expression in these cells does not affect the development of the 5-HT arborization. Although the presence of the 5-HT arborization is dependent on the presence of the LON, the opposite is not true. In *Ddc* mutants lacking serotonin expression the LON morphology is indistinguishable from wild-type, suggesting that the LON does not require exposure to 5-HT for development or maintenance (data not shown). Our results do not exclude the possibility that continuous contact with the LON is required

for maintenance of the 5-HT arborization. In order to address this issue we would need to ablate the larval visual system in the late third instar larva rather than during embryonic development as is the case with the mutations employed in this study, and then follow the fate of the serotonergic arborization. Thus we conclude that the serotonergic innervation of the larval optic center is dependent upon afferent innervation from the larval photoreceptor cells for development and possibly maintenance.

Similar cellular interactions have been suggested for the development of the adult neuropil in *Drosophila*. Previous studies demonstrated that adult photoreceptor innervation is required for the proliferation of lamina precursor cells (Selleck and Steller, 1991). It has been suggested that at least two different signals operate during retinal axon-mediated development of the lamina ganglionaris, one that directs the lamina precursor cells to the proliferative phase and the other that triggers the differentiation program of the precursor cells (Meinertzhagen and Hanson, 1993).

Anterograde retina–lamina interactions have also been reported in the adult visual system of *Drosophila*. Photoablation of the afferent retinal innervation causes terminal degeneration and synaptic disassembly but no transsynaptic degeneration of the deafferented targets (Brandstatter *et al.*, 1991). Our observations in the larval visual system are consistent with those of Brandstatter and colleagues in the adult visual system in that no overt signs of degeneration were observed in the serotonergic cell bodies in the absence of larval optic nerve innervation.

The observations discussed above suggest that factors secreted by or associated with the photoreceptor membrane are responsible for anterograde retina–lamina interactions during or after development is completed. It is possible that neurotransmitters present in the photoreceptor neurons play a role in some of these interactions. In *Drosophila* and other insects, histamine is the only neurotransmitter known so far to be expressed in the adult photoreceptor neurons and presumably in the larval photoreceptor neurons as well (reviewed by Nassel, 1991). It is unlikely that activity plays a role in the anterograde interaction reported here, given that maintenance of larvae in the dark throughout development did not alter the morphology of the 5-HT projection in the larval optic neuropil (data not shown).

The adult visual system of *Drosophila* is invaded by extensive serotonergic processes. In the Fleshfly, absence of synaptic connection between the photoreceptor axons and the serotonergic processes in the lamina suggested a paracrine action of serotonin in this system (Nassel *et al.*, 1983). Whether the serotonergic processes in the larval optic center make synaptic contact with the larval optic nerve terminal is yet to be determined.

Developmental analysis of the serotonin processes showed that the contact of the LON by the 5-HT arborization takes place during early third instar larval stage. During early pupal stages, concomitant with the degeneration of the LON, the 5-HT processes retract from the larval optic center and are not seen again projecting toward the developing adult optic ganglia (data not shown). These results suggest that this 5-HT projection has a primary role in the function of the larval visual system during the third instar stage.

Drosophila larvae display marked aversion to light during the first, second, and first half of the third larval instar (Sawin *et al.*, 1994; Sawin-McCormack *et al.*, 1995). At the onset of the wandering phase larval photobehavior becomes progressively less photonegative, achieving photo neutrality just before pupariation (Sawin-McCormack *et al.*, 1995). In several invertebrates serotonin has been proposed to have a role in modulating the photosensitivity of the eye (Barlow *et al.*, 1977; Eskin and Maresh, 1982; Arechiga *et al.*, 1990). Thus, it is possible that the contact of the LON by this serotonergic process mediates the transition in photobehavior observed during the mid third instar larval stage.

Identification of additional mutants displaying a normal larval visual system morphology but with defective larval photobehavior will aid in the investigation of the significance of the serotonin arborization in the developing optic lobe area of the larval brain. The presence of serotonin processes in intimate association with the LON and the simplicity of the larval visual system in *Drosophila* makes it an excellent model to study the role of serotonin in visual system function and development.

The authors thank A. Bedard, R. Jacobs, and C. Nurse for critically reading the manuscript, H. Steller and V. Budnik for mutant strains, G. Rubin for the generous gift of anti-GLASS monoclonal antibody, and Tina Avolio for help in the preparation of the manuscript. A.R.C. is specially thankful to M. L. Ashton for help in the confocal microscope at York University. A.R.C. is the recipient of a WFA (Woman Faculty Award) from NSERC (National Science and Engineering Research Council of Canada). This work was supported by an NSERC Operating Grant to A.R.C.

REFERENCES

Antonini, A., and Stryker, M. P. (1993). Rapid remodeling of axonal arbors in the visual cortex. *Science* **260**, 1819–1821.

Arechiga, H., Banuelos, E., Frixione, E., Picones, A., and Rodriguez, S. L. (1990). Modulation of crayfish retinal sensitivity by 5-hydroxytryptamine. *J. Exp. Biol.* **150**, 123–143.

Ashburner, M. (1989). "A Laboratory Handbook." Cold Spring Harbor Laboratory, Cold Spring Harbor, NY.

Barlow, R. B., Chamberlein, S. C., and Kaplan, E. (1977). Efferent inputs and serotonin enhance the sensitivity of the *Limulus* lateral eye. *Biol. Bull.* **153**, 141.

Bolwig, N. (1946). Senses and sense organs of anterior end of the

housefly larvae. *Vidensk. Medd. Dansk. Naturh. Foreni. Kbh.* **109**, 81-217.

Brandstatter, J. H., Shaw, S. R., and Meinertzhagen, I. A. (1991). Terminal differentiation and synaptic disassembly following receptor photoablation in the retina of the fly's compound eye. *J. Neurosci.* **11**, 1930-1941.

Byrd, C. A., and Burd, G. D. (1993). The quantitative relationship between olfactory axons and mitral/tufted cells in developing *Xenopus* with partially deafferented olfactory bulbs. *J. Neurobiol.* **24**, 1229-1242.

Campenot, R. B. (1982a). Development of sympathetic neurons in compartmentalized clusters. I. Local control of neurite growth by nerve growth factor. *Dev. Biol.* **93**, 1-12.

Campenot, R. B. (1982b). Development of sympathetic neurons in compartmentalized clusters. II. Local control of neurite survival by nerve growth factor. *Dev. Biol.* **93**, 13-21.

Campos, A. R., Lee, K. J., and Steller, H. (1995). Establishment of neuronal connectivity during development of the *Drosophila* larval visual system. Submitted for publication.

Cohen, B., Wimmer, E. A., and Cohen, S. M. (1991). Early development of leg and wing primordia in the *Drosophila* embryo. *Mech. Dev.* **33**, 229-240.

Consolazione, A., Milstein, C., Wright, B., and Cuello, A. C. (1981). Immunocytochemical detection of serotonin with monoclonal antibodies. *J. Histochem. Cytochem.* **29**, 1425-1430.

De Koninck, P., Carbonetto, S., and Cooper, E. (1993). NGF induces neonatal rat sensory neurons to extend dendrites in culture after removal of satellite cells. *J. Neurosci.* **13**, 577-585.

Ellis, M. C., O'Neill, E. M., and Rubin, G. M. (1993). Expression of *Drosophila glass* protein and evidence for negative regulation of its activity in non-neuronal cells by another DNA-binding protein. *Development* **119**, 855-865.

Eskin, A., and Maresh, R. D. (1982). Serotonin or electrical optic nerve stimulation increases the photosensitivity of the *Aplysia* eye. *Comp. Biochem. Physiol.* **73**, 27-31.

Fischbach, K. F. (1983). Neural cell types surviving congenital sensory deprivation in the optic lobes of *Drosophila melanogaster*. *Dev Biol.* **95**, 1-18.

Fischbach, K. F., and Technau, G. (1984). Cell degeneration in the developing optic lobes of *sine oculis* and *small optic lobes* mutants of *Drosophila melanogaster*. *Dev. Biol.* **104**, 219-239.

Fischbach, K. F., and Heisenberg, M. (1984). Neurogenesis and behavior in insects. *J. Exp. Biol.* **112**, 65-93.

Goodman, C. S., and Shatz, C. J. (1993). Developmental mechanisms that generate precise patterns of neuronal connectivity. *Cell* **72**, 77-98.

Green, P., Hartenstein, A. Y., and Hartenstein, V. (1993). The embryonic development of *Drosophila* visual system. *Cell Tissue Res.* **273**, 583-598.

Heilig, J. S., Freeman, M., Leverty, T., Lee, K. J., Campos, A. R., Rubin, G. M., and Steller, H. (1991). Isolation and characterization of the *disconnected* gene of *Drosophila melanogaster*. *EMBO J.* **4**, 809-815.

Hofbauer, A., and Campos-Ortega. (1990). Proliferation pattern and early differentiation of the optic lobes in *Drosophila melanogaster*. *Roux's Arch. Dev. Biol.* **198**, 264-274.

Kalb, R. G. (1994). Regulation of motor neuron dendrite growth by NMDA receptor activation. *Development* **120**, 3063-3071.

Katz, L. C., and Constantine-Patton, M. (1988). Relationships between segregated afferents and post synaptic neurons in the optic tectum of three eyed frogs. *J. Neurosci.* **8**, 3160-3180.

Kunes, S., and Steller, H. (1991). The ablation of *Drosophila* photoreceptor cells by conditional expression of a toxin gene. *Genes Dev.* **5**, 970-983.

Kunes, S., Wilson, C., and Steller, H. (1993). Independent guidance of retinal axons in the developing visual system of *Drosophila*. *J. Neurosci.* **13**, 752-767.

Laski, F. A., Rio, D. C., and Rubin, G. M. (1986). Tissue specificity of *Drosophila* P-element transposition is regulated at the level of m-RNA splicing. *Cell* **44**, 7-19.

Lee, K. J., Freeman, M., and Steller, H. (1991). Expression of the *disconnected* gene during development of *Drosophila melanogaster*. *EMBO. J.* **10**, 817-826.

Le Roux, P. D., and Reh, T. A. (1994). Regional differences in glial-derived factors that promote dendritic outgrowth from mouse cortical neurons *in vitro*. *J. Neurosci.* **14**, 4639-4655.

Loer, C. M., and Kristan, W. B., Jr. (1989). Central synaptic inputs to identified leech neurons determined by peripheral targets. *Science* **244**, 64-66.

Meinertzhagen, I. A., and Hanson, T. E. (1993). The development of the optic lobe. *In* "The Development of *Drosophila melanogaster*" (M. Bate, and A. M. Aries, Eds.), pp. 1363. Cold Spring Harbor Laboratory, Cold Spring Harbor, NY.

Meyerowitz, E. M., and Kankel, D. R. (1978). A genetic analysis of visual system development in *Drosophila melanogaster*. *Dev. Biol.* **62**, 112-142.

Moses, K., Ellis, M. C., and Rubin, G. M. (1989). The *glass* gene encodes a zinc-finger protein required by *Drosophila* photoreceptor cells. *Nature* **430**, 531-538.

Nassel, D. R., Hagberg, M., and Seyan, H. S. (1983). A new, possibly serotonergic neuron in the lamina of the blowfly optic lobe: An immunocytochemical and Golgi-EM study. *Brain Res.* **280**, 361-367.

Nassel, D. R. (1987). Serotonin and serotonin-immunoreactive neurons in the nervous system of insects. *Prog. Neurobiol.* **30**, 1-85.

Nassel, D. R., Ohlsson, L., and Sivasubramanian, P. (1987). Postembryonic differentiation of serotonin-immunoreactive neurons in Fleshfly optic lobes developing in situ on cultured in vitro without eye discs. *J. Comp. Neurol.* **255**, 327-340.

Nassel, D. R. (1991). Neurotransmitters and neuromodulators in the insect visual system. *Prog. Neurobiol.* **37**, 179-254.

Power, M. E. (1943). The effect of reduction in numbers of ommatidia upon the brain of *Drosophila melanogaster*. *J. Exp. Zool.* **94**, 33-71.

Prochiantz, A., Rousselet, A., and Chamak, B. (1990). Adhesion and the *in vitro* development of axons and dendrites. *Prog. Brain. Res.* **86**, 331-336.

Qian, J., Bull, M. S., and Levitt, P. (1992). Target-derived astroglia regulate axonal outgrowth in a region-specific manner. *Dev. Biol.* **149**, 278-294.

Robertson, H. M., Preston, C. R., Phillis, R. W., Johnson-Schiltz, D. M., Benz, W. K., and Engels, W. R. (1988). A stable source of P-element transposase in *Drosophila melanogaster*. *Genetics* **118**, 461-470.

Rousselet, A., Autillo-Touati, A., Aruaud, D., and Prochiantz, A. (1990). *In vitro* regulation of neuronal morphogenesis and polarity by astrocyte-derived factors. *Dev. Biol.* **137**, 33-45.

Sawin, E. P., Harris, L. R., Campos, A. R., and Sokolowski, M. B. (1994). Sensorimotor transformation from light reception to phototactic behavior in *Drosophila* larvae. *J. Insect Behav.* **7**, 553-567.

Sawin-McCormack, E. P., Sokolowski, M. B., and Campos, A. R. (1995). Characterization and genetic analysis of *Drosophila melanogaster* photobehavior during larval development. Submitted for publication.

Schilling, K., Dickinson, M. H., Connor, J. A., and Morgan, J. I. (1991). Electrical activity in cerebellar cultures determines Purkinje cell dendritic growth patterns. *Neuron* **7**, 891-902.

Schmucker, D., Taubert, H., and Jackle, H. (1992). Formation of the *Drosophila* larval photoreceptor organ and its neuronal differentiation require continuous *kruppel* gene activity. *Neuron* **9**, 1029-1039.

Schwartz, J. P. (1992). Neurotransmitters as neurotrophic factors: A new set of functions. *Int. Rev. Neurobiol.* **34**, 1-23.

Selleck, S. B., Steller, H. (1991). The influence of retinal innervation on neurogenesis in the first optic ganglion of *Drosophila*. *Neuron* **6**, 83-99.

Steller, H., Fischbach, K. F., and Rubin, G. M. (1987). *disconnected*: A locus required for neural pathway formation in visual system of *Drosophila*. *Cell* **50**, 1139-1153.

Tieman, S. B., and Hirsch, H. V. B. (1982). Exposure to lines of only one orientation modifies dendritic morphology of cells in the visual cortex of the cat. *J. Comp. Neurol.* **211**, 353-362.

Tix, S., Minden, J. S., and Technau, G. M. (1989). Preexisting neuronal pathways in the developing optic lobes of *Drosophila*. *Development* **105**, 739-746.

Valles, A. M., and White, K. (1988). Serotonin-containing neurons in *Drosophila melanogaster*: Development and distribution. *J. Comp. Neurol.* **268**, 414-428.

Van der Zee, C. E. E. M., Rashid, K., Le, K., Moore, K. A., Stanisz, J., Diamond, J., Racine, R. J., and Fahnestock, M. (1995). Intraventricular administration of antibodies to nerve growth factor retards kindling and blocks mossy fiber sprouting in adult rats. *J. Neurosci.*, in press.

Wolff, T., and Ready, D. F. (1993). Pattern formation in the *Drosophila* retina. *In* "The Development of *Drosophila melanogaster*" (M. Bate, and A. M. Arias, Eds.), pp. 1277-1325. Cold Spring Harbor Laboratory, Cold Spring Harbor, NY.

Zipursky, S., Venkatesh, D., Teplow, B., and Benzer, S. (1984). Neuronal development in the *Drosophila* retina: Monoclonal antibodies as molecular probes. *Cell* **36**, 15-26.

Chapter 3

Identification of DISCO-interacting proteins.

Introduction

Disconnected (*disco*) gene is required for proper neuronal connections in both larval and adult visual system of *Drosophila* (Steller *et al.*, 1987; Campos *et al.* 1995). The *disco* gene codes for a protein with two C2H2 type zinc-finger domains, a feature shared by many transcription factors (Pieler and Bellefroid, 1994). A human gene called *basonuclein*, contains zinc finger motifs similar to the motifs present in DISCO (Tseng and Green, 1992). The striking conservation of the zinc finger sequences in evolution suggests an important role for this motif in the function of the DISCO protein. A portion of the DISCO protein including the zinc finger motifs has been shown *in vitro* to confer sequence specific DNA binding activity (Kevin Lee, Ph. D. thesis, 1993).

Expression of the *disco* gene is seen in several cell types including neuronal, nonneuronal and glial cells, throughout the life cycle of *Drosophila* (Lee *et al.*, 1991). Of particular importance to the visual system development is its expression in glial cells that are intimately associated with the larval optic nerve (LON) and three so called "optic lobe pioneer cells" (OLPs), also contacted by the LON. The OLP cells are neuronal cells in the optic lobe primordium that are thought to guide the LON in the brain (Campos *et al.*, 1995). It has been suggested that the *disco* gene activity may be required in the optic nerve glia and the OLPs for the development of proper connections between the LON and its target cells in the brain (Campos *et al.*, 1995).

Among other cell types, *disco* expression is seen in visceral mesoderm, gnathal segments, thoracic segment, leg imaginal discs and cardioblasts. *disco* expression is differentially regulated in different tissues. For example, *disco* expression in the primordia of leg imaginal disc is dependent on the homeodomain-containing protein DISTALLESS (Cohen *et al*, 1991), whereas, *disco* expression in the cardioblasts is dependent on TINMAN (Bodmer, 1993), another homeodomain protein.

In two apparent null mutant alleles of *disco*, carrying changes in the highly conserved Cysteins of the zinc finger motifs, expression of a non-functional DISCO protein is seen in all embryonic tissues that normally express *disco* except the cells in the optic lobe region (Lee *et al.*, 1991). The absence of *disco* expression in the optic lobe tissue of these mutants has been shown to be due to a tissue specific autoregulatory activity of *disco* which is localized only to the cells of the optic lobe primordium (Kevin Lee, Ph. D. thesis, 1993). The tissue specific autoregulatory function of *disco* suggests that interaction of *disco* with other tissue specific factors restrict *disco* autoregulatory activity to the optic lobe primordium.

There are a variety of different approaches one might use to identify factors that interact in a tissue specific manner with DISCO. These include, traditional approaches, such as genetic screens or immunoprecipitation assay, as well *in-vitro* approaches using synthetic machinery such as that used in "interaction trap" assays. In our study we chose to use the latter approach (Gyuris *et al.*, in 1993) to identify DISCO interacting proteins.

The yeast interaction trap.

The yeast interaction trap used in this study is an implementation of the yeast two-hybrid system developed by Gyuris *et al.* in 1993. The method uses the transcription of yeast reporter genes as a synthetic phenotype to detect protein-protein interactions (reviewed by Finlay and Brent, 1995). It provides a convenient way of cloning cDNAs for interacting protein.

Most eukaryotic transcription factors contain two distinct domains; a DNA binding domain and an activation domain required for transcription activation. These domains can be exchanged between different transcription factors while retaining their function. For example, the DNA binding domain of Gal4 by itself is not sufficient to activate transcription of reporters with upstream Gal4 binding sites. However, when it is fused to activation domains of other proteins, the fusion protein is able to activate transcription of the same reporter gene. Another important feature is that the DNA binding domain and the activation domain need not be covalently attached to each other for activation to occur (Ma and Ptashne, 1988). If two proteins, one carrying the DNA binding domain and the other carrying the activation domain, interact with each other activation of reporter gene transcription can occur. This is the basis for the yeast interaction trap.

There are three basic components in any two-hybrid system: (i) a yeast vector for expression of a protein of interest fused to a DNA binding domain, (ii) a yeast vector for expression of an unknown cDNA (from a library) encoded protein fused to a transcription activation domain, and (iii) a yeast reporter gene that contains binding sites for the DNA binding domain. All systems utilize the DNA binding domain from either the yeast transcription factor Gal4 or from the

bacterial transcription factor LexA. The yeast interaction trap developed by Gyuris *et al.* (1993) uses the LexA system. Here, a LexA-fusion protein, containing the protein of interest fused to the LexA DNA binding domain, is referred to as a 'bait'. The activation domain B42 used in this system is derived from *E. coli* and is fused to the library proteins expressed from cDNA libraries made in the yeast interaction trap expression vector pJG4-5. The expression of the activation domain tagged library proteins is under the control of the galactose inducible promoter from the yeast Gal1 gene. The library vector not only provides the activation domain, but also a nuclear localization signal and an epitope tag (for convenient detection of the fusion protein) fused at the N-terminus of the expressed library proteins. Two reporter gene constructs are used in this system; a yeast *leucine2* derivative that has its normal upstream sequences replaced with *lexA* operator and a *lacZ* reporter construct with upstream LexA binding sites. Transcription of the *lexA*-operator-*leu2* gene is detected by the ability of a *leu*$^-$ yeast strain to grow in the absence of Leucine. While, transcription of the *lacZ* reporter is detected by the ability of the strain to form blue colonies on X-gal plates.

The yeast interaction trap is schematically represented in Figure1. The bait proteins used in our study are different LexA-DISCO fusions carrying either N-terminal or C-terminal DISCO fragments. The bait protein is constitutively expressed. It binds to the *lexA* operator located upstream of the *lacZ* gene (or *leu2* gene) in the reporter construct. The activation tagged library protein is expressed conditionally from the Gal1 promoter. In glucose medium the Gal1 promoter is repressed. Only when the yeast is growing on galactose medium, the library protein expression is induced. Those library proteins that interact

with the bait activate transcription of the *leu2* and *lacZ* reporter genes. As a result, cells containing activation-tagged library proteins that interact with the bait form colonies on galactose medium lacking Leucine and form blue colonies on galactose X-gal plates.

Figure 1

The yeast interaction trap scheme:

The yeast interaction trap is schematically represented in this Figure. The bait (LexA-DISCO fusion protein) binds to the LexA operator (LexA OP) located upstream of the reporter genes (*lacZ* or *leu2*). The binding of the bait does not itself activate transcription of the *lacZ* reporter gene. Only when an activation domain-tagged library protein (X) interacts with DISCO, the activation domain fused to the library protein activates the transcription of the reporter gene.

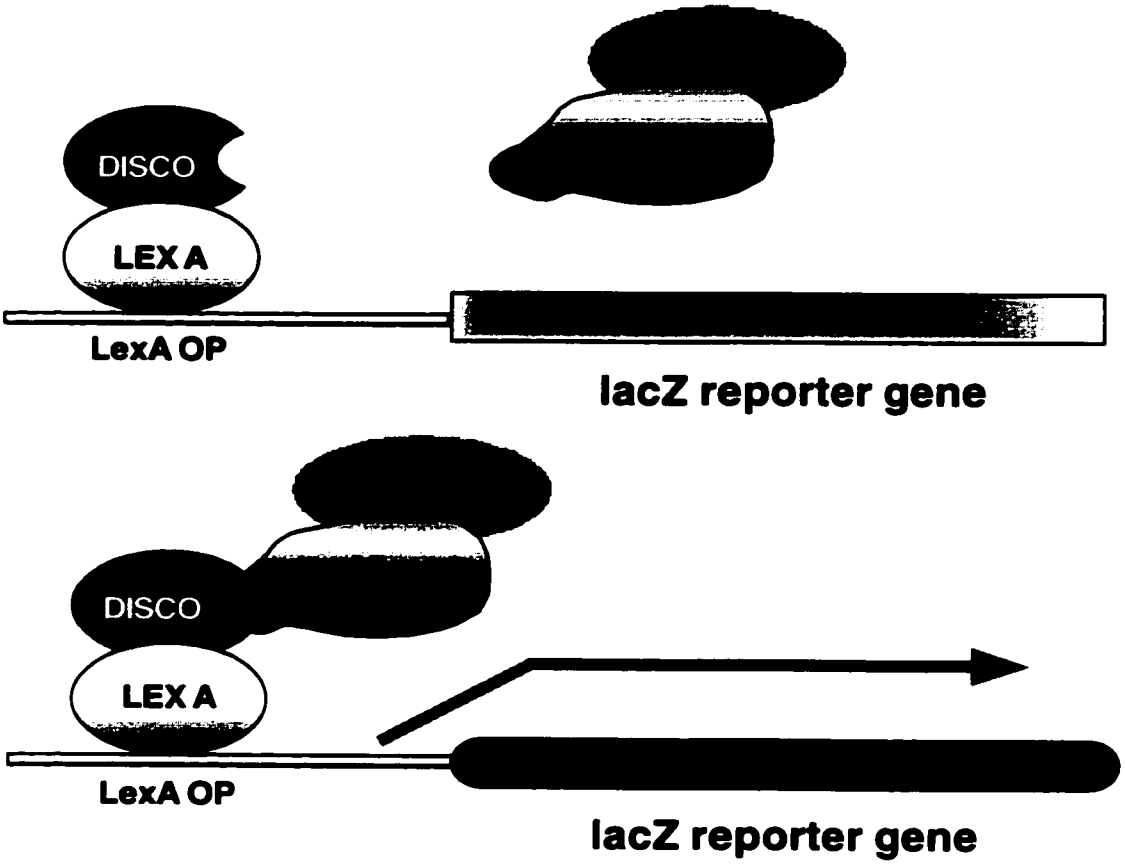

AD = Activation Domain
X = Library protein that interacts withs DISCO

Results:

I. The yeast interaction trap screening.

A. Testing the DISCO baits: Repression assay.

The size of an exogenous protein that can be efficiently expressed in yeast is limited. Since the expression of bait with the full-length DISCO protein (92 kDa) was poor in yeast, we used smaller *disco* fragments to construct baits for the "interactor hunt".

The middle portion of DISCO contains a 40 amino acids glutamate-rich acidic region (Heilig *et al.*, 1991). Glutamate- and aspartate-rich acidic regions are known to act as activation domains in several transcription factors (e.g., Ma and Ptashne, 1987; Triezenberg *et al.*, 1988). Therefore, presence of both a DNA binding domain and an activation domain in the bait may cause activation of the reporter gene in the absence of any interaction with activation tagged library proteins. Indeed a recent study in our lab has demonstrated that binding of the *LexA* promoter by the glutamate-rich region of DISCO as a LexA fusion protein was sufficient to cause activation of the *lacZ* reporter gene (Figure 3). Therefore, the glutamate-rich region was excluded from our study and only the N-terminal and C-terminal portions of DISCO were used as baits for the interaction trap assay (Figure 2).

The C-terminal DISCO bait used in our study contained a 153 amino acids DISCO fragment. The N-terminal DISCO fragment used for the interactor hunt was 186 amino acids long. To our surprise, this DISCO bait caused activation of

reporter gene transcription in the absence of a activation-tagged library protein (Figure 3).

In order to be able to use the N-terminal portion of the *disco* gene in the interaction trap screen, a DISCO bait was constructed where the cysteine (Cys) residue at position 127 was replaced with a serine (Ser) residue. The presence of the Cys residue at position 127 of the second zinc-finger domain of DISCO is crucial, since, replacement of this residue with Ser in the *disco1* mutant leads to a complete loss of *disco* function (Heilig *et al.*, 1991). The Cys127 to Ser substitution also abolished the transcription activation property of the N-terminal DISCO bait, which gave us the opportunity to use the mutated DISCO bait for our yeast interaction trap screening. The mutated DISCO bait was generated simply by PCR amplification of the N-terminal *disco* fragment from the chromosomal DNA of $disco^{1}$ mutant that carries the above mutation. The construct was subsequently sequenced to confirm the presence of the desired mutation.

In order to activate the transcription of the reporter genes, baits need to be localized in the nucleus (Finley and Brent, 1995). To examine nuclear localization and the ability of these baits to bind LexA operators, transcription repression of a *lacZ* reporter gene was monitored. Expression of the *lacZ* gene from the reporter gene construct pJK101 (Brent and Ptashne, 1984) is driven by yeast Gal1 promoter. The construct pJK101 also contains one *LexA* operator located between the Gal1 promoter and a TATA box. *lacZ* expression is thus galactose inducible. For reasons not completely understood, binding of a bait to the LexA operator causes 2-20 fold repression of the *lacZ* gene expression in galactose medium. This property of the reporter construct is used in the

repression assay to confirm nuclear localization and *LexA* operator binding ability of an experimental bait (Brent and Ptashne, 1984).

The repression assay was done on X-gal (5-bromo-4-chloro-3-indolyl-β-D-galactopyranoside)-galactose plates and the extent of blue coloration produced by the yeast colonies with or without the bait constructs were compared. Yeast colonies carrying the DISCO bait constructs showed distinct reduction in the expression level of the *lacZ* reporter gene compared to that produced by the colonies lacking the DISCO baits. The results of the repression assay show that both N- and C-terminal DISCO baits are able to localize to the nucleus and are able to bind *LexA* operator (data not shown).

B. Interactor hunt using the C-terminal DISCO bait:

A *Drosophila melanogaster* 0-12 hr. embryonic cDNA library made in the yeast interaction trap vector pJG4-5 was kindly provided by Dr. Brent (Harvard Medical school). This library was amplified and screened for all interactor hunts. In two trials, $1X10^6$ and $0.5X10^6$ colonies were screened with the C-terminal DISCO bait. No cells survived on galactose plates lacking Leucine. Thus, no interactor was isolated using the C-terminal DISCO bait.

C. Interactor hunt using the N-terminal DISCO bait:

About $2.5X10^6$ colonies from the 0-12 hr. *Drosophila* embryonic library were screened using the N-terminal DISCO bait carrying a Cys127-Ser127 mutation. 150 colonies survived on galactose plates lacking Leucine. To check the expression of the *lacZ* reporter gene, these 150 colonies were plated on galactose medium containing X-gal. 20 colonies appeared blue on the X-gal

plate. The other 130 colonies therefore may represent nonspecific interactions. Since, the library vector expression is induced by galactose and repressed by glucose, the above 20 colonies were replica plated on glucose medium containing X-gal. Out of 20 colonies 18 showed repression of *lacZ* expression on glucose X-gal medium, indicating that expression of the activation tagged library protein was necessary to activate transcription of the *lacZ* reporter gene in those colonies. Two colonies that failed to show repression of *lacZ* expression in glucose plate again represent non-specific interaction.

D. Classification and isolation of the cDNAs encoding the interacting proteins:

Since the *Drosophila* genome consists of approximately 12,000 genes (Miklos and Rubin, 1996), screening of $2.5X10^6$ cDNAs should lead to the isolation of several copies of a single interacting cDNA. The number of copies of a single cDNA present in 2.5 million clones depends on the abundance of the corresponding mRNA in the embryo. In order to classify the isolated positive yeast clones, the library cDNAs were PCR amplified from yeast plasmids isolated from the positive clones. The amplified products were digested with HaeIII and AluI enzymes and the restriction patterns were compared. From the restriction pattern, the 18 cDNAs were classified into three groups: 16 out of 18 showed a similar restriction pattern with both enzymes (group 1) while the other two showed distinct restriction patterns (group 2 and 3).

The plasmids isolated from positive yeast colonies represented a mixture of three different plasmid constructs; the library construct, the bait construct and the reporter gene construct. The selectable marker on the library plasmid was *tryptophan*. In order to isolate the library plasmid containing the interacting

cDNA, the plasmid mixture isolated from a positive yeast clone was transformed into a *trp*$^-$ *E. coli* strain MC1066. The colonies that survived on M9 minimal medium lacking Tryptophan represented colonies carrying the library plasmid. Yeast library plasmids isolated from 4 out of the 16 interacting colonies from group 1 and the two single interacting colonies from group 2 and 3 were transformed into the *trp*$^-$ *E. coli* strain. The library plasmids from the positive *trp*$^+$ bacterial colonies were isolated and transformed back in yeast together with the N-terminal DISCO bait to confirm the interactions detected previously (Figure 4).

Figure 2

Diagrammatic representation of baits used in the interaction trap assay: The baits used in the interactor hunt are schematically shown in this Figure. The entire DISCO protein and the fragments used in the baits are represented with horizontal bars. A 186 amino acids N-terminal DISCO fragment (amino acids 1-186) carrying a Cys127 to serine127 substitution, and a 153 amino acid C-terminal DISCO fragment (amino acids 415-568) were used for the interaction trap screening. The red box shows the location (amino acids 89-149) of the two repeats of the zinc finger motif present in DISCO. The yellow box shows the 40 amino acids glutamate rich region (from residue 311 to 351) located in the middle portion of the DISCO protein.

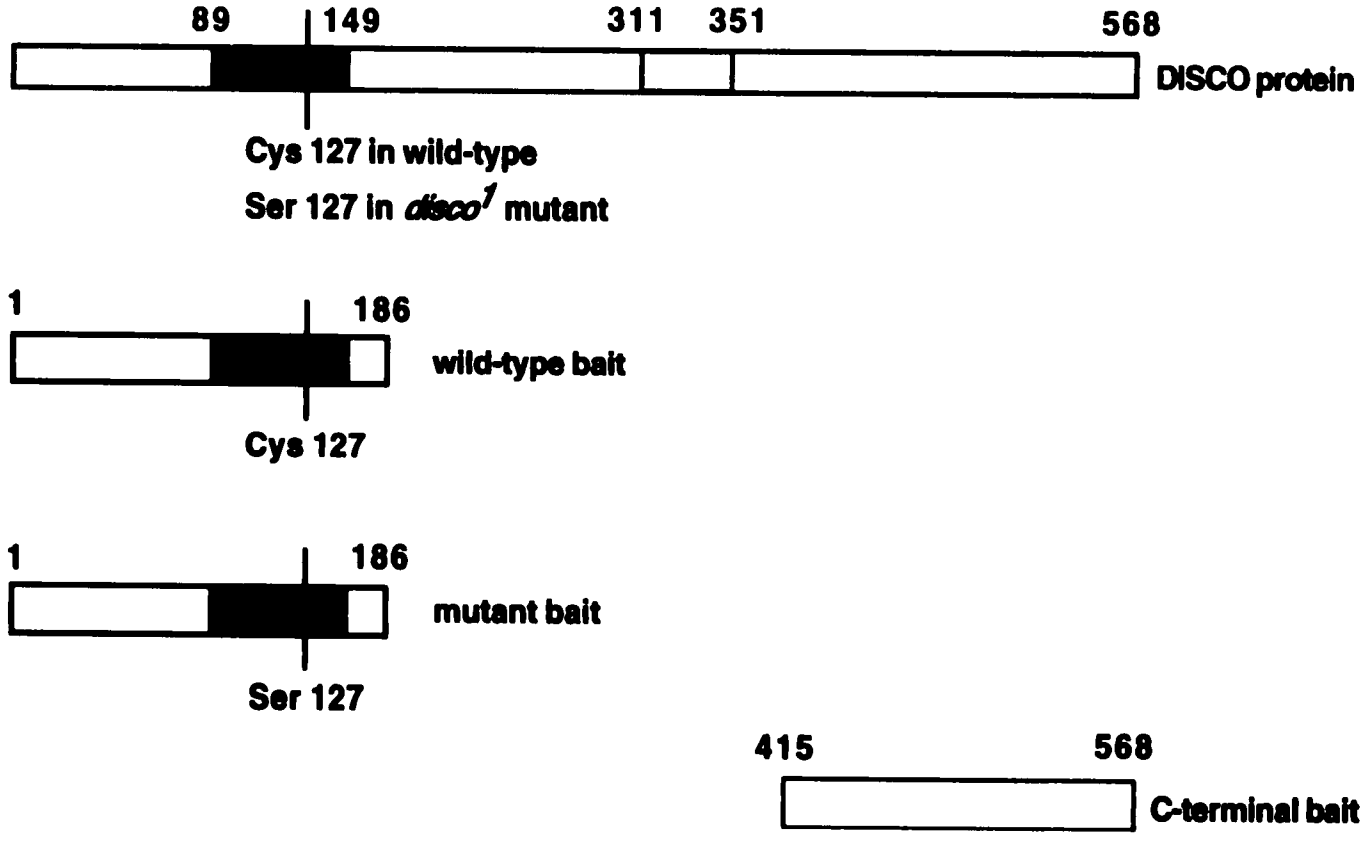
89
149
311
351
568
DISCO protein
Cys 127 in wild-type
Ser 127 in disco1 mutant
1
186
wild-type bait
Cys 127
1
186
mutant bait
Ser 127
415
568
C-terminal bait
Zinc finger domain of DISCO
Glutamine rich region of DISCO

Figure 3

Transcription activation ability of the N-terminal and glutamate-rich regions of DISCO:

This Figure shows the ability of the zinc finger domain and the glutamate rich region of DISCO to activate *lacZ* reporter gene transcription from the reporter construct used for interactor hunt. **Panel A** shows a schematic representation of the DISCO protein. The zinc-finger domains and the glutamate-rich region are indicated with different shades of blue.

Panel B shows the effects of different DISCO baits on reporter gene expression. The ability of the DISCO baits with the N-terminal (From amino acids 1-186, including the zinc-finger domain) and Glu-rich regions of the protein (From amino acids 186-414) to activate the *lacZ* reporter gene expression is revealed from the blue colour of the colonies containing these baits. Substitution of cysteine residue at position 127 by a serine residue in the mutated DISCO bait (indicated with an asterix) abolishes the transcription activation ability of the N-terminal bait as revealed from the white colour of the colony. The C-terminal bait is also unable to activate the reporter gene expression.

A

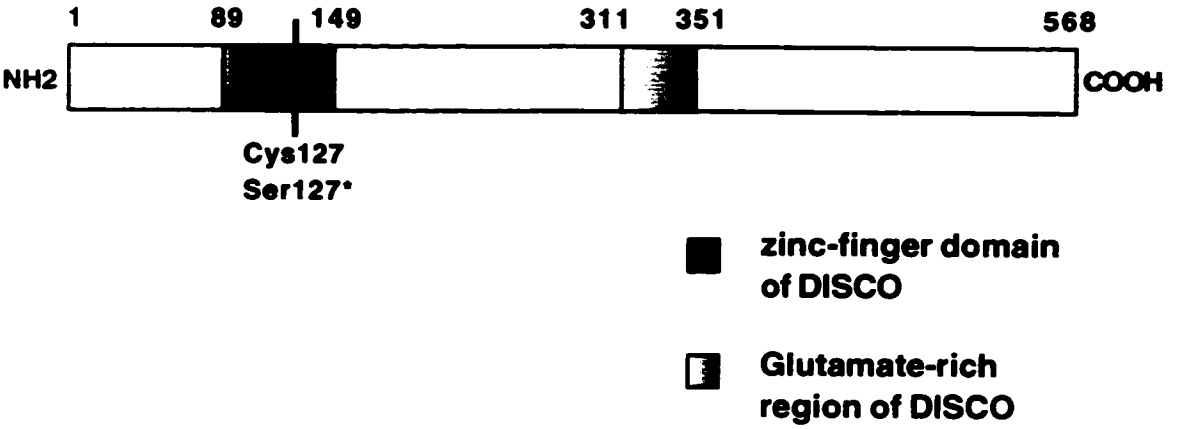
1
89
149
311
351
568
NH2
COOH
Cys127
Ser127*
zinc-finger domain of DISCO
Glutamate-rich region of DISCO

B

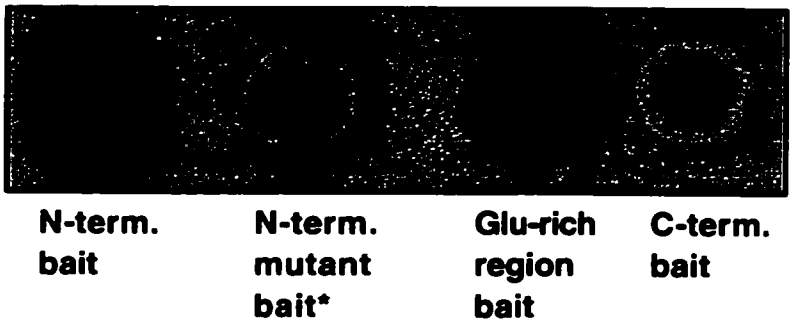
N-term. bait
N-term. mutant bait*
Glu-rich region bait
C-term. bait

Figure 4

Results of the interaction trap screening:

Screening of a *Drosophila* cDNA library constructed in a yeast expression vector with the N-terminal DISCO bait led to the identification of three interacting proteins. This Figure shows three positive yeast clones (blue colonies = *lacZ* reporter gene expression). All of the three interacting proteins; a putative ATPase subunit of the *Drosophila* 26S proteasome complex, the DIP1 protein and the DIP2 protein activate *lacZ* gene expression in galactose X-gal plate (blue colonies) in the presence of mutated N-terminal DISCO bait. The *lacZ* gene expression is activated only when both the DISCO protein and one of the interacting proteins are present simultaneously. Presence of either of these proteins alone is not sufficient to activate the transcription of the reporter gene. LexA alone without the DISCO fragment is also unable to produce blue colonies in the presence of any of the interacting proteins. The LexA-DISCO fusion protein in the presence of the activation domain alone without an interacting protein, also does not activate transcription of the *lacZ* reporter.

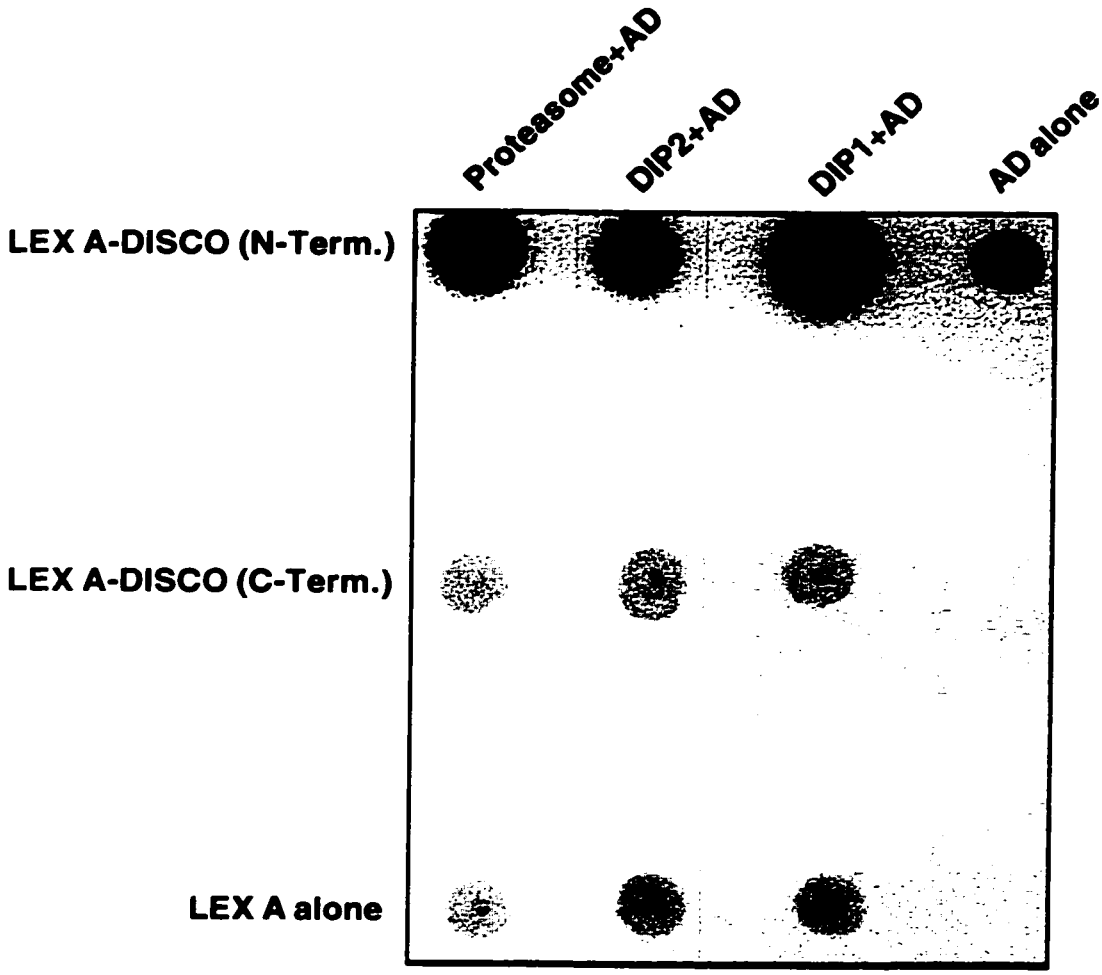

AD=activation domain

E. Sequence analysis of the cDNAs encoding interacting proteins:

The cDNAs corresponding to 4 interacting clones from group 1 and single interacting clone from both group 2 and group 3 were sequenced. Sequence analysis confirmed that all members of group 1 represent the same cDNA. We denoted the interacting protein encoded by the group 1 cDNA as "DISCO interacting protein 1" (DIP1).

The partial *dip1* cDNA isolated from the interacting clone contained a 1.1 kb fragment corresponding to the 3' end of *dip1* mRNA. Sequence analysis using 'BLAST' tool (Basic Local Alignment Search Tool; Altschul *et al.*, 1990) revealed that the putative DIP1 protein contains a region that shows sequence similarity to dsRNA binding domains (dsRBDs) (Figure 5). A consensus for dsRBDs has been determined through mutational analysis, *in-vitro* binding experiments and comparison of dsRBD sequences from several dsRNA-binding proteins (St. Johnston *et al.*, 1992). The putative dsRBD sequence of DIP1 matches well with the C-terminal short domain consensus but shows poor similarity with the N-terminal long domain consensus (Figure 13). The putative dsRBD of DIP1 shows extensive similarity to the dsRBDs of mammalian glutamate receptor editases (Melcher *et al.*, 1996; Lai *et al.*, 1997). The similarity extends beyond the conserved residues of the dsRBD consensus (Figure14). One striking feature of the *dip1* cDNA is the presence of 4 repeats of a 124 bp sequence at the 3'end of the cDNA (Figures 5, 12A.). Nucleotide sequences of the two 124 bp middle repeats are exactly equivalent, while, the first repeat contains two extra base pairs and the last repeat (120 bp) is interrupted by an EcoRI site (Figure 12B)

The group 2 cDNA is also a newly identified cDNA. We will refer to the interacting protein encoded by this cDNA as "DISCO interacting protein 2"

(DIP2). The cDNA clone contains a 1.2 kb 3' end fragment of *dip2* cDNA (Figure 6). Sequence analysis through 'BLAST' search (Altschul *et al.*, 1990) using the NCBI BLAST search server showed a high degree of similarity with a human cDNA isolated in the Human Genome project (Accession # D80006). The C-terminal 100 amino acids segment and N-terminal 155 amino acids segment of the predicted partial *Drosophila* DIP2 protein share 82% and 66% identities respectively with that of the human homolog. Both the predicted human protein and DIP2 share a high degree of similarity with a protein sequence predicted from a *Caenorhabditis elegans* genomic DNA sequence (Accession # 2088703, Wilson *et al.*, 1994). The degree of similarity shared between these proteins (Figure 26) suggests that these proteins are human and *C. elegans* homologs of *Drosophila* DIP2.

Sequence analysis showed that the group 3 cDNA codes for an ATPase, the fourth subunit of the *Drosophila* 26S proteasome complex. This cDNA was originally cloned based on its similarity to the ATPase component of the mouse 26S proteasome (Hoyle and Fisher, 1996).

Figure 5

Partial *dip1* cDNA sequence.

This Figure shows the sequence of the 1.1 kb partial *dip1* cDNA isolated from the yeast interaction trap screening. The predicted partial protein sequence is also shown. The cDNA lacks the 5′ end of the corresponding mRNA including a portion of the coding region. The putative dsRNA-binding domain in the partial protein sequence is highlighted. The first 3 nucleotides of all four 124 bp repeats in the 3′ UTR are shown in boldface. The stop codon (denoted with an asterix) lies at the beginning of the first repeat. The EcoRI site (GAATTC) that interrupts the fourth repeat is also shown in boldface and is underlined. The EcoRI site is followed by a 48 bp sequence and a polyA tail.

Partial *dip1* cDNA sequence and the predicted protein sequence:

```
GCCTGCGAGAAGGCTTGGCGCGATTTTATTATTGCAAAAATGACCCCCAAGCCGCCCCGT 60
 A  C  E  K  A  W  R  D  F  I  I  A  K  M  T  P  K  P  P  R
ATTCACCAGGTGGAGATGGGTTCGGAGCCAATGGATATCAACGAGGATGAGGCCGATGCA 120
 I  H  Q  V  E  M  G  S  E  P  M  D  I  N  E  D  E  A  D  A
CCGGATGATGATCTGCCCATGTTGAATCTGGCCTCGTTTGCCATCTACAAGCTGTTCGCG 180
 P  D  D  D  L  P  M  L  N  L  A  S  F  A  I  Y  K  L  F  A
GAGTGGGAACGGGAGGGCTATGTCGTGCCCGAGATGCACCCTTCGGCCAATGCTGCCCAA 240
 E  W  E  R  E  G  Y  V  V  P  E  M  H  P  S  A  N  A  A  Q
CAGGCGGGAGGGGATGCCGGAACTCCAGTTCCCCCCGTGCCGAAGGAGCCAAAGAAGCCG 300
 Q  A  G  G  D  A  G  T  P  V  P  P  V  P  K  E  P  K  K  P
CCAGTGCGCACCGAGCTACCCTCTGGCTGGGAGACCATGCACCCGGCGACCATTCTTTGC 360
 P  V  R  T  E  L  P  S  G  W  E  T  M  H  P  A  T  I  L  C
ATTATGCGTCCGGGACTCAACTACGTGGACTACGGGTCATCTGGCGACAAGACCAACGGC 420
 I  M  R  P  G  L  N  Y  V  D  Y  G  S  S  G  D  K  T  N  G
ATGCAGCATCTGGGAATCATGGTGGACAACCAGGAGTTCCACGCCAACGGCAGATCAAAG 480
 M  Q  H  L  G  I  M  V  D  N  Q  E  F  H  A  N  G  R  S  K
AAAATCGCCCGTCGCAACGTGGCCGTGAAAGTGTGCAACTCTCTGTTCGGCACCAACTTC 540
 K  I  A  R  R  N  V  A  V  K  V  C  N  S  L  F  G  T  N  F
ACCTACAGCGACACCACTTAAGACACCAACTCCAACCGCAGACTCCAACTGCCGACGACA 600
 T  Y  S  D  T  T  *
ACACACATAACGGACACTCTTAACGGACAGCAATCAGAAGATTGCGACCCTGACGTCAAT 660
TGCGCAACTTTAAGCGACACCACTTAAGACACCAACTCCAACCGCAGACTCCAACTGCCG 720
ACGACAACACACCTATGCCTCTCTTAACGGACAGCAATCAGAAGATTGCGACCCTGACGT 780
CAATGGCGCAACTTTAAGCGACACCACTTAAGACACCAACTCCAACCGCAGACTCCAACT 840
GCCGACGACAACACACCTATGCCTCTCTTAACGGACAGCAATCGGAAGATTGCGACCCTG 900
ACGTCAATGGCGCAACTTTAAGCGACACCACTTAAGACACCAACTCCAACCGCAGACTCC 960
AACTGCCGACGACAACACACCTATGCCTCTCTTAACGGACAGCAATCAGAAGATTGCGAC 1040
CCTGACGTCAATGGCGCAACTTTAAGAATTCCTTTTCTGTCAAAGTGAAGAGGCATATTA 1100
AACAAGAATTTCCCAATTTAAAAAAAAAAAAAAAAAAAAAAAAAAAAAAAAAAAAAAAA 1119
```

Figure 6

Partial *dip2* cDNA sequence.

This Figure shows the sequence of the 1.2 kb partial *dip2* cDNA isolated in yeast interaction trap screening. The partial amino acid sequence (337 residues) of the predicted protein is also shown. It contains no known functional domain. The stop codon on the cDNA is indicated with an asterix. The cDNA fragment belongs to the 3' end of the corresponding mRNA. The 53 amino acids sequence that is unique to the *Drosophila* DIP2 homolog is highlighted.

Partial *dip2* cDNA and the predicted amino acids sequence:

```
AGAGTGCAACTGACCCAGCAGTTCTGCAAGCTATTTCAAGCCCTTGGTCTGAATACGCGC 60
 R  V  Q  L  T  Q  Q  F  C  K  L  F  Q  A  L  G  L  N  T  R
TGCGTGTCAACTTCGTTTGGATGTCGTGTAAATCCGGCCATTTGTGTCCAAGGGGCTAGT 120
 C  V  S  T  S  F  G  C  R  V  N  P  A  I  C  V  Q  G  A  S
TCTGCAGAGAGTGCTCAAGTGTATGTAGATATGAGAGCATTGCGAAATAATCGTGTTGCT 180
 S  A  E  S  A  Q  V  Y  V  D  M  R  A  L  R  N  N  R  V  A
CTGGTAGAGCGTGGAGCGCCAAATTCGTTGTGTGTAATTGAATCAGGTAAACTTTTACCA 240
 L  V  E  R  G  A  P  N  S  L  C  V  I  E  S  G  K  L  L  P
GGCGTAAAAGTGATAATTGCAAATCCCGAAACTAAGGGCCACTGTGGCGACTCGCATTTG 300
 G  V  K  V  I  I  A  N  P  E  T  K  G  H  C  G  D  S  H  L
GGAGAAATCTGGGTTCAAGCTCCTCACAACGCACATGGTTACTTTACAATTTATGGTGAC 360
 G  E  I  W  V  Q  A  P  H  N  A  H  G  Y  F  T  I  Y  G  D
GAAACTGACTACAATGATCACTTCAACGCGAAATTGGTAACTGGGGCCACCTCAGAACTA 420
 E  T  D  Y  N  D  H  F  N  A  K  L  V  T  G  A  T  S  E  L
TATGCACGCACTGGGTATTTAGGATTCTTACGCCGCACCGAATGCTCGCAATCAGCATCA 480
 Y  A  R  T  G  Y  L  G  F  L  R  R  T  E  C  S  Q  S  A  S
CTGCTTGACGAGACCACACCAAGTGTGGCAAGTCGCGATAGTGATACAGAATCTTTGAAT 540
 L  L  D  E  T  T  P  S  V  A  S  R  D  S  D  T  E  S  L  N
TCGATAAGTCAATTGCAACTAAATTTTTCAAATGTTTCCTTGGGTGGAAATTCCGAGCAT 600
 S  I  S  Q  L  Q  L  N  F  S  N  V  S  L  G  G  N  S  E  H
AGCCTGGTAGGCGGCGCAAGCAATGCTAATGATCAAGAACTACACGACGCAGTGTATGTA 660
 S  L  V  G  G  A  S  N  A  N  D  Q  E  L  H  D  A  V  Y  V
GTCGGAGCTGTTGATGAAATGATCTCTTTACGTGGCATGAACTATCACCCAATTGATATC 720
 V  G  A  V  D  E  M  I  S  L  R  G  M  N  Y  H  P  I  D  I
GAAAATTCGGTAATGCGCTGTCACAAAAAAATTGCTGAGTGCGCCGTTTTCACCTGGACT 780
 E  N  S  V  M  R  C  H  K  K  I  A  E  C  A  V  F  T  W  T
AACTTATTAGTCGTTGTTGTCGAGTTGGACGGCAATGAATCAGAAGCTTTGGATTTGGTT 840
 N  L  L  V  V  V  V  E  L  D  G  N  E  S  E  A  L  D  L  V
CCCTTGGTCACAAACACAGTATTAGAAGATCATCAGCTTATAGTCGGCGTTGTAGTGGTC 900
 P  L  V  T  N  T  V  L  E  D  H  Q  L  I  V  G  V  V  V  V
GTTGATCCAGGTGTGGTGCCTATTAATAGTCGGGGCGAAAAGCAACGGATGCATTTACGG 960
 V  D  P  G  V  V  P  I  N  S  R  G  E  K  Q  R  M  H  L  R
GATGGTTTTCTGGCCGACCAATTGGATCCCATATACGTAGCATATAACATGTAAATACAC 1020
 D  G  F  L  A  D  Q  L  D  P  I  Y  V  A  Y  N  M  *
AATTATTCTTATGATGAAATCGCCGTATTAAGAAACGTTACAAAACGTTGTNTTNGTATC 1080
ATAATTCAAAACAACCGCAATCCACAAAAAAACAGAAATGGCTCATTTTGGTAACACGCA 1140
CGCCTAATTACACATTTCCTTTTAGAGTATTAGCAAAGATGGTAAAACATTCTTACAATA 1200
AAATGACTATTTATCTTTATATGACCATAT 1230
```

II. Verification of the interactions between DISCO and its interacting proteins DIP1 and DIP2 seen in the interaction trap assay.

A. In-Vitro Binding Assay.

The specificity of interaction between DISCO and the proteins isolated from the interaction trap screening were examined *in-vitro*. For this study, the individual proteins were prepared as follows; *disco* was expressed as a GST-fusion protein in *E. coli*, the *dip1* and *dip2* cDNAs were transcribed and translated *in-vitro*.

The 186 amino acids N-terminal DISCO fragment used in the yeast interaction trap was also used for the *in-vitro* binding assay. Since we were unable to use the wild-type DISCO protein for the yeast interactor hunt, to rule out the possibility of a non-specific interaction between the mutated DISCO protein and the library proteins, we used both wild-type and mutated N-terminal DISCO fragments for the *in-vitro* analysis.

For *in vitro* expression of the *dip1* and *dip2*, the corresponding cDNAs were cloned into the *in vitro* expression vector pSPUTK (MBI Fermentas). SP6 RNA polymerase was used to drive transcription of these cDNAs. The translation was done in rabbit reticulocyte lysate (MBI Fermentas). [S^{35}]Methionine was used to radiolabel the translated protein.

Purified GST-DISCO fusion proteins (bound to glutathione beads) were allowed to bind to the *in-vitro* expressed DIP1 and DIP2 proteins. Bound proteins were eluted from the glutathione-agarose beads and analyzed on denaturing SDS-polyacrylamide gel. Only if *in-vitro* translated DIP1 and DIP2 are able to bind DISCO will these proteins be present in the eluant, and the radiolabeled

proteins can be detected by autoradiography. Results of this experiment are shown in Figure 7. Both wild-type and mutated DISCO fragments were able to bind the *in-vitro* expressed DIP1 (lanes 6 and 7) and DIP2 (lanes 2 and 3) proteins to the same extent. GST alone, without the N-terminal DISCO fragment was unable to bind either one of these proteins (lanes 8 and 4). Therefore, the *in-vitro* binding assay showed a direct physical association between DISCO and DIP1/ DIP2.

B. The mRNA expression pattern of *disco* overlaps with that of *dip1* and *dip2*:

The expression pattern of the genes encoding the interacting proteins in *Drosophila* embryo should overlap with that of *disco* at least partially if these are true *in-vivo* interactors of DISCO. To examine this we determined the mRNA expression pattern of *dip1*, and *dip2* during various stages of embryogenesis. For *in-situ* expression studies, a digoxygenin labeled RNA probe was synthesized from a *dip2* cDNA and non-repeated portion of the *dip1* cDNA.

The *dip1* mRNA shows a ubiquitous expression pattern at all stages of embryogenesis. However, the expression is not homogeneous, rather, more concentrated in the developing CNS (Figure 8). Expression pattern of the *dip1* mRNA overlaps with that of *disco* in the developing optic lobe. The cells of the optic lobe primordium invaginate from the posterior portion of the procephalic lobe (embryonic head) during stages 12. This tissue remains attached to the larval brain until stages 15-16, when it is completely incorporated into the brain hemispheres (Green *et al.*, 1993). Figure 10 shows stage 13 embryos to compare overall expression patterns of *dip1* and *disco*. The *dip1* expression also overlaps with *disco* in the visceral mesoderm and the epidermis of gnathal and thoracic

segments. Visceral mesoderm staining becomes evident during stages 12 and 13, the last stages of germ band retraction. Following these stages, the cells of the visceral mesoderm elongate and contact the midgut primordia and eventually form a sheet around the gut (Campos-Ortega and Hartenstein, 1985).

The *dip2* mRNA shows extensive expression in the CNS throughout embryogenesis (Figure 9). Expression is seen in the optic lobe (OL) primordium starting from stage 12. Expression in the OL is seen at later stages as well. Staining in this tissue is shown in a stage 15 embryo, at which stage the OL has already been incorporated in the larval brain. A lower level of expression of the *dip2* mRNA may also be present at least in a portion of the peripheral nervous system. However, due to the lower resolution of the *in-situ* procedure, we were unable to unambiguously detect the peripheral nervous system expression pattern of the *dip2* mRNA. In addition, expression of the *dip2* mRNA is also seen in the visceral mesoderm during stages 12 and 13 (expression in a stage 12 embryo is shown in Figures 9 and 10). The expression pattern of the *dip2* mRNA partially overlaps with that of *disco* in the optic lobe primordium, and the visceral mesoderm (Figure 10).

Figure 7

Results of the *in vitro* binding assay:

Panel A depicts the results of the *in-vitro* binding assay. *In-vitro* translated partial DIP2 (40 kDa) and DIP1 (29 kDa) proteins are shown in lane 1 and 5 respectively. Both the wild-type and the mutated DISCO proteins are able to bind the *in-vitro* translated DIP2 (lanes 2 and 3) and the DIP1 (lanes 6 and 7) proteins. GST alone is not able to bind either protein (shown in the control lanes 4 and 8).

Panel B shows the expression of the GST-DISCO fusion proteins (48 kDa) expressed and purified from *E. coli.* BL21 strain. Lane 1 shows expression of the GST protein alone. Lane 2 and 3 show expression of GST-fusion proteins (48 kDa) containing the wild-type N-terminal DISCO fragment and a mutated N-terminal DISCO fragment respectively. The mutated DISCO fragment contains a Cys127 to Ser127 substitution.

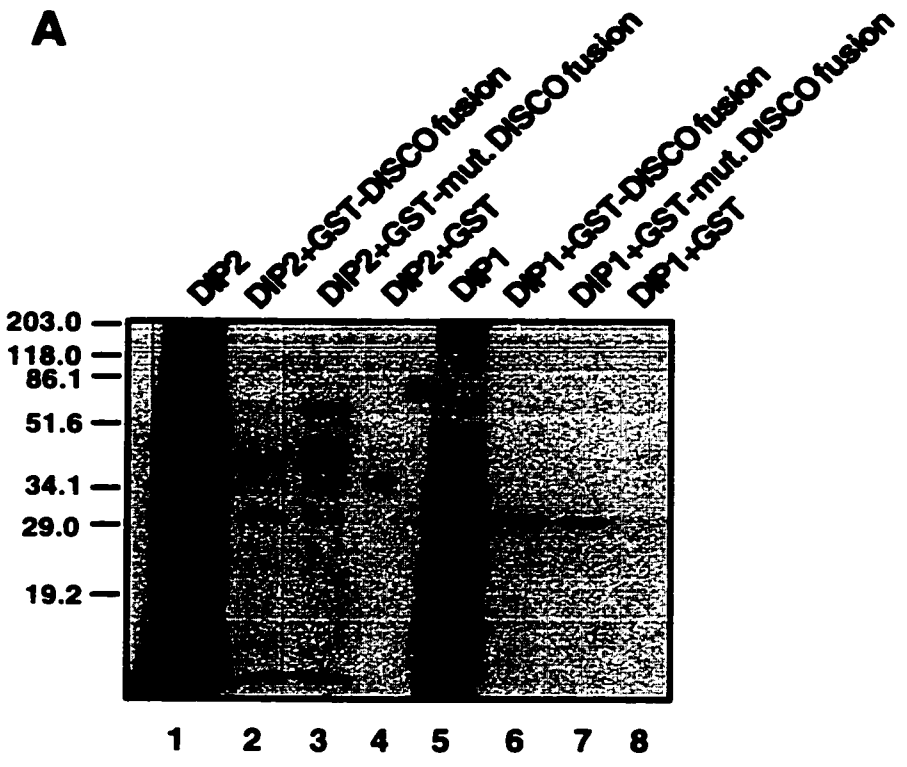
A
DIP2
DIP2+GST-DISCO fusion
DIP2+GST-mut. DISCO fusion
DIP2+GST
DIP1
DIP1+GST-DISCO fusion
DIP1+GST-mut. DISCO fusion
DIP1+GST
203.0
118.0
86.1
51.6
34.1
29.0
19.2
1 2 3 4 5 6 7 8
B
GST
GST-DISCO fusion
GST-mut. DISCO fusion
203.0
118.0
86.1
51.6
34.1
29.0
19.2
1 2 3

Figure 8

mRNA expression pattern of the *dip1* gene:

The results of the *in situ* mRNA expression study are shown in this Figure. Expression in three different stages of embryogenesis (stages 9, 12 and 14) are shown. Only lateral views are shown. Anterior is to the left and dorsal side is up. Embryo staging was done according to Campos-Ortega and Hartenstein, 1985. A ubiquitous expression pattern of *dip1* mRNA is seen at all stages of embryogenesis. Expression of the *dip1* mRNA in the optic lobe primordium (arrow) is shown in the stage 12 embryo, the last stage of germ band retraction. Because of the superficial view of the embryo, expression in the invaginated optic lobe primordium can not be seen clearly. At this stage expression of the *dip1* mRNA is evident in the visceral mesoderm (VM) and in a variety of other tissues, including the epidermis of gnathal (GN) and thoracic segments (T). At all stages, the expression appears to be more concentrated in the developing CNS than other parts of the embryo. In the stage 14 embryo, the CNS is indicated with an arrow with white arrowhead.

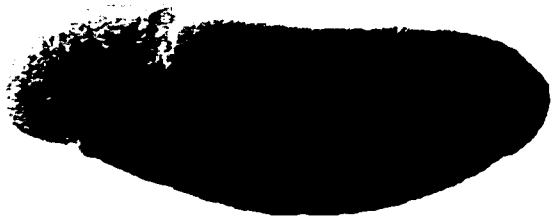

Stage 9

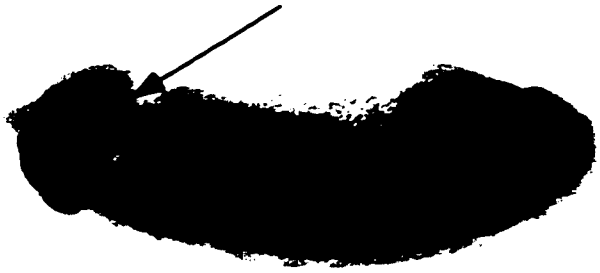

Stage 12

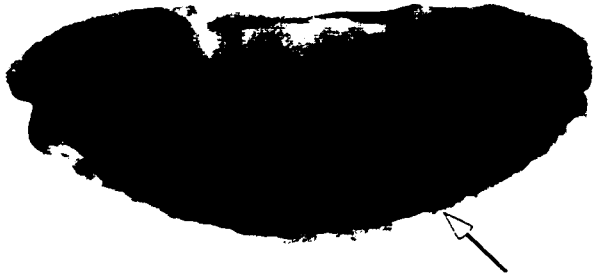

Stage 14

Figure 9

mRNA expression pattern of the *dip2* gene:

This Figure shows the *dip2* mRNA expression pattern during different stages (stage 11, 12 and 15) of embryogenesis. Expression in the CNS (arrows with white arrowheads) is seen at all stages of development. At around stage 12 expression in the visceral mesoderm (VM) is clearly visible. The location of the optic lobe primordium is indicated with an arrow. Because of the superficial view of the embryo, the OL can not be clearly seen.

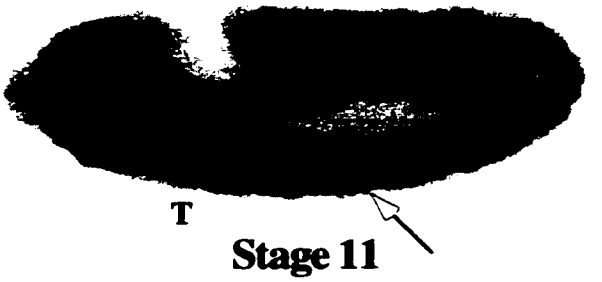

Stage 11

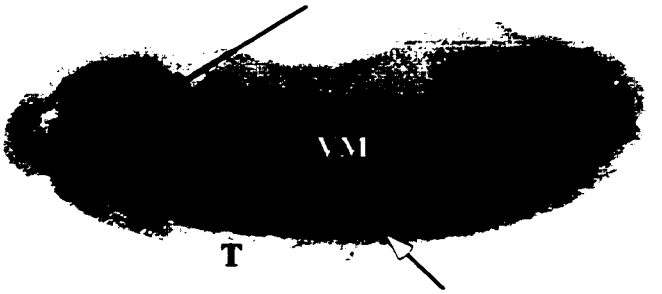

Stage 12

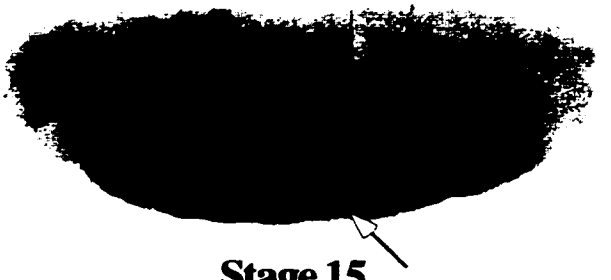

Stage 15

Figure 10

Expression patterns of *dip1* and *dip2* overlap with that of *disco*.

In this Figure, expression patterns of the *dip1* and *dip2* mRNAs are compared with that of the *disco* at embryonic stage 12. *disco* expression is seen in the optic lobe primordium (arrow) , in the gnathal (GN) segments, in the ectoderm of thoracic segments (T) and in the visceral mesoderm (VM). The expression pattern of *dip1* and *dip2* mRNAs overlap with that of *disco* in the optic lobe primordium (arrow) and the visceral mesoderm (VM). *dip1* and *disco* expression patterns also overlap in the ectoderm of gnathal and thoracic segments.

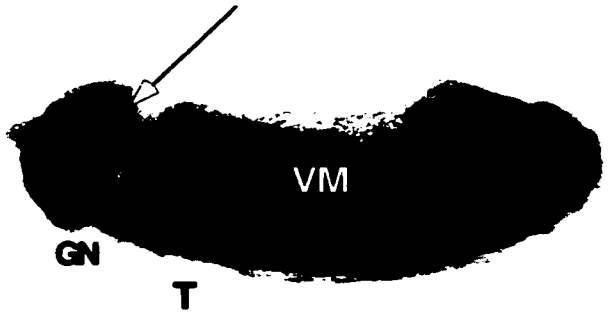

DIP1

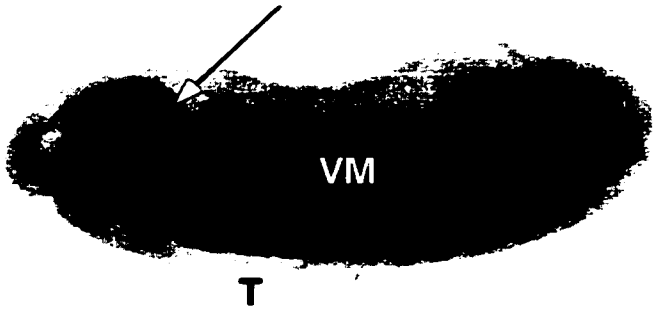

DIP2

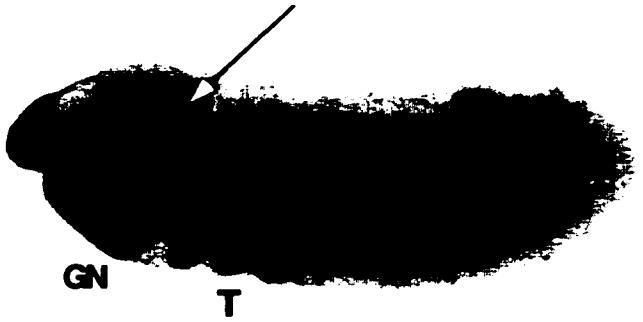

DISCO

III. Characterization of the *dip1* cDNA:

A. Cloning of the full-length *dip1* cDNA:

A partial 1.1 kb 3' end fragment of the *dip1* cDNA was isolated in the interaction trap screen. In order to isolate the full-length *dip1* cDNA, another 12-24 hours *Drosophila* embryonic cDNA library made in λgt11 phage vector was amplified and screened. The library (obtained from Dr. Roger Jacobs, McMaster University) was made by cloning cDNAs synthesized from embryonically expressed *Drosophila* mRNAs into the EcoRI site of the phage-vector.

About 2 X 10^6 plaques from the library were screened with a probe made from the *dip1* cDNA fragment isolated from the yeast interaction trap library. Three positive plaques containing *dip1* cDNA fragments were isolated. The sizes of the cDNA inserts were examined by digesting the phage DNA with EcoRI. Two of the positive plaques contained only a small fragment, about 1 kb in length. The third plaque contained two EcoRI fragments of approximately 2.5 kb and 0.5 kb length. Both fragments were subcloned into the EcoRI site of the SK^- pPBluescript vector and sequenced. Since, we used only a 1.1 kb 3' end dip1 cDNA fragment as probe, the two smaller cDNAs (~ 1kb) are presumably part of the larger cDNA isolated in this screen. However, we can not exclude the possibility that the smaller cDNAs may also represent the differentially spliced *dip1* transcript.

B. Sequence analysis of the *dip1* cDNA:

Sequence analysis of the 2.5 kb and 0.5 kb fragments of the *dip1* cDNA showed that the 0.5 kb fragment corresponds to the 3' end and the 2.5 kb

fragment corresponds to the 5′ end of the cDNA. The 2.5 kb fragment contained the full coding region of the *dip1* cDNA (Figure 11).

The number of 124 bp repeats present in the two cDNAs isolated from the yeast interaction trap library and the λgt11 library differ from each other. The newly isolated cDNA contains estimated 8-10 repeats as opposed to 4 repeats present in the previously isolated cDNA (Figure 12A.). Following the repeated region, an EcoRI site and a 48 bp sequence are common in both cDNAs. The 48 bp sequence is followed by a poly A tail in the *dip1* cDNA isolated from the yeast vector. On the other hand, the cDNA isolated from the λgt11 vector contained an extra 348 bp sequence between the 48 bp sequence and the polyA tail. This difference in sequence might indicate that these cDNAs represent two alternatively spliced forms of the *dip1* mRNA. The differences between the two cDNAs are diagrammatically represented in Figure 12A. The sequence of each individual repeat is shown in Figure 12B.

Considering the presence of 8 repeats, the cDNA isolated from the λgt11 vector is about 2.6 Kb. The exact number of repeats present, and as a result the exact size of the cDNA, was difficult to determine due to difficulty in generating primers with unique sequences. There is a putative start codon 263 bp downstream from the 5′ end of the cDNA fragment and a 927 bp open reading frame that may represent the full coding sequence for the DIP1 protein. It is not certain if this cDNA contains the complete 5′ untranslated region of full-length *dip1* cDNA. Sequence analysis through 'BLAST' search (Altschul et al., 1990) showed that the putative 309 amino acids DIP1 protein contains an additional dsRNA-binding motif N-terminal to the motif predicted before. Double stranded RNA binding domains (dsRBD) are usually about 70 bp long. A

consensus sequence for dsRNA binding domains has been determined (St. Johnson et al., 1992) from seven copies of the dsRBD motifs in Xlrbpa, Staufen and human TRBP proteins. Each full-length motif consists of an N-terminal large domain and a C-terminal short domain. Two types of dsRBDs have been recognized and are denoted as type A and type B (St. Johnston *et al.*, 1992). The type A dsRBDs show strong similarity to the entire length of consensus sequence defined for dsRBDs. While type-B dsRBDs match well with the basic C-terminal short domain consensus, but show only poor similarity to the N-terminal long domain consensus. The putative DIP1 protein contains two type B dsRBDs . Figure 13 shows alignment of the putative dsRNA binding domains of DIP2 with that of other proteins known to bind dsRNA. The two dsRNA- binding motifs of the DIP1 protein share significant similarity with the C-terminal consensus, but, match poorly with the N-terminal large domain consensus. The dsRNA binding domains of DIP1 share striking similarity with that of mammalian glutamate receptor editases (Melcher, T. et al., 1996; Lai *et al.*, 1997). The similarity extends far beyond the consensus for dsRNA binding motifs (Figure 14). In addition, the predicted protein also contains a putative bipartite nuclear localization signal similar to that present in the glutamate receptor editases. Bipartite nuclear localization motifs are composed of: two basic amino acids, a spacer region of any ten amino acids followed by a basic cluster of five amino acids, three of which must be basic (Dingwall and Laskey, 1991). Figure 11. shows that the putative nuclear localization signal in the predicted DIP1 protein (**KR**KKSSERTRDK**KLRQN**) meets this criterion. The sequence similarity between the nuclear localization signal and the dsRBDs of the predicted DIP1 protein with mammalian glutamate receptor editases are shown in Figure 14.

Figure 11

Sequence of the *dip1* cDNA that contains the full coding region:
This Figure shows the sequence of the *dip1* cDNA (about 2.6 kb) isolated from the λgt11 library. Eight repeats in the 3'UTR are shown. The first three nucleotides of each repeat are shown in (boldface). The repetitive region ends with an EcoRI site (GAATTC, shown in boldface and is underlined). The EcoRI site is followed by a 396 bp sequence and a polyA tail. The 348 bp sequence preceding the polyA tail is unique to this *dip1* cDNA. The predicted protein sequence is also shown. The putative start codon is located 263 bp downstream from the 5' end of the cDNA. The stop codon (*) is located at the very beginning of the first repeat (at nucleotide position 1188). The putative bipartite nuclear localization signal (NUC) in the predicted protein (from amino acids 45-62) is underlined. The consensus for NUC consists of two basic amino acids, a 10 amino acids spacer region and a cluster of five amino acids out of which at least three should be basic. The basic amino acids in the bipartite signal are shown in boldface. Two putative dsRNA-binding domains of the protein are highlighted.

Sequence of *dip1* cDNA and the predicted DIP protein:

```
ACGATTCTTTCTGTGACCTGAGCAGTGAAAAATTAAATTACAAAAGCGAAAAAGCGAATT 60
ACAAAAGCCGCCAATGTCCAGGAGCAGCAGTCTTCTCCGGTGGCTTTATATCCGACATCG 120
GCCTCCCCCGGTGGCTGTTCAATCGCCACAGGACGCATTTTTGGCTGTTCAGTCGCCAGGG 180
GCTCCTGCCCCCGTTCAACTGGCCAACTCGTCCGACCAGCAGAATAATCCGGATGCGGAC 240
GCCATTGCCTCCAAACTGCCCATGCCAGTTATCATCAAGGAGGAGCCGATCTCTGTCAAC 300
                          M  P  V  I  I  K  E  E  P  I  S  V  N  13
GATGAACCGTCCGTCGACAATATAGAGGACAATACCAGTGCCAGTACCAGTGCCAGCGGC 360
 D  E  P  S  V  D  N  I  E  D  N  T  S  A  S  T  S  A  S  G  33
ATCGGGGGCAAGATCCCATTTAAAAAAATCTTCCAAAAGCGCAAGAAGTCGTCTGAACGC 420
 I  G  G  K  I  P  F  K  K  I  F  Q  K  R  K  K  S  S  E  R  53
ACTCGGGACAAGAAGTTGCGACAGAACCGCCAGCTGCGCAAGTCCATGCTCCCCAAGAAC 480
 T  R  D  K  K  L  R  Q  N  R  Q  L  R  K  S  M  L  P  K  N  73
GCTCTGATGGCCCTCAACGAGGTGAAGGGCGTGACCATCAGCGATTTCACCATCGACAGC 540
 A  L  M  A  L  N  E  V  K  G  V  T  I  S  D  F  T  I  D  S  93
AATACCGACGGGGGATTCACGGCCGTTGTCACTGTCAACTCGAATCAGTACGAGGGCAAG 600
 N  T  D  G  G  F  T  A  V  V  T  V  N  S  N  Q  Y  E  G  K  113
GGTACCTCGAAAATGACAGCCAAGAACGCGGCCTGCGAGAAGGCTTGGCGCGATTTTATT 660
 G  T  S  K  M  T  A  K  N  A  A  C  E  K  A  W  R  D  F  I  133
ATTGCAAAAATGACCCCCAAGCCGCCCCGTATTCACCAGGTGGAGATGGGTTCGGAGCCA 720
 I  A  K  M  T  P  K  P  P  R  I  H  Q  V  E  M  G  S  E  P  153
ATGGATATCAACGAGGATGAGGCCGATGCACCGGATGATGATCTGCCCATGTTGAATCTG 780
 M  D  I  N  E  D  E  A  D  A  P  D  D  D  L  P  M  L  N  L  173
GCCTCGTTTGCCATCTACAAGCTGTTCGCGGAGTGGGAACGGGAGGGCTATGTCGTGCCC 840
 A  S  F  A  I  Y  K  L  F  A  E  W  E  R  E  G  Y  V  V  P  193
GAGATGCACCCTTCGGCCAATGCTGCCCAACAGGCGGGAGGGGATGCCGGAACTCCAGTT 900
 E  M  H  P  S  A  N  A  A  Q  Q  A  G  G  D  A  G  T  P  V  213
CCCCCCGTGCCGAAGGAGCCAAAGAAGCCGCCAGTGCGCACCGAGCTACCCTCTGGCTGG 960
 P  P  V  P  K  E  P  K  K  P  P  V  R  T  E  L  P  S  G  W  233
GAGACCATGCACCCGGCGACCATTCTTTGCATTATGCGTCCGGGACTCAACTACGTGGAC 1020
 E  T  M  H  P  A  T  I  L  C  I  M  R  P  G  L  N  Y  V  D  253
TACGGGTCATCTGGCGACAAGACCAACGGCATGCAGCATCTGGGAATCATGGTGGACAAC 1080
 Y  G  S  S  G  D  K  T  N  G  M  Q  H  L  G  I  M  V  D  N  273
CAGGAGTTCCACGCCAACGGCAGATCAAAGAAAATCGCCCGTCGCAACGTGGCCGTGAAA 1140
 Q  E  F  H  A  N  G  R  S  K  K  I  A  R  R  N  V  A  V  K  293
GTGTGCAACTCTCTGTTCGGCACCAACTTCACCTACAGCGACACCACTTAAGACACCAAC 1200
 V  C  N  S  L  F  G  T  N  F  T  Y  S  D  T  T  *           309
TCCAACCGCAGACTCCAACTGCCGACGACAACACACATAACGGACACTCTTAACGGACAG 1260
CAATCAGAAGATTGCGACCCTGACGTCAATTGCGCAACTTTAAGCGACACCACTTAAGAC 1320
ACCAACTCCAACCGCAGACTCCAACTGCCGACGACAACACACCTATGCCTCTCTTAACGG 1380
ACAGCAATCAGAAGATTGCGACCCTGACGTCAATGGCGCAACTTTAAGCGACACCACTTA 1440
AGACACCAACTCCAACCGCAGACTCCAACTGCCGACGACAACACACCTATGCCTCTCTTA 1500
ACGGACAGCAATCAGAAGATTGCGACCCTGACGTCAATGGCGCAACTTTAAGCGACACCA 1560
CTTAAGACACCAACTCCAACCGCAGACTCCAACTGCCGACGACAACACACCTATGCCTCT 1620
CTTAACGGACAGCAATCAGAAGATTGCGACCCTGACGTCAATGGCGCAACTTTAAGCGAC 1680
ACCACTTAAGACACCAACTCCAACCGCAGACTCCAACTGCCGACGACAACACACCTATGC 1740
CTCTCTTAACGGACAGCAATCGGAAGATTGCGACCCTGACGTCAATGGCGCAACTTTAAG 1800
CGACACCACTTAAGACACCAACTCCAACCGCAGACTCCAACTGCCGACGACAACACACCT 1860
ATGCCTCTCTTAACGGACAGCAATCGGAAGATTGCGACCCTGACGTCAATGGCGCAACTT 1920
TAAGCGACACCACTTAAGACACCAACTCCAACCGCAGACTCCAACTGCCGACGACAACAC 1980
ACCTATGCCTCTCTTAACGGACAGCAATCAGAAGATTGCGACCCTGACGTCAATGGCGCA 2040
ACTTTAAGCGACACCACTTAAGACACCAACTCCAACCGCAGACTCCAACTGCCGACGACA 2100
ACACACCTATGCCTCTCTTAACGGACAGCAATCAGAAGATTGCGACCCTGACGTCAATGG 2160
CGCAACTTTAAGAATTCCTTTTCTGTCAAAGTGAAGAGGCATATTAAACAAGAATTTCCC 2220
```

AATTTAGTTTGTATTTGGGACAGCTCTTACTTATGATTTTTTAGGTGGGCCGGAGCCGTT 2280
TTCAACAACGAATAATTTTGAACTGCAAGAGCCGATAAGATTATCCGAATAATCTAAACC 2340
AGGATTCCTTGGTAATGCTGATTAATTTTTTCCGTGTATTTTGCGACACACTGTGGGTTT 2400
GGTTTTTTTGAAAACGCTTCCACAGAAGAGGATTTCAGTGGCAGATTGGGTATCAAATAT 2460
TAATTATGCTTACCAGTGAATTACATTTTTGTCGTAAACTAGATTAAGCTAAATGGGTGG 2520
TATAATTACTTGATTTTTTAAAAACATGAAGACATAAGTACATGTATTGAATATAAAAAAA 2580

Figure 12

Difference in the 3'UTR of the *dip1* cDNAs:

Panel A shows the features of the two *dip1* cDNAs. In this Figure, the cDNA (1104 bp) isolated from the yeast interaction trap library is denoted as $cDNA^1$. It is a partial cDNA that lacks the 5′ end of the corresponding mRNA. The cDNA isolated from the λgt11 library is denoted as cDNA2. The exact size of the cDNA is not known. It contains at least 8 repeats. The first and the last repeats of $cDNA^1$ and $cDNA^2$ are identical. The last repeat is interrupted with an EcoRI site. The numbers of middle repeats are different in the two cDNAs. All of the middle repeats in either cDNA have exactly same nucleotide sequence. In $cDNA^2$, the location of the putative start codon at 263 bp and the stop codon at 1188 bp from the 5′ end of the cDNA are indicated with vertical lines. The location of the putative nuclear localization signal coding sequence (nuc, nucleotides 396-447 and the two dsRNA-binding motif coding sequence (nucleotides 462-660 and 1020-1164 respectively) are shown in $cDNA^2$. The position of the C-terminal dsRNA-binding domain coding sequence present in $cDNA^1$ is also shown. **Panel B** shows the sequences of the individual repeats. The first repeat is 126 bp long. The nucleotide sequences of all the 124 bp middle repeats in either cDNA are exactly equivalent. The last repeat is 121 bp long. The nucleotide sequence of the first repeat is different from that of other repeats in the region that is underlined.

A

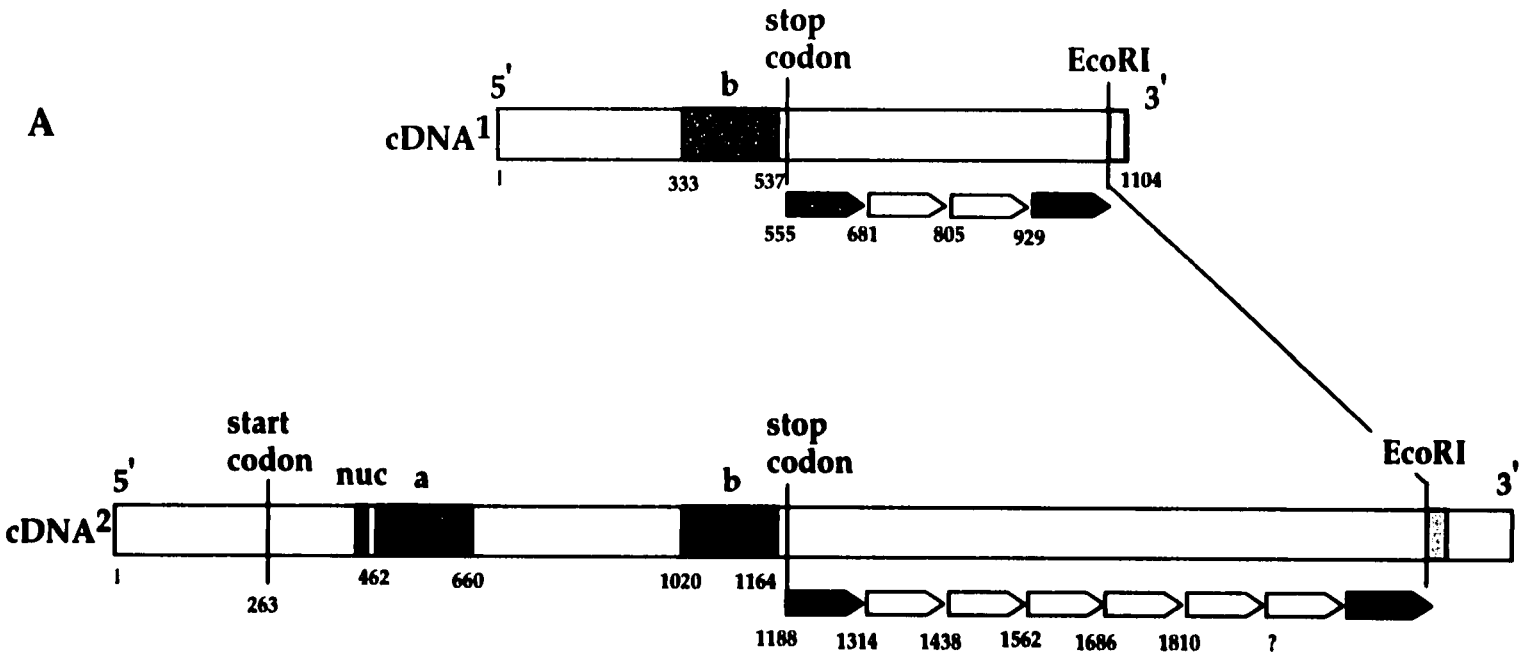

B

First repeat (126 bp)

CACCACTTAAGACACCAACTCCAACCGCAGACTCCAACTGCCGACGACAACACACATAACGGACA
CTCTTAACGGACAGCAATCAGAAGATTGCGACCCTGACGTCAATTGCGCAACTTTAAGCGA

Middle repeats (124 bp)

CACCACTTAAGACACCAACTCCAACCGCAGACTCCAACTGCCGACGACAACACACCTATGCCTCTC
TTAACGGACAGCAATCAGAAGATTGCGACCCTGACGTCAATGGCGCAACTTTAAGCGA

Last repeat (121 bp)

CACCACTTAAGACACCAACTCCAACCGCAGACTCCAACTGCCGACGACAACACACCTATGCCTCTC
TTAACGGACAGCAATCAGAAGATTGCGACCCTGACGTCAATGGCGCAACTTTAAG

Figure 13.

Alignment of the putative dsRNA binding domains of DIP1 with the RNA-binding domain consensus:

The top portion shows the predicted protein sequence for *dip1*. The positions of the two dsRNA-binding domains (67-135 and 234-301) are shown in blue.

The bottom part shows the alignment of the putative RNA binding domains of DIP1 with those of known dsRNA binding proteins and the consensus for dsRNA binding domains (dsRBD). In the consensus, the uppercase letters indicate the most frequently found conserved residues, while the lower case amino acids are conserved in relatively fewer number of dsRBDs. The consensus sequence (about 70 amino acids long) has two distinct segments, denoted as N-terminal long domain consensus (shown in green), and C-terminal short domain consensus (shown in red). The dsRNA-binding domains of DIP1 represent type-B dsRBDs that match well with the C-terminal short domain consensus (orange), but show only a weak similarity with the N-terminal long domain consensus. The dsRNA-binding domains used for the alignment are as follows: first dsRBDs of *Drosophila* Staufen-1 and human TAR-binding protein hTRBP1; the dsRBD of the mammalian transcription factor NF-NT90 and two dsRBDs of the glutamate receptor editases hRED1-1 and hRED1-2.

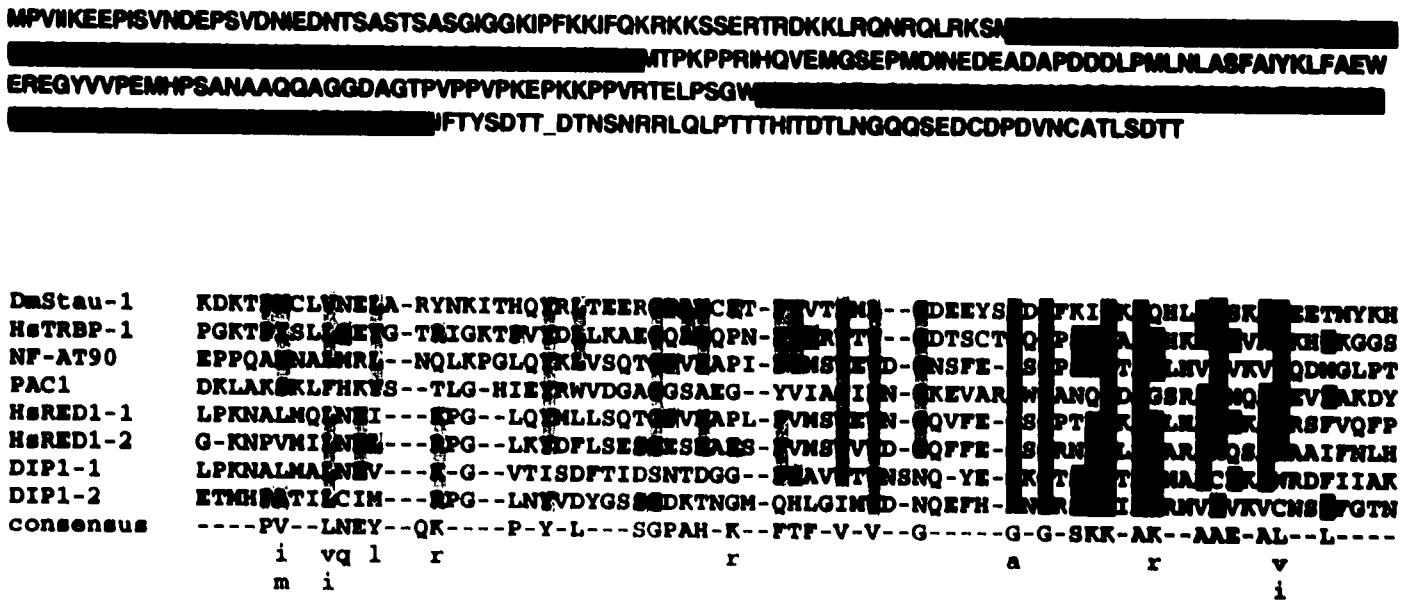
MPVNKEEPISVNDEPSVDNEDNTSASTSASGIGGKIPFKKIFQKRKKSSERTRDKKLRQNRQLRKSA
MTPKPPRIHQVEMGSEPMDNEDEADAPDDDLPMLNLASFAIYKLFAEW
EREGYVVPEMHPSANAAQQAGGDAGTPVPPVPKEPKKPPVRTELPSGW
IFTYSDTT_DTNSNRRLQLPTTTHITDTLNGQQSEDCDPDVNCATLSDTT
DmStau-1
HsTRBP-1
NF-AT90
PAC1
HsRED1-1
HsRED1-2
DIP1-1
DIP1-2
consensus

Figure 14

Alignment of the predicted DIP1 protein with the N-terminal region of mammalian glutamate receptor editases:

This Figure shows the alignment of the putative nuclear localization signal (nuc) and dsRNA binding domains of DIP1 with those of human and rat glutamate receptor editases (hRED1, and rRED1 respectively). The putative DIP1 protein shares similarity with the bipartite nuclear localization signals (nuc) of hRED1 and rRED1. Identical amino acids are shown in blue (purple), conserved changes are shown in violet (pink) and similar amino acids are shown in yellow. The consensus for dsRNA-binding domains (shown in red) is underlined. It is evident that the similarity between the dsRBDs of DIP1 and glutamate receptor editases extends beyond the conserved amino acids.

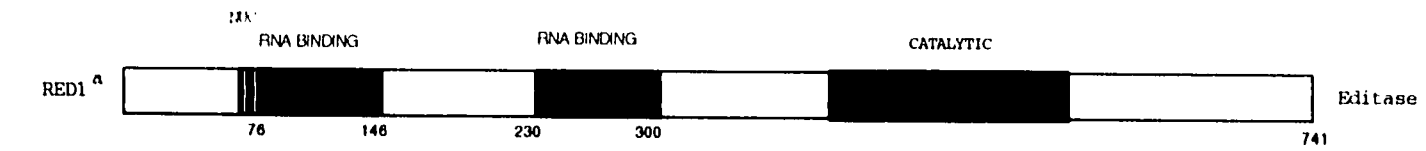


```
rRED1   M D I ED  E E IM   S S ST D VE   RR NIDN N   E   S S T   G PG DRIP  L  N QRRRS  TS R KR PL  E  GS  G  R  KYR LK FP R KT   73
hRED1   M D I ED  E E IM   S S ST D VE   RR NIDN V   E   G S T   G PG DRQ  L  N QRRRS  RG R KR HL  E  GS  G  R  KYR LK FP R KT   73
DIP1    M P V II  K E  E   I S VN D EP   VD N IED N   A   T S A   G IG GEIP  P  K      IF Q KR EE   ER  R  R  KLR QN   R Q L   65

CONSENSUS b  Pv   LnEy   qk     p  Y l   sGPaH   k  FTf   v v     g     G G   SKK   AK   AAe   AL    L

rRED1   RG  V LPKNALM  Q LNE  I K PG LQYML  LS QT  P  RG  PL P  MS VE VN  Q V P BG  G  TK E  AK IH A  EKA  L R  P V QFP   100
hRED1   RG  V LPKNALM  Q LNE  I K PG LQYTL  LS QT  P  RG  PL P  MS VE VN  Q V P BG  G  TK E  AK IH A  EKA  L R  P V QFP   100
DIP1    RK  M LPKNALM  A LNE  V K G VTIPD  FT ID  H  DG  G P  AV VT VN  N Q Y BG  G  SK N  AK NA A  EKA  WR  P I IIA    91

rRED1   NA  E HLAMGRT  L VN T D F  D QAD FPD      T LP NG FE TID K S E IPF YVG    D  DD SF  S  GDV  L    PVP A  LTQ PP L IPI   226
hRED1   NA  E HLAMGRT  L VN T D F  D QAD FPD      T LP NG FE TID K A E IPF YVG    D  DD SF  S  GDL  L    PVP A  LAQ PP L IVL   226
DIP1    MT  K IRIHQVE  M SE IN D I  D EAD APD DLLIHIL  A SP AI YK LPA EW E PBG YVV PPMI  N NA AQ  A  GDA  T    PVP E  IEK PP V RTEL  229

CONSENSUS b  Pv   L nE y   qk     p  Y l   sGPaH   k  FTf   v v     g     G G   SE K AK   AA e   AL    L

rRED1   PFIPF  SGE N P  MIL IE L RPGL KY IFL  SG E  HAFSFV  M  VV VD  Q F P  GR  KK LA KA  AQ  IA TV P  L HL IQ T P S FQPVL   311
hRED1   PFIPF  SGE N P  MIL IE L RPGL KY IFL  SG E  HAFSFV  M  VV VD  Q F P  GR  KK LA KA  AQ  IA AI P  L HL IQ T P S FQPII   311
DIP1    PSMME  T M H P  TIL CI M RPGL NY VVV  SG D  TD AQH  L  IM VD  Q E P  GR  KK IA RR  AV  CN SL P  T NF TY S D T  T     309
```

[a] Lai, F., Chen, C-X., Carter, K. C. and Nishikura, K. (1997).

[b] St. Johnston, D., Brown, N. H., Gall, J. G. and Jantsch, M. 1992.

C. Northern analysis for *dip1* transcripts:

To examine the size of the *dip1* transcript(s) and detect expression of alternatively spliced forms (if any) of *dip1*, northern analysis was done. Northern analysis was done with polyA$^+$ RNA isolated from 0-22 hours embryos of *Drosophila*.

Two different probes for *dip1* cDNA (with and without the repeated region) were used for northern analysis. Three bands of different size were obtained with the probe lacking the repeated region, indicating the expression of at least three different transcripts for *dip1* during embryogenesis. The sizes of these transcripts are about 3 kb, 2.2 kb and 1.8 kb (Figure15). The cDNA isolated from the λgt11 vector is larger in size than the middle transcript seen on the northern blot. It might represent a partial form of the largest transcript.

Similar sized bands were detected in the northern blots hybridized with probes made from the *dip1* cDNA containing both the repeated and the unique regions. However, the signal was stronger and more diffused when the probe with the repeated region was used (data not shown), indicating the presence of other RNA species that can be detected with the repeated region only.

D. Chromosomal location of the *dip1* gene:

To understand the physiological role of the *dip1* gene, isolation of mutants in which *dip1* gene function is disrupted is essential. In order to identify existing mutants with mutation in a particular gene, the knowledge of its chromosomal location is important. Due to the presence of large polytene chromosomes in *Drosophila*, the chromosomal location of a gene can be readily determined by hybridizing the corresponding probe to a polytene chromosomal preparation

made from salivary glands of third-instar larvae. There are about 5000 polytene bands and the limit of cytological resolution with in-situ hybridization is about 50 kb (Sorsa, 1988). The in-situ hybridization to polytene chromosome was performed with a biotin labeled *dip1* probe. The 1.1 kb *dip1* cDNA fragment isolated from the yeast interaction trap library was used as template to make the biotin labeled probe.

The in-situ hybridization studies localized the *dip1* signal to two locations on the polytene chromosome; band 20A at the base (adjacent to centromere) of the X-chromosome and band 91F on right arm of the third chromosome (Figure 16A). Since the results of northern analysis suggested the possibility of presence of the repeated element of the *dip1* cDNA in other *Drosophila* messages as well, one of the two hybridized regions on the polytene chromosome may represent location of another gene containing the same repeated sequence. To test this hypothesis, an in-situ probe was generated from the non-repeated region of the *dip1* cDNA. This probe hybridized to only band 20A (Figure 16B), confirming that the repeated sequence seen in the *dip1* cDNA is not unique to the *dip1* gene, but, is also present in at least another gene located on the right arm of the third chromosome (Figure 16A). These results implicated the location of the *dip1* gene to be on the band 20A of X-chromosome of *Drosophila*.

Figure 15

Northern analysis for *dip1* mRNA:

This Figure shows the result of northern analysis for *dip1* mRNA. Poly A^+ RNAs isolated from *Drosophila* embryos were hybridized to a probe made from the nonrepetitive region of the *dip1* cDNA. Three distinct bands of approximate molecular weights 3.0 kb, 2.2 kb and 1.8 kb can be seen.

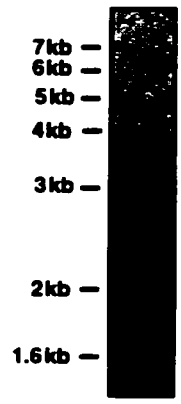
7kb
6kb
5kb
4kb
3kb
2kb
1.6kb

Figure 16

Localization of the *dip1* gene on *Drosophila* polytene chromosome:

Panel A shows that the probe made from the *dip1* cDNA containing both the nonrepetitive and repetitive regions hybridizes to two polytene bands; the band 20A located at the base of the X-chromosome (empty arrow) and band 91F on the right arm of *Drosophila* chromosome III (solid arrow).

Panel B (next page) shows that the probe made from the nonrepetitive region of the *dip1* cDNA hybridizes to only one region of the polytene chromosome: band 20A of the X-chromosome.

A

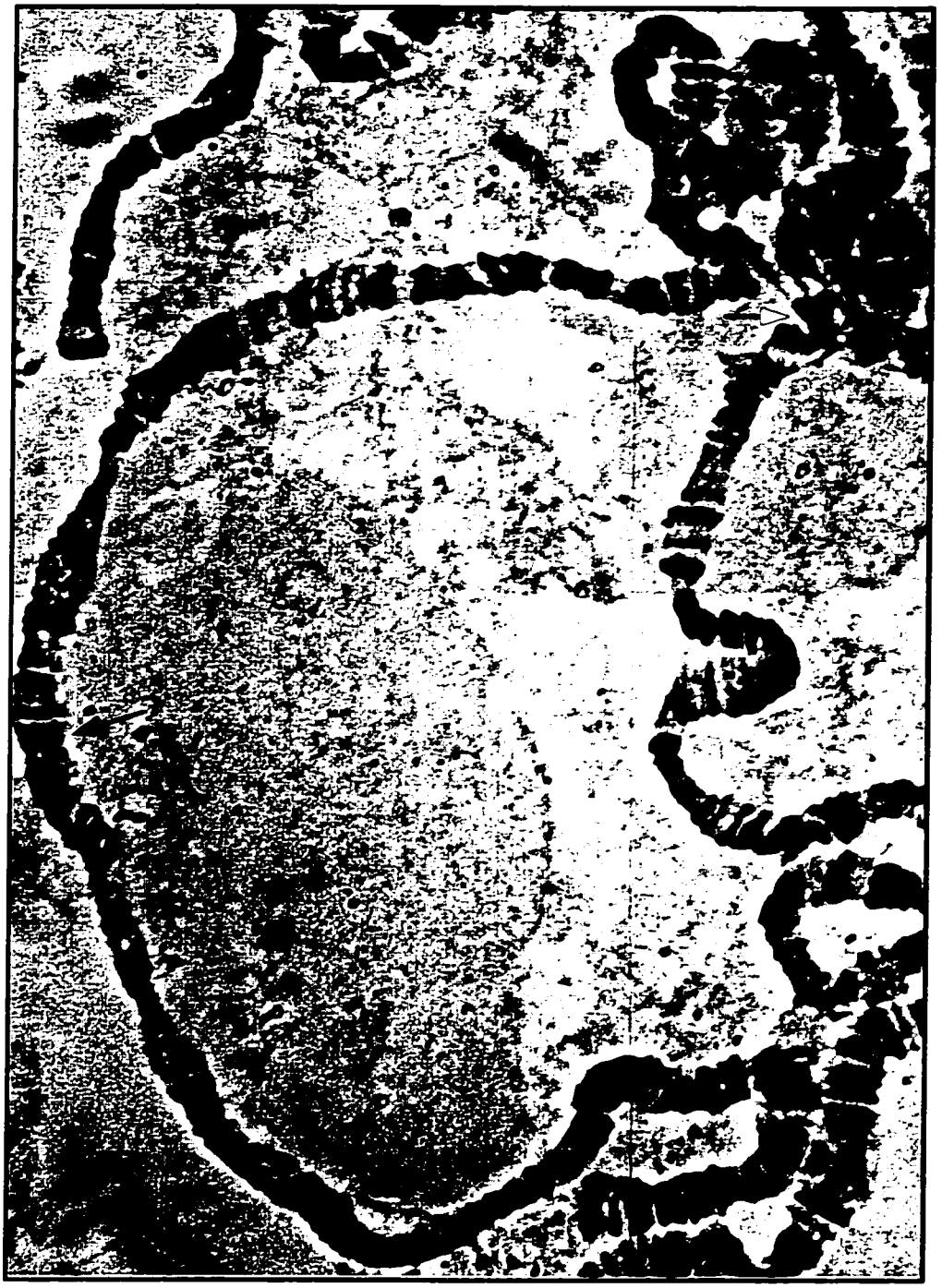

B

E. Deficiency mapping of the *dip1* gene:

In order to determine the genetic location of the *dip1* gene, deficiency mapping was done. This was done by southern analysis of deficiency lines that carry a deletion in the 20A region of the X-chromosome. The presence or absence of the *dip1* gene was followed by a restriction fragment length polymorphism that exists in this region. Since homozygosity of deficiency chromosomes lead to lethality, heterozygous lines in which deficiency chromosomes are kept either under a wild-type or a balancer chromosome were used. For southern analysis the chromosomal DNA was digested with EcoRI or BamHI and hybridized to a probe made from the *dip1* cDNA. Due to the polymorphism, the wild-type, balancer and deficiency chromosomes generated distinct restriction patterns on southern blots.

The results of this study are shown in Table 1 Here, '-' indicates deletion and '+' indicates inclusion of the gene in the deficiency chromosome. The genotypes of the deficiency lines are shown in the 'Materials and Methods' section of this chapter.

Table 1: Results of the deficiency mapping for *dip1*:

Deficiency	Result
Df(1)DCB1-35b	-
Df(1)17-137	-
Df(1)16-2-13	-
Df(1)R22	-
LB6	-
Df(1)S54	-

Df(1)17-257	-
Df(1)A209	+
Df(1)HM430	+
Df(1)R21	+
Df(1)B12	+
Df(1)B1-35C	+
Df(1)R38	+
Df(1)GA22	+

The southern blots from this study are shown in Figure 17. Deficiency map of the *dip1* gene is shown schematically in Figure18. The deficiency map of the *dip1* gene is similar to that of a gene called *flamenco* (Prud'homme *et al.*, 1995). Furthermore, the deficiency maps of the genes located on either side of *flamenco* {*extra organ* (*eo*) and *touch insensitive larvae B* (*tilB*)} do not match with that of the *dip1* gene. These findings raise the possibility that *flamenco* and *dip1* represent the same gene (additional evidence is presented in the discussion section). Therefore, through deficiency mapping we were able to narrow down the genetic location of the *dip1* gene in between *eo* and *tilB*.

Figure 17

Results of the deficiency mapping of *dip1* by southern analysis:
This Figure shows three southern blots that determined the genetic location of the *dip1* gene. **Panel A, B and C** show EcoRI digested chromosomal DNA isolated from flies heterozygous for deficiency chromosomes and wild-type (CS, Canton S) or balancer chromosomes. The CS, balancer and deficiency chromosomes produced restriction fragments of distinctly different sizes when hybridized to a [^{32}P] labeled *dip1* probe. In the control lane containing only EcoRI digested DNA from homozygous wild-type flies (CS), a single band is hybridized to the *dip1* probe. In each of the two lanes, R21/CS, and B12/CS two bands, one corresponding to the CS chromosome and one corresponding to the deficiency chromosome are hybridized, indicating that these three deficiencies do not delete the *dip1* gene. In the lane B1-35c/CS, the bands corresponding to the CS and the deficiency chromosomes show almost same electrophoretic mobility. However, in the B1-35c/balancer lane two distinct bands, one corresponding to the deficiency chromosome and one corresponding to the balancer chromosome are seen indicating that this deficiency does not delete the *dip1* gene either. In the lanes, 16-2-13/CS, R22/CS, LB6/CS, S54/CS, B1-35b/CS, R22/CS, 17-257/CS , only one band corresponding to the CS chromosome can be seen. Similarly, in lanes where the same deficiencies are over a balancer chromosome, only one band corresponding to the balancer chromosome can be seen. Therefore, the above deficiencies delete the *dip1* gene. The balancer chromosome used for the 16-2-13 deficiency is different from the FM7 balancer used for

other deficiencies. The electrophoretic mobility of the EcoRI fragment from this chromosome is close but distinctly different from that of CS fragment. The electrophoretic mobilities of the R38 and GA22 deficiency chromosomes are identical to that of CS. However, presence of two bands in the R38/FM7 and GA22/FM7 shows that these deficiencies do not delete the *dip1* gene.

Panel D shows another southern blot which was done with chromosomal DNA digested with two different enzymes, EcoRI (lanes 1-5) and BamHI (6-10). Both EcoRI digests and BamHI digests of B1-35b/balancer and 17-137/balancer show only one band corresponding to the balancer chromosome. Therefore, B1-35b and 17-137 delete the *dip1* gene. Whereas, A209/balancer and HM430/balancer show two bands each, one corresponding to the balancer chromosome and the other corresponding to the deficiency chromosome. Therefore, these deficiencies do not delete the *dip1* gene.

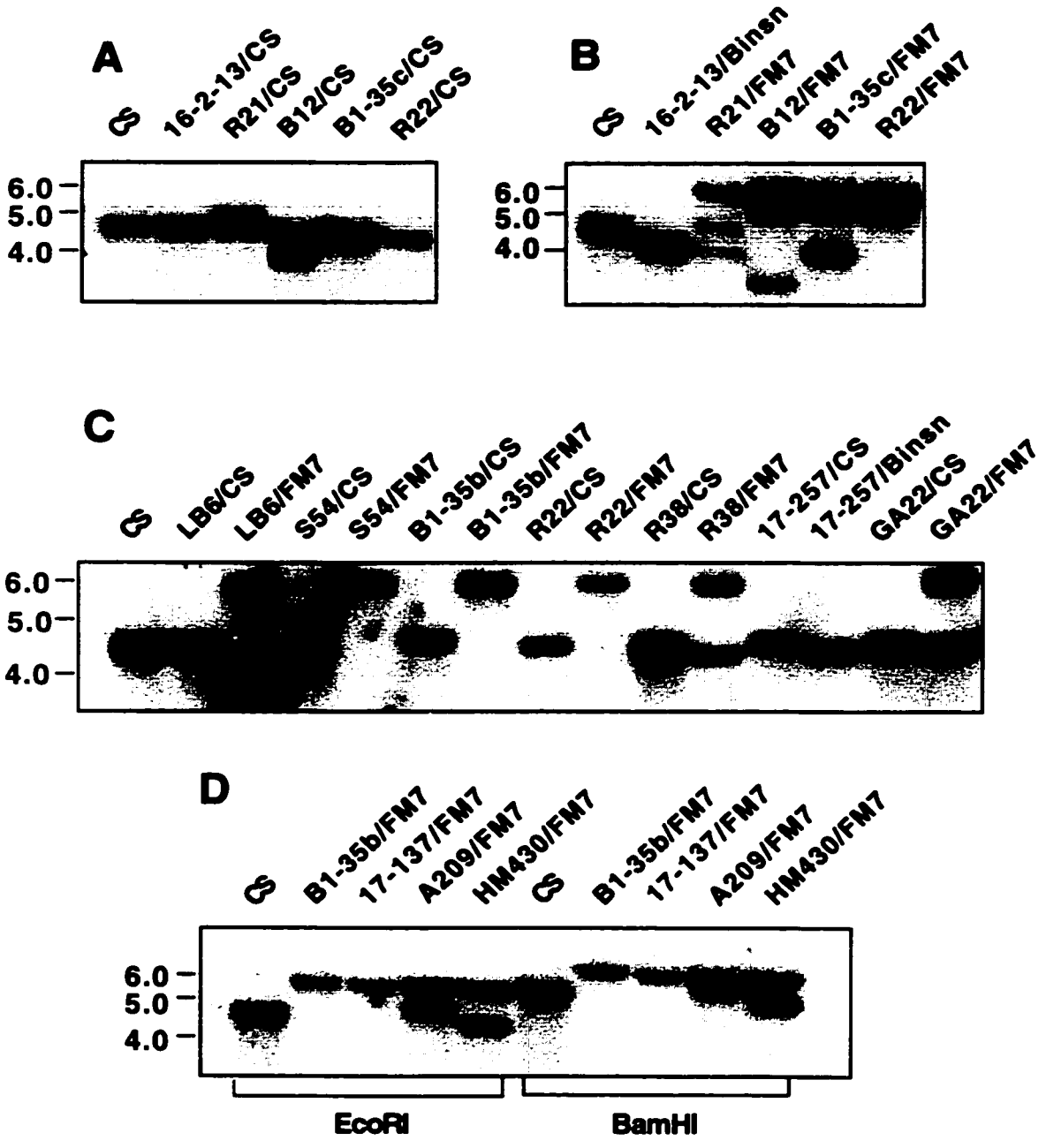
A
CS
16-2-13/CS
R21/CS
B12/CS
B1-35c/CS
R22/CS
6.0
5.0
4.0
B
CS
16-2-13/Binsn
R21/FM7
B12/FM7
B1-35c/FM7
R22/FM7
6.0
5.0
4.0
C
CS
LB6/CS
LB6/FM7
S54/CS
S54/FM7
B1-35b/CS
B1-35b/FM7
R22/CS
R22/FM7
R38/CS
R38/FM7
17-257/CS
17-257/Binsn
GA22/CS
GA22/FM7
6.0
5.0
4.0
D
CS
B1-35b/FM7
17-137/FM7
A209/FM7
HM430/FM7
CS
B1-35b/FM7
17-137/FM7
A209/FM7
HM430/FM7
6.0
5.0
4.0
EcoRI
BamHI

Figure 18

Deficiency map of the *dip1* gene:

This Figure shows a schematic representation of the deficiency map of the 20A region of the X-chromosome. The relative locations of several genes that map to the 19A to 20D region are shown. These are, *extra organ* (*eo*), *flamenco* (*flam*), *touch-insensitive larvae B* (*tilB*), *wings apart* (*wap*), *introvert* (*intro*), l(1)20Ad, *stoned A* (*stnA*), *suppressor of forked* [su(f)], A112, LB20, *tumerous head* (*tuh1*), *maroon-like* (*mal*), *melanized* (*mel*) and l(1)carot2. The extent of the deleted region for each deficiency chromosome is indicated with a horizontal line. The deficiencies that delete the *dip1* gene are indicated with asterix. The map shows that the genetic location of the *dip1* gene matches well with that of the *flam* gene.

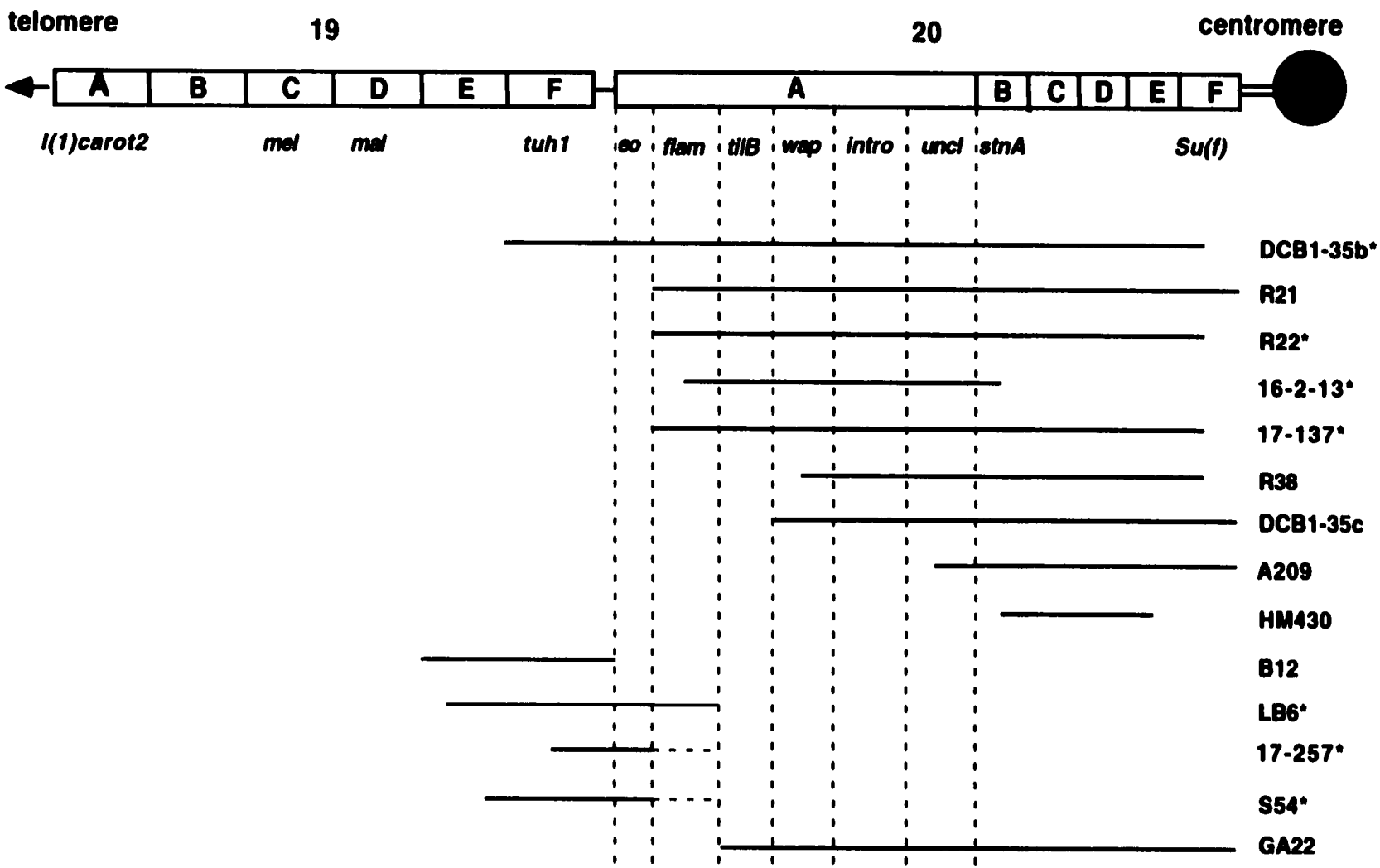
telomere
19
20
centromere
A
B
C
D
E
F
A
B
C
D
E
F
l(1)carot2
mel
mal
tuh1
eo
flam
tilB
wap
intro
uncl
stnA
Su(f)
DCB1-35b*
R21
R22*
16-2-13*
17-137*
R38
DCB1-35c
A209
HM430
B12
LB6*
17-257*
S54*
GA22

F. Expression of the *dip1* mRNA in the follicle cells of the ovary:

The possibility of *dip* gene being *flamenco* was examined by determining its expression in the follicle cells of the ovary, the previously identified site of *flam* gene function (Song *et al.*, 1997). To that end the wild-type expression pattern of the *dip1* mRNA was examined. This experiment was done in collaboration with Dorothy DeSousa, a graduate student of the lab.

During oogenesis (reviewed by Spradling, 1993), *Drosophila* ovarioles contain a series of progressively older egg chambers that represent 14 successive developmental stages. Each egg chamber contains cells from germ line origin as well as somatic cells. The cells of germ line origin consists of 16 interconnected sister cells, the posterior-most of which is the oocyte (OO) and the other 15 differentiate into giant polyploid nurse cells (N). The cells of somatic origin are called follicle cells. These cells form an epithelial sheath that completely covers the egg chamber. Ovarioles containing egg chambers from various stages were dissected from young *Drosophila* females (2-3 days old) to study *dip1* expression pattern. In wild-type ovarioles we were able to detect *dip1* expression in the follicle cells (arrow) and nurse cells of the ovary (Figure 19, Panel B). The arrow shows the localization of the *dip1* gene expression at the basal level of the columner follicle cell layer just adjacent to the oocyte.

Figure 19

Expression pattern of *dip1* mRNA in the ovary:

Panel A shows one ovariole that contains egg chambers from different stages of oogenesis. Expression of the *dip1* gene can be seen in the nurse cells and the follicle cells at all stages. **Panel B** shows one egg chamber from stage 10 at higher magnification. Expression of the *dip1* mRNA is clearly seen in the nurse cells (N) and at the base of the columnar follicle cells (arrow with a white arrowhead), that surround the oocyte.

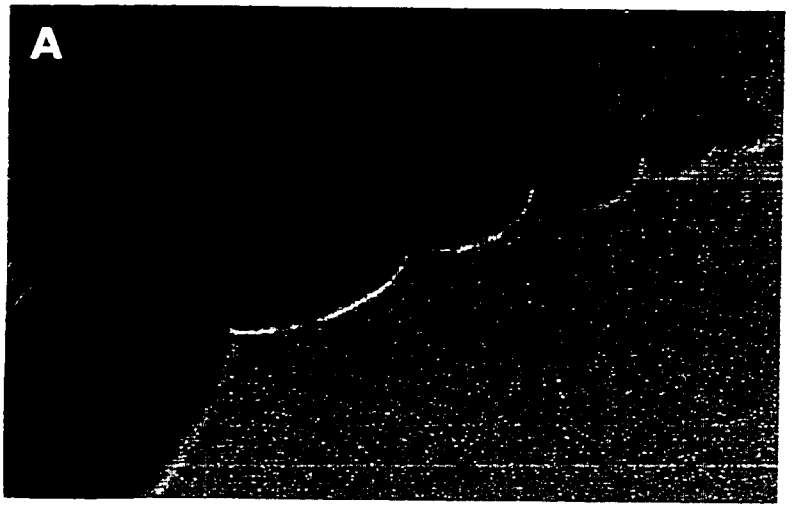
A

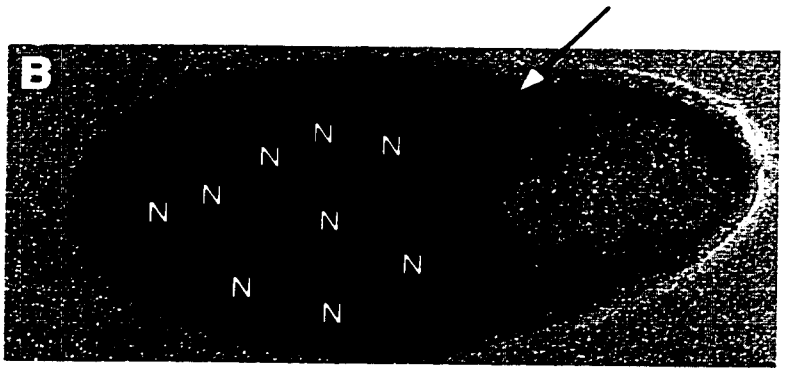
B
N
N
N
N
N
N
N
N
N

G. Screening of genomic P1 and cosmid clones for the *dip1* gene:

A number of genomic P1 and cosmid clones that map to the 20A region of the polytene chromosome of *Drosophila* were screened in an attempt to sequence the genomic region of the *dip1* gene.

The genomic P1 clones for *Drosophila* were generated by infecting its bacterial host *E. coli* NS3145 with P1 phage vector containing *Drosophila* genomic DNA fragments (Hartl *et al.*, 1994). This modified P1 phage is lysis defective. It is replicated and maintained inside its host as a plasmid vector. The P1 vector can hold foreign DNA as large as 100 kb. Due to this advantage, a *Drosophila melanogaster* genomic DNA library was constructed in this vector (Hartl *et al.*, 1994).

A physical map of the *Drosophila melanogaster* genome has also been constructed with about 20,000 cosmid clones and the available P1 clones (Siden-Kiamos et al., 1990). Screening of 32 P1 clones and four cosmid clones that map to the 20A region of *Drosophila* polytene chromosome showed absence of the *dip1* gene in any of those clones.

The results of this study are shown in Table 2. The '-' sign indicates absence of the *dip1* gene in the genomic clones.

Table 2: Results of the screening for *dip1* genomic clones.

P1 clones	DS00349	-
	DS06959	-
	DS00847	-
	DS08593	-

P1 clones	DS04319	-
	DS02066	-
	DS03063	-
	DS04564	-
	DS04565	-
	DS04568	-
	DS05092	-
	DS05127	-
	DS05241	-
	DS05244	-
	DS05529	-
	DS06218	-
	DS06350	-
	DS06586	-
	DS02945	-
	DS06287	-
	DS01584	-
	DS02138	-
	DS02234	-
	DS03356	-
	DS05833	-
	DS05892	-
	DS06580	-
	DS06744	-

Cosmids	DS02983	-
	DS02995	-
	DS03783	-
	DS04430	-
	146B9	-
	115G9	-
	6H2	-
	37F7	-

IV. Characterization of *dip2*

A. Screening of λgt11 and λEXlox cDNA libraries for *dip2* cDNA:

A partial 1.2 kb 3′ end fragment of the *dip2* cDNA was isolated from the yeast interaction trap library vector. In an attempt to isolate the 5′ portion of the cDNA we screened two other *Drosophila* cDNA libraries made in λ phage vectors. A 12-24 hours *Drosophila* embryonic cDNA library made in λgt11 phage vector and 20-22 hours embryonic cDNA library made in λEXlox (Novagen) vector were screened. These libraries were screened with a radiolabeled probe made from the 1.2 kb *dip2* cDNA fragment isolated from the yeast interaction trap library. Five positive plaques from the λgt11 library and four positive clones from the λEXlox library were isolated. The size of the cDNA inserts were examined by restriction digestion of the phage DNA from the positive plaques isolated from the λgt11 library with EcoRI, and that of λEXlox library with ApaI and SacI. All five positive plaques from the λgt11 library contained only a small fragment, about 1 kb in length corresponding to the 3′ end of the *dip2* cDNA. One of the four positive plaques isolated from the λEXlox library contained a 2.5 kb fragment also from the 3′ end of the *dip2* cDNA. The other three positive plaques contained cDNA inserts of larger that 2 kb, but smaller that 2.5 kb, all corresponding to the 3′ end of the *dip2* cDNA. The largest fragment isolated from these libraries was 2.5 kb, which lacked the 5′ end of the *dip2* cDNA. Thus, none of the three libraries (including the yeast interaction trap library) screened contained a full-length cDNA clone for the *dip2* gene.

In collaboration with an undergraduate (Peter Pelka) in the lab the mouse homolog of the *dip2* gene was also cloned. Screening of a 8.5 day old mouse

embryonic cDNA library made in λgt10 led to the isolation of a single clone with a partial 1.1 kb 3′ end fragment of the mouse *dip2* cDNA. The probe used for this study was made from a 4.6 kb partial human *dip2* cDNA that was cloned in the human genome project from the human cell line KG1 (Accession# D80006). Sequence analysis of the 1.1 kb mouse cDNA fragment showed that the clone isolated contained a recombinant cDNA with only a 382 bp sequence from the middle portion of the 1.1 kb fragment representing the desired cDNA. This 382 bp fragment corresponded to the 3′ end of mouse *dip2* cDNA. A 124 amino acids sequence predicted from the 382 bp 3′ end fragment showed 100% amino acid identity with that of its human homolog (Figure 26). The mouse and the corresponding *Drosophila* fragments shared 82.3% amino acid identity and 97.6% positives. The sequence of the partial mouse cDNA is shown in Figure 25.

B. Northern analysis for *dip2* transcript:

Northern analysis was done to determine the size of the *dip2* transcript expressed during *Drosophila* embryonic development. The analysis was done with polyA$^+$ RNA isolated from 0-22 hours embryos. The probe used for this study was made from the 1.2 kb *dip2* cDNA fragment isolated in the yeast interaction trap. The probe hybridized to a single band. As judged from the northern blot, the size of the single *dip2* transcript is about 5 kb (Figure 20).

Figure 20

Northern analysis for *dip2* mRNA:

Result of the northern analysis done with polyA$^+$ RNA isolated from 0-22 hours *Drosophila* embryos is shown. The *dip2* probe hybridized to a single band of approximately 5 kb in length.

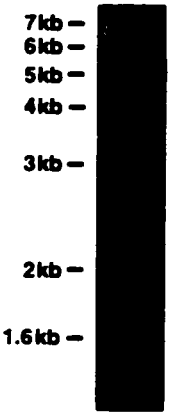
7kb
6kb
5kb
4kb
3kb
2kb
1.6kb

C. Chromosomal location of the *dip2* gene:

In order to understand the physiological role of *dip2*, knowledge of its chromosomal location is essential. *In-situ* hybridization to polytene chromosomes of *Drosophila* was done to determine the chromosomal location of the *dip2* gene. This was done using a 1.2 kb biotin labeled *dip2* probe isolated from the yeast interaction trap library.

The *dip2* probe hybridized to a single location on the polytene chromosome, the band 61B, at the tip of the left arm of the third chromosome (Figure 21).

D. Deficiency mapping of the *dip2* gene:

In order to narrow down the chromosomal location of the *dip2* gene its genetic location was determined through deficiency mapping. This was done through southern analysis of chromosomal DNA from deficiency lines from the 61B region, the location of the *dip2* gene on polytene chromosomes. Only three deficiency lines were available in *Drososphila* stock centers with breakpoints in the vicinity of the 61 B region. These were; Df(3L)Ar12-1, Df(3L)Ar11 and Df(3L)emc-E12. Unlike the *dip1* locus we did not detect a polymorphism at the *dip2* locus. Therefore, to identify deficiencies that delete the *dip2* gene, the amount of DNA loaded in each lane was estimated by rehybridizing the experimental blot with a control probe (*disco* probe). This allowed us to determine if one copy of the *dip2* gene was deleted in any of the heterozygous deficiency lines. Absence of one copy of the gene led to a reduction in band intensities in the experimental blot as compared to the control blot. Since the *disco* gene is an X-linked gene, only one copy of the gene is present in the male as

opposed to two copies in females. Therefore, in order to be able to use *disco* as a control probe, only chromosomal DNA of heterozygous female flies from the above deficiency lines was used.

The deficiencies Ar12-1 and Ar11 carry deletions from bands 61C to 61F. Whereas, Df(3L)emc-E12 is the only one in which the 61B region is deleted. As expected from the in-situ result, Df(3L)emc-12 was the only deficiency from the 61 region that deleted the *dip2* gene. The results obtained with these deficiencies are shown in table 3, where '-' indicates deletion, and '+' indicates inclusion of the *dip2* gene in the deficiency.

Table 3: Results of the deficiency mapping for *dip2*:

Df(3L)emc-E12	-
Df(3L)Ar12-1	+
Df(3L)Ar11	+

Due to the absence of smaller deficiencies from the 61B region we were unable to further narrow down the genetic location of the *dip2* gene. The southern blots from this study are shown in Figure 23. The deficiency map is schematically represented in Figure 22.

Figure 21

Localization of the *dip2* gene on *Drosophila* polytene chromosome: This Figure shows the *in situ* chromosomal localization result for the *dip2* gene. The *dip2* probe hybridized to band 61B (arrow) on the left arm of chromosome III of *Drosophila*.

Figure 22

Results of the deficiency mapping of *dip2* by southern analysis:
This Figure shows the southern blots done to identify a third chromosome deficiency (emc-E12) that delete the *dip2* gene. **Panel A** shows the southern blot done with the EcoRI and BamHI digested chromosomal DNA isolated from the heterozygous deficiency lines that carry one third chromosome deficiency from the 61 region and one balancer chromosome. The intensity of the bands hybridized to the *dip2* probe appears to be lower in the lanes corresponding to the deficiency line emc-E12 compared to other lanes.
Panel B shows the same blot hybridized to a *disco* probe as a control to examine the amount of DNA loaded in each lane. The amount of DNA loaded in the lane containing chromosomal DNA from the emc-E12 line does not appear to be less than that loaded in other lanes. This shows that the lower band intensities of the emc-E12 lane in the blot in panel A is due to the absence of one copy of the *dip2* gene in that deficiency line. In other words, the deficiency emc-E12 deletes the *dip2* gene.

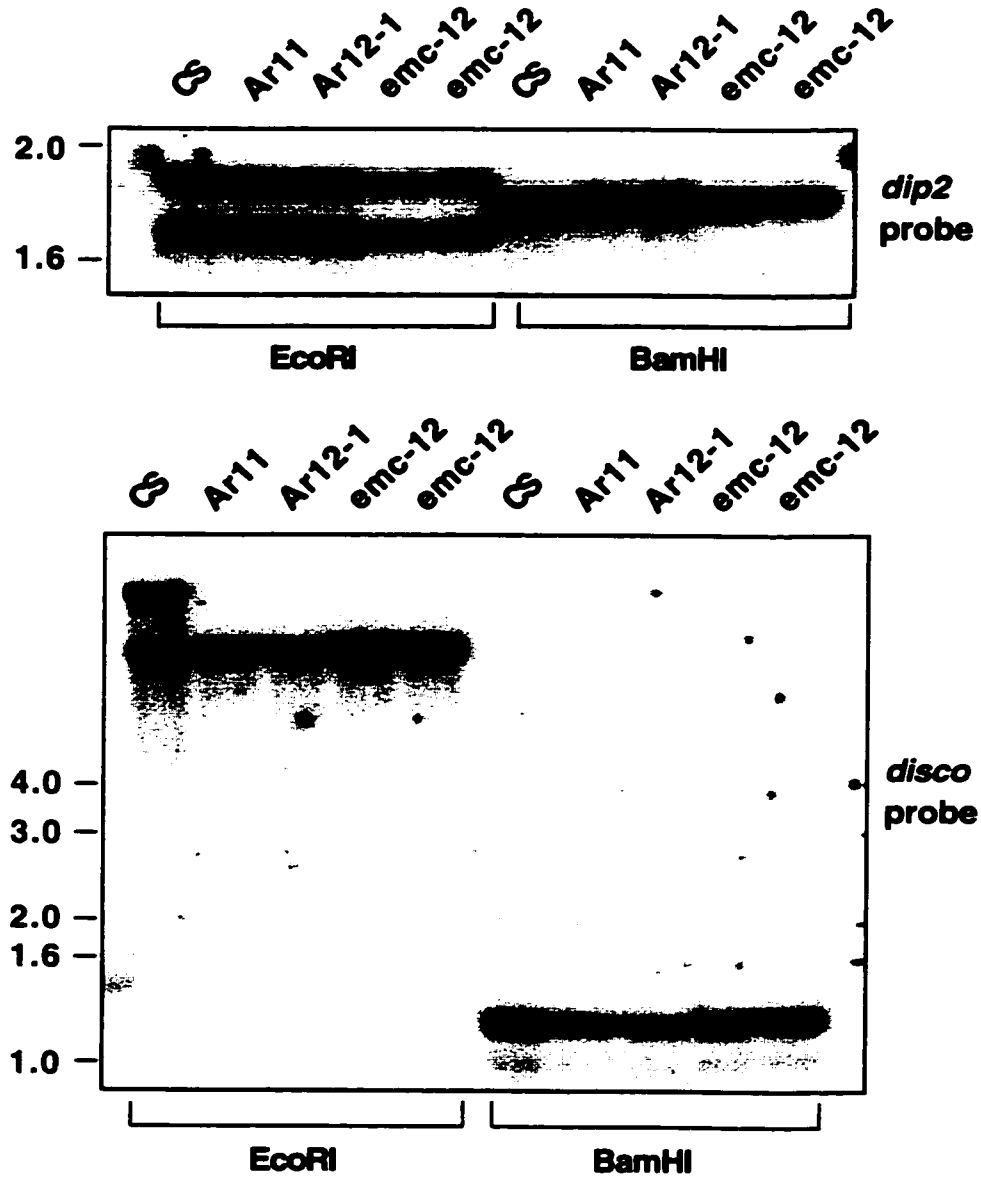
CS
Ar11
Ar12-1
emc-12
emc-12
CS
Ar11
Ar12-1
emc-12
emc-12
2.0
1.6
dip2
probe
EcoRI
BamHI
CS
Ar11
Ar12-1
emc-12
emc-12
CS
Ar11
Ar12-1
emc-12
emc-12
4.0
3.0
2.0
1.6
1.0
disco
probe
EcoRI
BamHI

Figure 23

Deficiency map of the *dip2* gene:

The genetic location of the *dip2* gene is shown in the deficiency map of the 61 region on the left arm of the third chromosome of *Drosophila*. The extent of the deleted region for each deficiency chromosome is indicated with a horizontal line. The deficiencies that were used for southern analysis are Df(3L)Ar12-1, Df(3L)Ar11 and Df(3L)emcE12. Only the deficiency emc-E12 deletes the *dip2* gene (shown with an asterix). Mutations that map to the 61A-D region are shown. These are *trachealess* (*trh*), *marble* (*marb*), *extra macrochaete* (*emc*), *smell impaired 61A*(*smi61A*), *pointless* (*ptl*), *forewheel drive* (*fwd*), l(3)122 and l(3)06240.

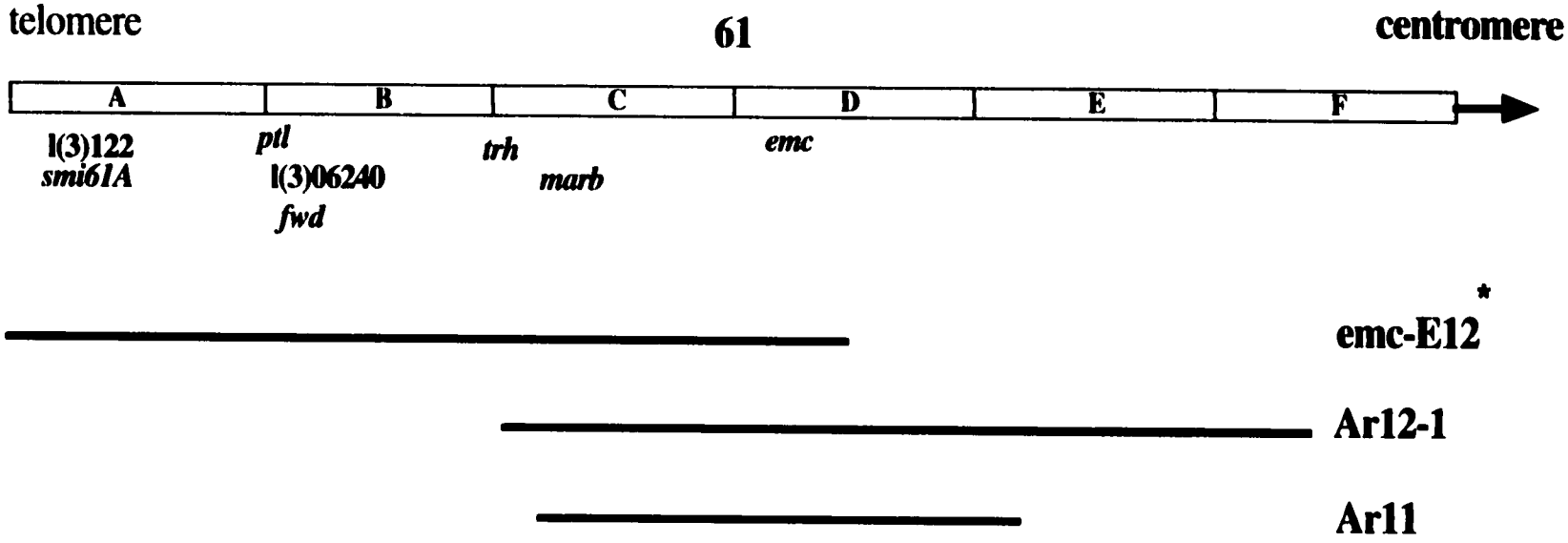
telomere
61
centromere
A
B
C
D
E
F
l(3)122
smi61A
ptl
l(3)06240
fwd
trh
marb
emc
*
emc-E12
Ar12-1
Ar11

E. Isolation of genomic P1 clones for the *dip2* gene:

In order to sequence the genomic region of the *dip2* gene, three genomic P1 clones that map to the 61B region of *Drosophila* polytene chromosome, were screened. These are shown in Table 4. Of the three, two (DS05688 and DS03215) contained the chromosomal DNA for *dip2*. Because of technical difficulties only a portion of the *dip2* genomic DNA was sequenced (Figure 24). A portion of the P1 clone sequencing was done partly by Peter Pelka, a graduate student of the lab. The results of the sequence analysis are presented following this section.

Table 4: Results of the screening for dip2 genomic clones: In this table '+' indicates inclusion and '-' indicates absence of the *dip2* gene in the P1 clones.

P1 clones	Result
DS05688	+
DS03215	+
DS00583	-

F. Sequence analysis of the *dip2* genomic DNA:

A 2.7 kb fragment of the *dip2* gene was sequenced from the P1 clone DS03215. This 2.7 kb sequence corresponds to the 3' end of *dip2* mRNA. BLAST search analysis of the *dip2* genomic DNA sequence determined from the clone DS03215 showed sequence homology with a human and a *C. elegans* gene, both isolated from the corresponding genome projects.

The 2.7 kb sequence has a continuous open reading frame that stops at the nucleotide position 2509 (Figure 24). Both, the genomic sequence and the partial

dip2 cDNA sequence of *Drosophila* showed the presence of an extra 159 bp fragment (124 bp upstream of the stop codon) which was absent in any other *dip2* homolog. Absence of a putative splice acceptor site (Padgett *et al.*, 1986) adjacent (5') to the 159 bp genomic sequence, and a splice donor site (usually G) at the 3' end of this sequence also indicates that this region of the *dip2* gene constitutes part of *dip2* cDNA coding sequence. Thus, the predicted *Drosophila* DIP2 protein contains an extra 53 amino acid sequence that is lacking in other DIP2 homologs.

The protein predicted from the putative open reading frame show no significant similarity to any known functional domain. BLAST search analysis (Altschul et al., 1990) for DIP2 homologs show a weak similarity to the AMP-binding motif (PROSITE database, accession number PDOC00427) found in several enzymes such as insect luciferase, acetyl CoA ligases, 4-coumarate-CoA ligase and others. 'Block' database (Henikoff and Henikoff, 1994) searches show that the amino acid sequence of the *C. elegans* DIP2 homolog (for which the complete protein sequence is known) shows weak similarity to an N-terminal 30 amino acids fragment of adenosine deaminases and a similar fragment from AMP-deaminases (BLOCK number BL00485A). The sequence of the *dip2* gene determined from the P1 clone is shown in Figure 24.

Figure 24

Partial *dip2* genomic sequence:

The sequence of the 2.7 kb partial *dip2* genomic region determined from the P1 clone DS03215 is shown in this Figure. It contains a continuous open reading frame that stops at the nucleotide position 2509 of the fragment. The amino acids sequence predicted from the open reading frame is also shown. A 53 amino acids region (residues 659-712) that is unique to the *Drosophila* DIP2 homolog is highlighted.

Partial genomic sequence for *dip2*

```
                ←  CCGTTACCGGTAGAAAAGCACAATGCGGATGACATTATTGCCACA 45
                     P  L  P  V  E  K  H  N  A  D  D  I  I  A  T
GTGTTAGCTGTGGAACCCATGCGGTTTATTTATCGAGGACGCATTGCTGTATTTAGCATT 105
 V  L  A  V  E  P  M  R  F  I  Y  R  G  R  I  A  V  F  S  I
AAAGTTTTGCGCGACGAACGCGTGTGCGTCATTGCTGAACAACGTCCGGACTGCTCGGAG 165
 K  V  L  R  D  E  R  V  C  V  I  A  E  Q  R  P  D  C  S  E
GAAGAAAGTTTCCAATGGATGTCACGTGTTCTGCAAGCAGTAGACTCCATTCACCAAGTC 225
 E  E  S  F  Q  W  M  S  R  V  L  Q  A  V  D  S  I  H  Q  V
GGAATTTACTGCCTGGCATTGGTTCCGCCGAATCATTTGCCAAAGACTCCTCTTGGGGGC 285
 G  I  Y  C  L  A  L  V  P  P  N  H  L  P  K  T  P  L  G  G
ATACATTTATGCGAAGCACGGGAAAGGTTCTTGGAGGGATCTCTCCACCCAGCGAATGTT 345
 I  H  L  C  E  A  R  E  R  F  L  E  G  S  L  H  P  A  N  V
TTAATGTGCCCACATACATGTGTTACCAATCTACCAAAGCCACGGGAACTACATCAAGGT 405
 L  M  C  P  H  T  C  V  T  N  L  P  K  P  R  E  L  H  Q  G
GTAGGACCAGCCTCTGTGATGGTTGGAAATTTAGTTCAGGGCAATCGCCTTGCTGAAGCC 465
 V  G  P  A  S  V  M  V  G  N  L  V  Q  G  N  R  L  A  E  A
CATGGACGGATGTTGTTGCGACTAAAAAACTGTCCAAAANTTCAACAGCTTCAATTGATA 525
 H  G  R  M  L  L  R  L  K  N  C  P  K  X  Q  Q  L  Q  L  I
ACAGGTGTGTTGCGTTGGCGAGCAAACACGTCCCCCGATCATATAATATTTACACTGCTG 585
 T  G  V  L  R  W  R  A  N  T  S  P  D  H  I  I  F  T  L  L
AACTCCAAGGGTAAGTTTTGTTCCGCTTCAGGTGCCATCGCGAAAACACTGACATGNTCT 645
 N  S  K  G  K  F  C  S  A  S  G  A  I  A  K  T  L  T  X  S
GAGTTGCATAAGCGGGCAGAGAAAATAGCGGCATTGTTACAAGAACGAGGAAGAATTGAG 705
 E  L  H  K  R  A  E  K  I  A  A  L  L  Q  E  R  G  R  I  E
CCAGGAGACCACGTTGGTAAGTTTTTCTGTGTACACACTATAGGAATGTTAATGAAGTCC 765
 P  G  D  H  V  G  K  F  F  C  V  H  T  I  G  M  L  M  K  S
GATTTTCCCGCAGCGCTTATATTTCCCCCAGGTCTCGATTTGCTGTGTGCATTTTATGGA 825
 D  F  P  A  A  L  I  F  P  P  G  L  D  L  L  C  A  F  Y  G
TGCCTTTATTTGGGTGCAATACCAATTACCATTCGGCCTCCACATCCACAAAATTTAAAT 885
 C  L  Y  L  G  A  I  P  I  T  I  R  P  P  H  P  Q  N  L  N
ACCACGTTACCCACTGTTCGGATGATTGTTGATGTCTCTAAAAGTGGCATTGTACTCTCC 945
 T  T  L  P  T  V  R  M  I  V  D  V  S  K  S  G  I  V  L  S
ATACAGCCAATTATTAAGTTACTCAAATCGCGAGAGGCAGCAACCTCGATTGATCCAAAG 1005
 I  Q  P  I  I  K  L  L  K  S  R  E  A  A  T  S  I  D  P  K
ACAGGGCCCCCTATATTAGATATTGATGACAACCCGAAACGAAAATATGCCGGCATAGCC 1065
 T  G  P  P  I  L  D  I  D  D  N  P  K  R  K  Y  A  G  I  A
ACGGTTTCCTTTGACTCTAGCGCCTATTTGGACTTTAGCGTATCAACTTGTGGACGTCTT 1125
 T  V  S  F  D  S  S  A  Y  L  D  F  S  V  S  T  C  G  R  L
AGCGGTGTTAACATTACGCATAGATCTCTCTCTAGTCTGTGCGCCAGTTTAAAATTGGCT 1185
 S  G  V  N  I  T  H  R  S  L  S  S  L  C  A  S  L  K  L  A
TGTGAGCTGTACCCTTCTCGACATGTTGCTTTATGTTTGGATCCGTACTGCGGCCTTGGA 1245
 C  E  L  Y  P  S  R  H  V  A  L  C  L  D  P  Y  C  G  L  G
TTTGTTATGTGGACTCTTATCGGAGTATACAGTGGCCACCATTCTATACTTATCGCGCCC 1305
 F  V  M  W  T  L  I  G  V  Y  S  G  H  H  S  I  L  I  A  P
TACGAGGTCGAAGCGAATCCCAGTTTATGGCTGTCAACTCTATCGCAACACCGCGTTCGC 1365
 Y  E  V  E  A  N  P  S  L  W  L  S  T  L  S  Q  H  R  V  R
GACACATTCTGTTCATATGGTGTAATTGAGTTATGCACTAAAGCTCTCAGCAATTCTATA 1425
 D  T  F  C  S  Y  G  V  I  E  L  C  T  K  A  L  S  N  S  I
CCTTCCTTAAAGCAACGAAACATAGATTTGAGATGCGTACGGACGTGTGTCGTGGTGGCA 1485
 P  S  L  K  Q  R  N  I  D  L  R  C  V  R  T  C  V  V  V  A
GAAGAGCGCCCCAGAGTGCAACTGACCCAGCAGTTCTGCAAGCTATTTCAAGCCCTTGGT 1545
 E  E  R  P  R  V  Q  L  T  Q  Q  F  C  K  L  F  Q  A  L  G
```

```
CTGAATACGCGCTGCGTGTCAACTTCGTTTGGATGTCGTGTAAATCCGGCCATTTGTGTC 1605
 L  N  T  R  C  C  V  S  T  S  F  G  C  R  V  N  P  A  I  C  V
CAAGGGGCTAGTTCTGCAGAGAGTGCTCAAGTGTATGTAGATATGAGAGCATTGCGAAAT 1665
 Q  G  A  S  S  A  E  S  A  Q  V  Y  V  D  M  R  A  L  R  N
AATCGTGTTGCTCTGGTAGAGCGTGGAGCGCCAAATTCGTTGTGTGTAATTGAATCAGGT 1725
 N  R  V  A  L  V  E  R  G  A  P  N  S  L  C  V  I  E  S  G
AAACTTTTACCAGGCGTAAAAGTGATAATTGCAAATCCCGAAACTAAGGGCCACTGTGGC 1785
 K  L  L  P  G  V  K  V  I  I  A  N  P  E  T  K  G  H  C  G
GACTCGCATTTGGGAGAAATCTGGGTTCAAGCTCCTCACAACGCACATGGTTACTTTACA 1845
 D  S  H  L  G  E  I  W  V  Q  A  P  H  N  A  H  G  Y  F  T
ATTTATGGTGACGAAACTGACTACAATGATCACTTCAACGCGAAATTGGTAACTGGGGCC 1905
 I  Y  G  D  E  T  D  Y  N  D  H  F  N  A  K  L  V  T  G  A
ACCTCAGAACTATATGCACGCACTGGGTATTTAGGATTCTTACGCCGCACCGAATGCTCG 1965
 T  S  E  L  Y  A  R  T  G  Y  L  G  F  L  R  R  T  E  C  S
CAATCAGCATCACTGCTTGACGAGACCACACCAAGTGTGGCAAGTCGCGATAGTGATACA 2025
 Q  S  A  S  L  L  D  E  T  T  P  S  V  A  S  R  D  S  D  T
GAATCTTTGAATTCGATAAGTCAATTGCAACTAAATTTTTCAAATGTTTCCTTGGGTGGA 2085
 E  S  L  N  S  I  S  Q  L  Q  L  N  F  S  N  V  S  L  G  G
AATTCCGAGCATAGCCTGGTAGGCGGCGCAAGCAATGCTAATGATCAAGAACTACACGAC 2145
 N  S  E  H  S  L  V  G  G  A  S  N  A  N  D  Q  E  L  H  D
GCAGTGTATGTAGTCGGAGCTGTTGATGAAATGATCTCTTTACGTGGCATGAACTATCAC 2205
 A  V  Y  V  V  G  A  V  D  E  M  I  S  L  R  G  M  N  Y  H
CCAATTGATATCGAAAATTCGGTAATGCGCTGTCACAAAAAAATTGCTGAGTGCGCCGTT 2265
 P  I  D  I  E  N  S  V  M  R  C  H  K  K  I  A  E  C  A  V
TTCACCTGGACTAACTTATTAGTCGTTGTTGTCGAGTTGGACGGCAATGAATCAGAAGCT 2325
 F  T  W  T  N  L  L  V  V  V  V  E  L  D  G  N  E  S  E  A
TTGGATTTGGTTCCCTTGGTCACAAACACAGTATTAGAAGATCATCAGCTTATAGTCGGC 2385
 L  D  L  V  P  L  V  T  N  T  V  L  E  D  H  Q  L  I  V  G
GTTGTAGTGGTCGTTGATCCAGGTGTGGTGCCTATTAATAGTCGGGGCGAAAAGCAACGG 2445
 V  V  V  V  V  D  P  G  V  V  P  I  N  S  R  G  E  K  Q  R
ATGCATTTACGGGATGGTTTTCTGGCCGACCAATTGGATCCCATATACGTAGCATATAAC 1505
 M  H  L  R  D  G  F  L  A  D  Q  L  D  P  I  Y  V  A  Y  N
ATGTAAATACACAATTATTCTTATGATGAAATCGCCGTATTAAGAAACGTTACAAAACGT 2565
 M  *
TGTNTTNGTATCATAATTCAAAACAACCGCAATCCACAAAAAAACAGAAATGGCTCATTT 2625

TGGTAACACGCACGCCTAATTACACATTTCCTTTTAGAGTATTAGCAAAGATGGTAAAAC 2685

ATTCTTACAATAAAATGACTATTTATCTTTATATGACCATATA 2728
```

Figure 25

Partial mouse *dip2* cDNA sequence:

This Figure shows the partial cDNA sequence corresponding to a 382 bp 3′ end fragment of the mouse *dip2* homolog. The predicted amino acids sequence corresponding to this fragment is shown. The stop codon is indicated with an asterix.

Partial mouse cDNA sequence and the predicted amino acids sequence:

```
GATGCACTGTATGTCGTTGGGTCTCTGGATGAAACGCTAGAACTGAGAGGCATGCGGTAT
 D  A  L  Y  V  V  G  S  L  D  E  T  L  E  L  R  G  M  R  Y
CACCCCATCGACATAGAAACCTCCGTGATCCGTGCACACAGGAGCATTGCAGAGTGTGCC
 H  P  I  D  I  E  T  S  V  I  R  A  H  R  S  I  A  E  C  A
GTGTTCACCTGGACCAACCTGCTGGTGGTGGTGGTGGAGCTGGATGGGCTGGAGCAGGAC
 V  F  T  W  T  N  L  L  V  V  V  V  E  L  D  G  L  E  Q  D
GCCCTGGACCTGGTGGCCCTGGTGACCAACGTCGTGCTGGAGGAGCACTACCTTGTGGTG
 A  L  D  L  V  A  L  V  T  N  V  V  L  E  E  H  Y  L  V  V
GGCGTGGTGGTCATCGTGGATCCCGGAGTGATCCCCATCAACTCTCGGGGCGAGAAGCAA
 G  V  V  V  I  V  D  P  G  V  I  P  I  N  S  R  G  E  K  Q
CGCATGCACCTGCGAGATGGCTTCCTGGCTGACCAGCTGGACCCCATCTACGTGGCCTAC
 R  M  H  L  R  D  G  F  L  A  D  Q  L  D  P  I  Y  V  A  Y
AATATGTGAGCCCAGCTG
 N  M  *
```

Figure 26

Alignment of the predicted DIP2 homologs:

This Figure shows the sequence homology between the predicted DIP2 homologs from *Drosophila*, mouse, human and *C. elegans*. The top portion shows a schematic representation. The bottom portion shows actual protein sequences. Except for the *C. elegans* protein, all other DIP2 sequences presented here are partial. The protein alignment was done using Clustal W alignment program. The C-terminal 124 amino acids sequence is identical in all DIP2 homologs. Just adjacent to the 124 amino acids C-terminal fragment, there is a 53 amino acids sequence (shown in orange) that is unique to the *Drosophila* DIP2 protein.

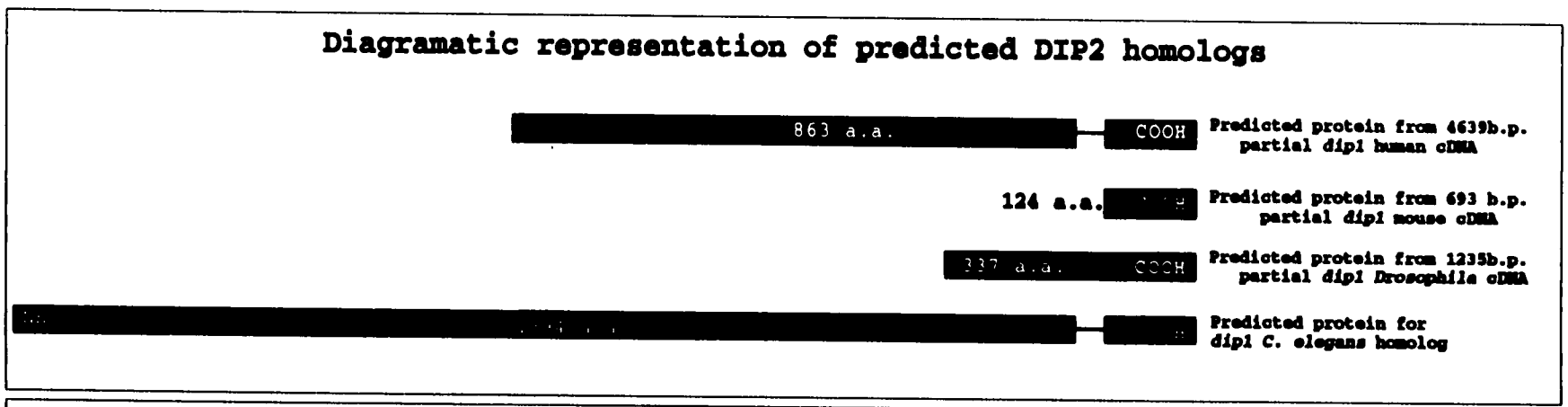
Diagramatic representation of predicted DIP2 homologs
863 a.a.
COOH
Predicted protein from 4639b.p. partial dip1 human cDNA
124 a.a.
Predicted protein from 693 b.p. partial dip1 mouse cDNA
337 a.a.
COOH
Predicted protein from 1235b.p. partial dip1 Drosophila cDNA
Predicted protein for dip1 C. elegans homolog

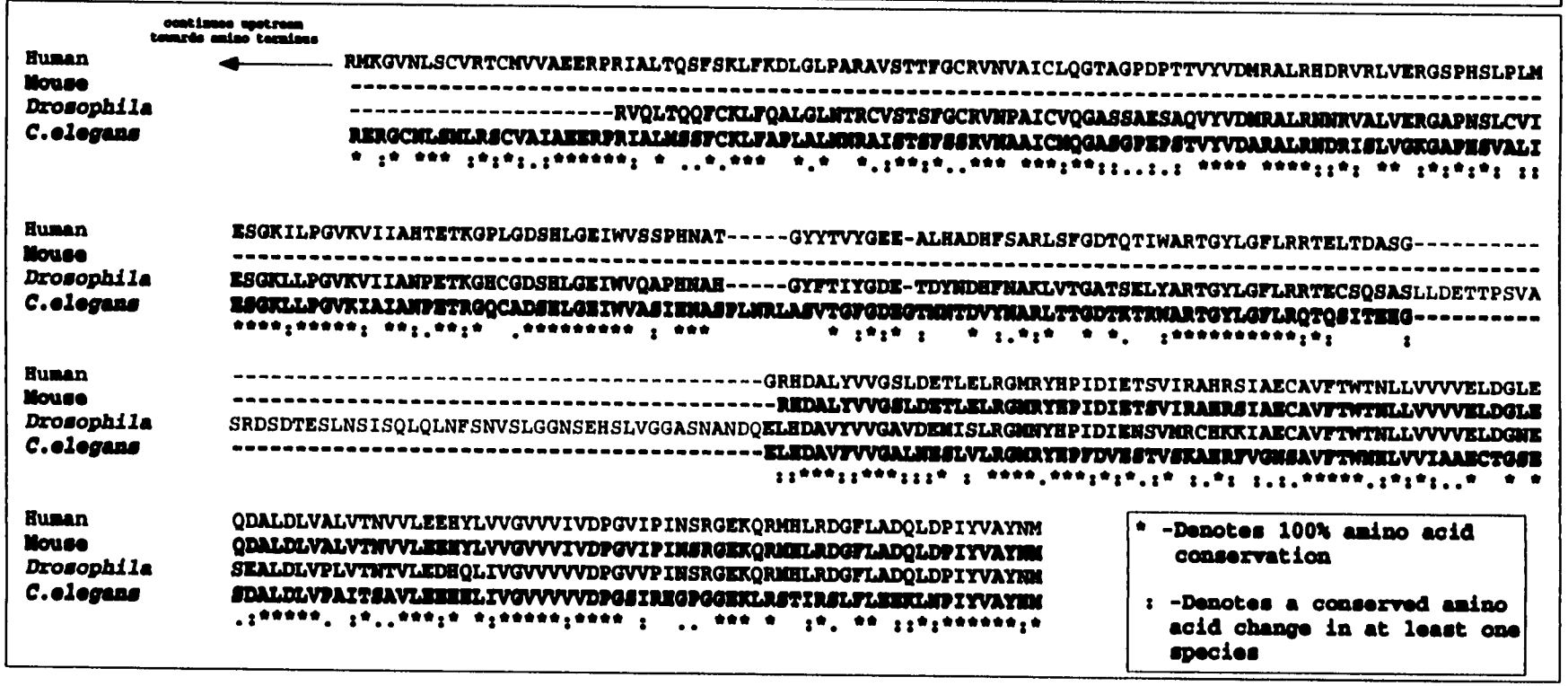
continues upstream towards amino terminus
Human
Mouse
Drosophila
C.elegans
* -Denotes 100% amino acid conservation
: -Denotes a conserved amino acid change in at least one species

G. Search for P-element insertion mutants at the *dip2* locus:

To search for mutations that affect *dip2* gene function, P-element insertion mutants from the 61 region of the polytene chromosome were screened. In these mutants, disruption of gene function is achieved through insertion of the *Drosophila* P-element (transposable element) in the coding or the regulatory regions of a gene. The nine P-element insertion mutant lines were screened for this study include insertion in the genes denoted as *forewheel drive, marbles, pointless* and several other lethal mutations. None of these genes have yet been cloned and might represent *dip2*. For the detailed genotype of these lines please refer to the materials and methods.

In order to identify lines(s) with insertion inside the *dip2* locus, size difference among the EcoRI and BamHI digested chromosomal DNA bands from different lines that hybridized to a *dip2* probe were examined. Insertion of a P-element should change the length of a restriction fragment from the region of the insertion. The probe used for this study was synthesized from the 1.2 kb *dip2* cDNA fragment isolated in the yeast interaction trap assay.

None of the nine P-element insertion lines from the 61 region showed any difference in restriction pattern when compared to each other and to the wild-type chromosomal DNA restriction pattern. In these lines, no P-element insertion was detected at the *dip2* locus, using a probe made from the 3′ portion of the *dip2* cDNA. However, these results do not exclude the possibility of an insertion at the 5′ end or in the regulatory region of the gene. The results of the screen are shown in Figure 27.

Figure 27

Results of the screening of P-element insertion mutants for *dip2*:
This Figure shows the result of the southern analysis done on the P-element insertion mutant lines to screen for mutations at the *dip2* locus. The P-element insertion lines are denoted with their Bloomington stock center numbers. For the actual genotype of these lines please refer to the materials and methods section of this chapter. None of the EcoRI or BamHI digested chromosomal DNA from any mutant line shows any difference in restriction pattern when hybridized to a *dip2* probe made from the 3′ 1.1 kb *dip2* cDNA fragment as template. Bands hybridized to the *dip2* probe from all mutant lanes are of same size as that obtained from the control lanes (digested chromosomal DNA from wild-type flies). For all mutant lines and the wild-type line, EcoRI digestion produced two bands of about 1.6 kb and 1.3 kb in length and Hind III digestion produced two bands of about 4.5 kb and 2 kb in length.

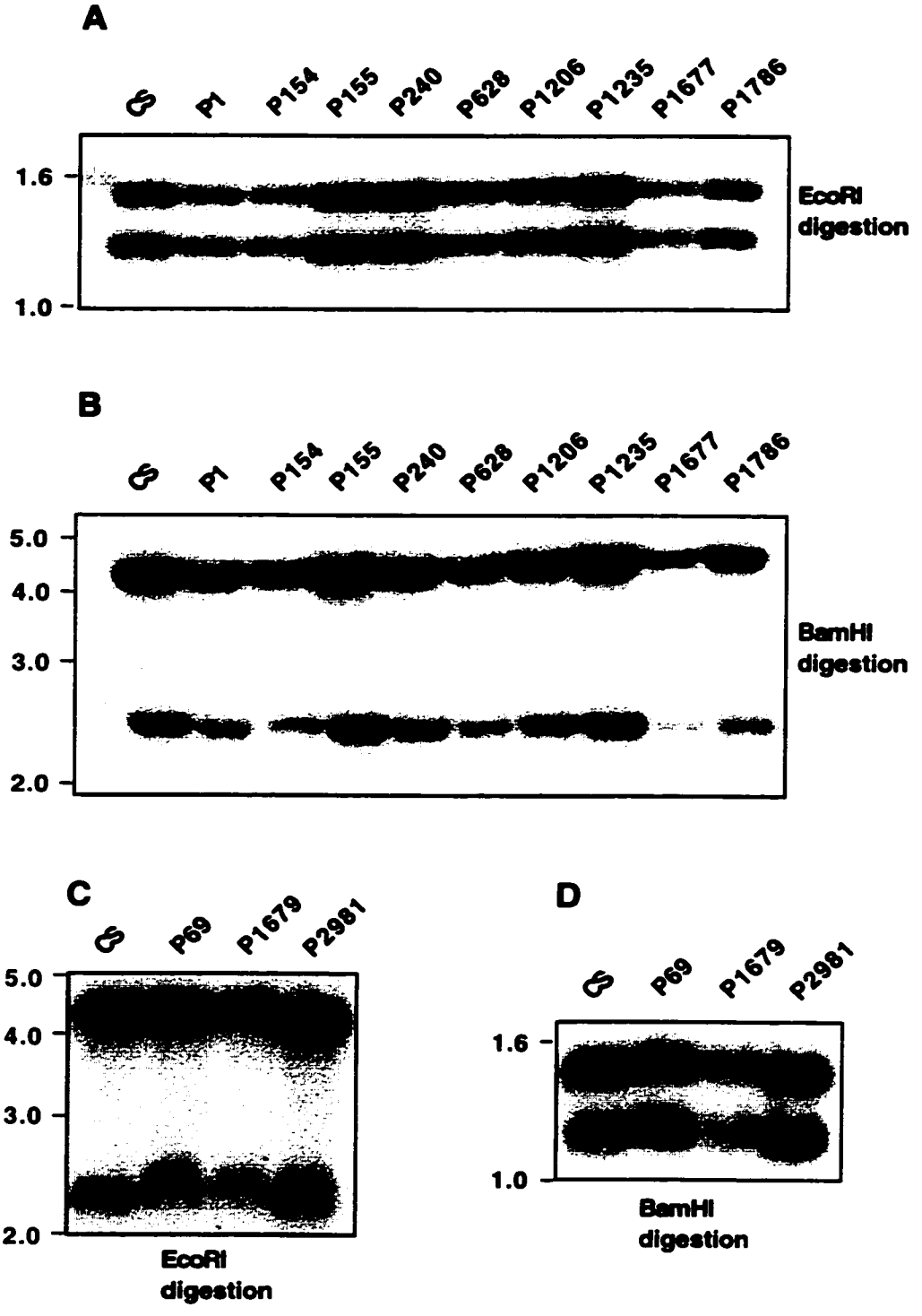
A
CS
P1
P154
P155
P240
P628
P1206
P1235
P1677
P1786
1.6
1.0
EcoRI digestion
B
CS
P1
P154
P155
P240
P628
P1206
P1235
P1677
P1786
5.0
4.0
3.0
2.0
BamHI digestion
C
CS
P69
P1679
P2981
5.0
4.0
3.0
2.0
EcoRI digestion
D
CS
P69
P1679
P2981
1.6
1.0
BamHI digestion

Discussion

The *disco* gene codes for a putative transcription factor:

The *disconnected* gene is required for proper development of the *Drosophila* larval visual system, and codes for a putative transcription factor with two Krüppel-like zinc-finger domains (Steller *et al.*, 1987; Heilig *et al.*, 1991). DISCO contains one complete C_2H_2 and one incomplete and unusual CCH Krüppel-like fingers.

The C_2H_2-type zinc-fingers are known to bind DNA in a sequence specific manner (reviewed by Bernstein *et al.*, 1994). The consensus for the C_2H_2-type motif is (Y,F)-X-C-$X_{2,4}$-C-X_3-F-X_3-L-X_2-H-$X_{3,5}$-H-$X_{2,6}$. In the 30 amino acids long motif, the seven conserved residues and the spacing between them are vital for its structure and DNA-binding activity (Bernstein et al., 1994; Berg, 1990). The two conserved cysteine and two histidine residues make direct contact with a zinc atom. Substitution of any of these four residues is sufficient to abolish the DNA binding activity of the domain. The *disco* gene function is completely disrupted by mutations that lead to substitution of one of the two conserved Cys residues in the zinc-finger domains of the encoded protein.

The possible role for DISCO as a transcription factor was first recognized from *in-situ* expression studies (Kevin Lee, Ph. D. thesis, 1993, Lee *et al.*, 1999). These studies demonstrated an autoregulatory function of *disco* in maintaining its own mRNA expression in the optic lobe primordium (the target area for photoreceptor axons). Subsequent *in vitro* studies have demonstrated a direct binding of the zinc-finger domain of *disco* to its own promoter region. Furthermore, substitution of the first conserved Cys residue of the N-terminal

zinc-finger domain of DISCO with tyrosine abolishes *disco* function *in vivo* and the *disco* promoter-binding ability of the domain *in vitro* (Heilig, *et al.*, . *et al.*, 1991, Kevin Lee, Ph. D. thesis, 1993, Lee *et al.*, 1999).

Although these studies were significant in understanding the *disco* gene function, the transcription regulatory function of DISCO has not yet been conclusively demonstrated due to the lack of any knowledge on DISCO targets. The results of the yeast two-hybrid assays reported in this chapter provide additional evidence that support the proposed transcription regulatory function of *disco*. It was observed that a LexA-DISCO fusion carrying the glutamate-rich (acidic) portion of DISCO, was able to activate transcription of the *lacZ* reporter gene from a yeast interaction trap-reporter gene construct (Figure 3). Activation of reporter gene transcription from this construct would otherwise need an activation domain. This result supports previous findings that have demonstrated the transcription activation ability of glutamate/aspartate-rich acidic domains in several transcription factors (e.g., Ma and Ptashne, 1987; Triezenberg, *et al.*, 1988). Identification of a putative transcription activation domain in *disco* argues in favor of the proposed transcription regulatory function of DISCO.

The N-terminal DISCO bait generated for the yeast interaction trap assay uncovered an interesting property of the second zinc-finger domain of DISCO. It was observed that the wild-type zinc-finger domain of DISCO was sufficient to activate transcription of the reporter gene in the absence of any activation domain provided by tagged library proteins. The transcription activation ability of this bait was abolished when one of the conserved Cys residues of the second zinc-finger domain was substituted with a Ser residue.

A possible mechanism by which the second zinc-finger domain of DISCO allows activation of reporter gene expression is suggested by studies on other zinc-finger containing transcription factors (reviewed in Mackay *et al.*, 1998). A number of these transcription factors contain several zinc-finger domains, some of which are involved in DNA binding, while others are dedicated to protein-protein interactions (Georgopoulos *et al.*, 1997; Tsang *et al.*, 1997; Merika and Orkin, 1995). For example, the transcription factor GATA-1 contains two CCCC-type zinc-finger domains, the C-terminal of which binds DNA, while the N-terminal domain interacts with zinc finger domains of other transcription factors including the sixth CCHC (an unusual Krüppel-like domain) zinc-finger domain of FOG (Friend of GATA) (Tsang, 1997) and the Krüppel-like zinc-finger domains of the transcription factors Sp1 and EKLF (Merika and Orkin, 1995). The Krüppel-like fingers in Sp1 and EKLF proteins appear to bind both DNA and protein. These observations suggest the possibility that the second zinc-finger domain of DISCO interacts with zinc-finger domains of other proteins to activate transcription. One may speculate that binding to an endogenous yeast transcription factor by the zinc-finger domain of DISCO may allow activation of the reporter gene expression.

Identification of DISCO partners:

Characterization of mutants in which *disco* gene function is disrupted has revealed a role for *disco* in photoreceptor axon pathfinding (Steller *et al.*, 1987). Since *disco* expression is absent in photoreceptor cells, *disco* expression in the photoreceptor target area, the optic lobe, appears to be important for proper neuronal connectivity formation in the visual system. In fact, the differentiation

of optic lobe pioneer cells (OLPs) that are contacted by the larval optic nerve (LON) during larval visual system development, is disrupted in *disco* mutants (Campos *et al.*, 1995). It has been proposed that expression of *disco* in these cells and in a subpopulation of glial cells, also contacted by the LON, direct the LON pathway formation. A tissue–specific autoregulatory activity of *disco* localized to the cells of the optic lobe primordium (Kevin Lee, Ph. D. thesis, 1993), and the importance of *disco* expression in this region (Lee *et al.*, 1999; Campos *et al.*, 1995), suggest that dissecting the *disco* autoregulatory pathway will be an important step towards understanding the role of *disco* in visual system connectivity.

To address the molecular mechanism of tissue-specific autoregulation of *disco*, we focused our study on identifying proteins that interact and cooperate with *disco*. To that end we used the yeast interaction trap technique (Gyuris *et al.*, 1993). The expectation is that some of the proteins identified in the screen may represent molecules that regulate tissue specific *disco* function.

Using the interaction trap assay, two new genes and one previously known gene (*dip1*, *dip2* and *dip3* respectively) were identified (Figure4). Sixteen independent cDNA clones were isolated for *dip1* alone. This suggests that the corresponding message is highly abundant in the embryo. Sequence analysis of four members of group 1 confirmed the single identity of the members of that group. All of them contained the same *dip1* fragment, corresponding roughly to the 3′ half of the *dip1* mRNA and code for C-terminal half of the predicted DIP1 protein. This observation demonstrates that the C-terminal half of the DIP1 protein is sufficient for interaction with DISCO. The DIP1 fragment identified in the interaction trap screen contains a 111 amino acid region with no known functional domain that precedes the putative dsRNA-binding domain present in

the C-terminal portion of the predicted protein. Whether the 111 amino acid region contains a domain that mediates interaction with DISCO, has to be determined through deletion analysis. The specificity of the DIP1-DISCO interaction seen in yeast was further tested in an *in-vitro* binding assay. A direct physical association was demonstrated between GST-DISCO fusion proteins expressed in *E. coli* and DIP1 protein synthesized *in vitro* (Figure7).

Unlike *dip1* cDNA, the *dip2* cDNA was isolated only once in the same interaction trap screen. The interaction was nevertheless quite strong as judged by the intensity of the blue colour produced on X-gal plates. Isolation of a single positive clone for *dip2* may indicate a lower relative abundance of the *dip2* transcript in *Drosophila* embryo compared to that of *dip1* transcripts. Furthermore, the library used in this study was amplified several times. Presumably these amplifications led to a further reduction in the percentage of low copy number cDNAs. However, direct association between DISCO and DIP2 *in-vitro* strengthened the argument that DIP2 is a true interactor of DISCO.

The third DISCO-interacting protein (DIP3) isolated in the interaction trap assay is a putative ATPase, the fourth subunit of the *Drosophila* 26S proteasomal complex (Hoyle and Fisher, 1996). The *dip3* cDNA was also represented once among the 18 interacting clones.

The *dip1* gene expresses three different size transcripts with repeated sequences at the 3' untranslated region:

A nearly full-length *dip1* cDNA was isolated from a *Drosophila* cDNA library made in λgt11 vector. This *dip1* cDNA clone contains the full coding region for the putative DIP1 protein. The size of the protein, predicted from the

open reading frame of the cDNA, is approximately 36.6 kDa. The yeast interaction trap screening led to the isolation of only a 1.1 kb partial cDNA clone that lacked the 5′ end of the corresponding mRNA. Both cDNAs contain an unusual 124 bp repeating element in the 3′ untranslated region (UTR). Sequence comparison of the two cDNAs isolated from two different libraries showed a difference in the 3′ UTR (Figure 12). The larger cDNA contains 8-10 repeats, while the shorter cDNA has only 4 repeats. The larger cDNA also contains an additional 348 bp sequence at the 3′ end. The difference in the 3′ UTR indicates that these cDNAs represent alternatively spliced transcripts for *dip1*. The possibility of alternative splicing of nascent *dip1* mRNA is supported by the results of the Northern analysis that showed expression of at least three different transcripts during embryogenesis (Figure 15). We were unable to determine the exact number of repeats and as a result the exact size of the *dip1* cDNA isolated from the λgt11 library. From the size estimated from agarose gel electrophoresis (~2.6 kb), the *dip1* cDNA appears to have 8 repeats and may represent the largest transcript (~3.0 kb) seen on the northern blot (Figure 15). It has not yet been determined if the above cDNA lacks a portion from the 5′ end of the corresponding transcript.

The presence of 124 bp repeating elements of almost identical sequence in the 3′ UTR is a unique feature of the *dip1* cDNAs. Results of our Northern analysis suggest the possibility that other RNA species expressed in *Drosophila* embryos may also contain the same repeat. This possibility is strengthened from the results of *in situ* chromosomal localization studies that showed hybridization of a *dip1* probe which included the repeated region to an additional location on the polytene chromosome. These observations suggest the presence of at least

one other gene in the *Drosophila* genome that contains the repeating element present in *dip1* cDNAs.

The striking identity in the nucleotide sequence of the individual repeats suggests an important regulatory role in gene regulation. The 3′ UTRs in several mRNAs have been shown to be involved in translational regulation, subcellular localization and stability (Gavis *et al.*, 1996; Singer, 1992; Sachs, 1993; Rastinejad and Blau, 1993). These processes are in turn important for regulation of gene expression during cell growth and development.

Repetitive sequences in the 3′UTR have been shown to mediate translational regulation of mRNAs. An example has been demonstrated for the gene *15-lipoxygenase* (*loxA*; Ostareck-Lederer *et al.*, 1994). The *loxA* mRNA codes for an enzyme that degrades phospholipids during breakdown of internal membranes of mitochondria during reticulocyte maturation. The *15-loxA* mRNA is transcribed in bone marrow during early stages of erythropoiesis, but is translated only when reticulocytes reach the peripheral blood. It was demonstrated that a 19 nucleotide sequence repeated 10 times in the 3′UTR of *loxA* mediates the translational repression of the mRNA during early stages of erythropoiesis (Ostareck-Lederer *et al.*, 1994). The fusion of *loxA* repeated elements to the 3′ UTR of a reporter gene was sufficient to cause translational repression of the reporter genes. Whether the varying number of the 124 bp repeats present in different *dip1* transcripts are involved in differential regulation of translation of the corresponding mRNAs and whether translational regulation confer spatial restriction to *dip1* gene function are important questions to be addressed in future.

Analysis of secondary structure of the repeated region of the *dip1* cDNAs using 'MFOLD' software (Walter *et al.*, 1994) predicts formation of stem-loop structures in the 3' UTR of the corresponding mRNAs. The analysis showed that the number of stem-loops that form depends on the number of repeats present in the cDNA. Approximately two repeats are required for each stem-loop. For example, analysis using four repeats led to the formation of 2 stem loops, while eight of them formed 4 stem-loops (results of the analysis are shown in the appendix). This secondary structure analysis thus predicts the formation of double-stranded RNA regions in the 3'UTR of *dip1* mRNAs. Double-stranded RNA regions formed by repeated elements may provide a mechanism for translational regulation of mRNAs by dsRNA-binding proteins.

The *dip1* gene codes for a putative double stranded RNA-binding protein:

Sequence analysis of the *dip1* cDNA that appear to contain the full coding sequence revealed the presence of two type B double stranded RNA-binding domains (dsRBDs) in the predicted DIP1 protein. The type B dsRBDs in general match well with the C-terminal short domain consensus (23 amino acids), but fit the N-terminal long domain consensus (47 amino acids) only poorly (St. Johnston *et al.*, 1992; Figure 13).

Examples of type B proteins that are known to bind dsRNA substrates include the PAC1 protein of fission yeast *S. pombe* (Iino *et al*, 1991). PAC1 shares similarity with RNaseIII and is known to degrade dsRNA substrates when expressed in *E. coli*. Several other dsRNA-binding proteins are known to contain both type A and type B dsRBDs. These include, the *Xenopus* protein Xlrbpa, its human homolog TRBP (TAR binding protein), and the STAUFEN protein of

Drosophila (St. Johnston *et al.*, 1992). TRBP is known to bind TAR (trans-activating region contained in 5' ends of human immunodeficiency virus transcripts) stem-loop of human immunodeficiency virus (HIV) RNA (Gatignol *et al.*, 1991). In *Drosophila* embryos, maternal *staufen* gene product is required for the correct localization of *bicoid* and *oskar* RNA to the anterior and the posterior poles of the egg (Kim-Ha *et al.*, 1991).

The dsRBDs of *dip1* are similar to those of mammalian glutamate receptor editases:

The dsRNA binding domains of DIP1 share significant similarity with those of human and rat glutamate receptor editases, hRED1 and rRED1 respectively (Lai *et al.*, 1997; Melcher *et al.*, 1996), which extends beyond the conserved residues of the dsRBD consensus. Figure 14 shows the alignment of the dsRBDs of DIP1 with that of the glutamate receptor editases. On average, the amino acids sequences of DIP1 and the mammalian glutamate receptor editases share 36% identity and 72% similarity within their dsRNA binding motifs. This similarity raises the question of whether these proteins recognize and bind similar RNA sequences.

Although the predicted DIP1 protein shares extensive similarity with the 300 amino acid N-terminal region of hRED1/rRED1, it lacks the C-terminal catalytic deaminase domain of the glutamate receptor editases. Editing (deamination) adenine residues of glutamate receptor mRNAs by these editases causes an adenine to inosine conversion. In the case of the glutamate receptor-B subtype, such a site-specific A to I conversion results in the substitution of an arginine for a glutamine in the protein (Lomeli *et al.*, 1994; Melcher, *et al.*, 1996;

Lai *et al.*, 1997). This in turn alters the calcium conductance properties of the glutamate receptor gated ion channel (Lomeli, *et al.*, 1994).

Although the predicted DIP1 protein lacks an editase domain, we can not entirely exclude the possibility of its involvement in an editing event. At present the genomic sequence for *dip1* is not known. In addition, the full coding sequence for only one alternatively spliced *dip1* transcripts is available. Therefore, one may consider the possibility that one of the two uncharacterized *dip1* transcripts contain a potential editase domain.

Another alternative view regarding the function of the predicted DIP1 protein is the possibility of it being a component of a multiprotein editase complex, where the editase activity is provided by a separate protein. One such example is seen in the case of apolipoprotein B mRNA editing (Navaratnam *et al.*, 1993; Mehta and Driscoll, 1998). Editing of the apolipoprotein B mRNA leads to the production of two forms of the protein, apo-B100 and apo-B48. Apo-B100 and apoB-48 perform distinct functions in lipoprotein structure and metabolism. Apo-B48 is translated from an edited RNA in which cytidine (position 6666) is deaminated to uracil. This results in a premature termination of translation. Interestingly, the editing is done by a multiprotein complex, called the editase complex. In this complex, the RNA-binding domain that binds the apolipoprotein B mRNA and the editase catalytic domain are located on two different proteins.

In addition, to the dsRBDs, the DIP1 sequence also shares similarity with a bipartite nuclear localization signal present in these editases (Figure 14). Nuclear targeting of the DIP1 protein would be necessary for it to function as *in-vivo* interactor of the transcription factor DISCO. Preliminary studies in the lab with

antibody raised against the DIP1 protein indeed shows its nuclear localization (data not shown).

The *dip1* gene maps close to or represents *flamenco*:

Southern analysis of 20A deficiencies showed that the genetic location of the *dip1* gene is very close or may be identical to the *flamenco* (*flam*) locus (Prud'homme *et al.*, 1995). *flam* is known to control the expression of gypsy retrovirus elements of *Drosophila melanogaster*. These viruses exist in the *Drosophila* genome as endogenous provirus. Establishment of the endogenous provirus arises from infection of germ cells by the viral particles and subsequent insertion of DNA corresponding to the RNA genome of these viruses in the *Drosophila* genome. In homozygous *flam* mutants, insertion rate of the retroviral elements in the germ line is increased several fold. Although, in the absence of the *flam* gene function, increased gypsy mobilization is seen in the germ line, the site of *flam* gene function is not the germ-line cells, but, the follicle cells of somatic origin that surround the germ-line cells (nurse cells and oocyte) (Song *et al.*, 1997). This was shown by demonstrating that the expression of the retroviral genome encoded proteins occur only in the follicle cells of the ovary. The complete virion particles expressed in the follicle cells of the *flam* mutant ovaries then infect the underlying oocyte (Pelisson *et al.*, 1994). Expression of the *dip1* mRNA in the follicle cells, the site of *flamenco* gene function, is consistent with the possibility that the *dip1* gene represents *flamenco*.

The production of complete infectious gypsy viral particles require expression of three transcripts, *gag*, *pol* and *env* (Marlor *et al.*, 1986; Pelisson *et al.*, 1994)). Gag and Pol proteins are expressed from the first and second open

reading frames of full-length gypsy mRNA. Env is expressed from an alternatively spliced transcript produced from the same mRNA. Interestingly, it was noted that the wild-type *flam* gene function inhibits expression of the alternatively spliced transcript (*env*) of the gypsy retroviral mRNA (Pelisson *et al.*, 1994). Since a functional *flam* gene prevents alternative splicing of the gypsy mRNA, complete virions are produced only in the absence of *flam* gene function. These observations suggest that the mechanism by which the wild-type *flam* gene function prevents expression of *env* is by blocking a splice acceptor site in the full-length gypsy mRNA. Since *dip1* codes for a putative RNA binding protein, a role for this gene in alternative splicing events may not be surprising.

A previous study has demonstrated intimate associations between transcription and splicing events in the nucleus (Jimenez-Garcia and Spector, 1993, reviewed by Neugebauer and Roth, 1997). Furthermore, several examples are known that show direct *in vivo* associations between transcription complexes and splicing factors. These include interaction of the transcription factor Spi-1/PU.1 with the splicing factor TSL (Translocated in Liposarcoma) and interaction of RNA polymerase II with SRrp129/CASP11, a member of the SR (serine-, arginine-rich domain) family of splicing factors, (Hallier *et al.*, 1998; Tanner *et al.*, 1997). The TSL protein promotes the use of a 5′ splice acceptor site during alternative splicing of the adenovirus E1A nascent mRNA in a IW1-32 erythroid cell line cotransfected with *tsl* and E1A genes (Hallier *et al.*, 1998). The transcription factor Spi-1 appears to interrupt the splicing process by trapping the splicing factor TSL. In addition to its role in alternative splicing, TSL has also been shown to interfere with the transcription regulatory function of Spi-1. These observations suggest the possibility that DIP1 may have a role in splicing

while being a component of the DISCO transcription machinery. The example of TSL and Spi-1 show how interaction between an RNA-binding protein and a transcription factor can regulate more than one biological process.

Although, proteins containing dsRBDs are generally known to bind dsRNA substrates, one exception is the mammalian transcription factor NF90, a component of the heterodimeric nuclear factor of activated T cells (Corthesy, 1994; Kao et al., 1994). The normal physiological function of NF90 is to regulate transcription of the *interleukin-2* gene by binding to its promoter (the ARRE element). However, during adenovirus infection, this protein may also be able to bind the highly structured single stranded RNA of these viruses (Liao *et al.*, 1998). It has been proposed that adenoviruses exert their control on cellular function through interaction with various RNA-binding proteins including NF90 (Liao *et al.*, 1998). The dual role of NF90 raises the possibility that the putative dsRBDs of the DIP1 protein may also have a dual function. On the other hand, under normal physiological conditions these domains may act as DNA-binding motifs. While, during retroviral infection of the *Drosophila* ovary, they may function as RNA binding motifs to activate the cellular defense mechanism that prevents infection of the germ line by the gypsy elements.

The example of NF90 suggests the possibility that the DIP1 protein might exert its effect on alternative splicing by binding to a single stranded region of the nascent gypsy mRNA. At the same time, the high similarity seen in the dsRBDs of DIP1 and the mammalian glutamate receptor editases might suggest similar substrate-binding specificity. The editases bind dsRNA substrates formed through base pairing between intronic and exonic sequences of newly transcribed target mRNAs (Lomeli *et al.*, 1994; Higuchi, *et al.*, 1993). Therefore,

we can not exclude the possibility that DIP1 binds to similar dsRNA substrates in order to mask certain splice acceptor sites.

The *dip2* gene codes for a highly conserved protein expected to play an important role in nervous system development:

Sequence analysis of the partial 1.2 kb *dip2* cDNA (Figure 6) revealed that it has the potential to code for a highly conserved protein of unknown function. The *C. elegans* and human homologs of the *dip2* gene have already been cloned in the corresponding genome projects. A partial 382 bp 3′ end fragment of mouse *dip2* cDNA has also been cloned in collaboration with another member of the lab (Figure 25). Alignment of the predicted amino acids sequences of all DIP2 homologs showed that the partial C-terminal mouse sequence shares 82.3% identity and 97.6% similarity in amino acid sequence with that of the *Drosophila* DIP2 protein (Figure 26). The C-terminal 31 amino acids of the DIP2 proteins from all species are identical. The predicted *Drosophila* protein contains an extra 53 amino acids segment 124 amino acids upstream from the stop codon, which is not present in any other DIP2 homolog. Whether this extra 53 amino acid sequence in the *Drosophila* protein confers any unique property to it compared to homologs in other organisms will be a subject for future investigation.

Northern analysis of *dip2* transcript revealed expression of a single mRNA approximately 5 kb in length during embryogenesis (Figure 20). The size of the full-length *C. elegans* DIP2 protein predicted from its genomic sequence is about 1414 amino acids in length. The protein coding sequence therefore corresponds to about 4.2 kb of mRNA. The size of the *dip2* transcript on the Northern blot

suggests that the size of the *Drosophila* DIP2 protein may be comparable to the size of its *C. elegans* homolog.

The *dip2* mRNA shows a highly tissue-specific expression pattern during embryogenesis. Extensive expression is seen in the developing nervous system at all stages of embryogenesis. Recently, in collaboration with Dr. M. Rudnicki's lab (McMaster University) the expression of the mouse *dip2* mRNA has also been determined. Interestingly, expression in mouse is also localized to a subset of cells in the developing nervous system. These results may implicate an important role for *dip2* homologs in nervous system development.

The location of the *dip2* gene on *Drosophila* polytene chromosomes was determined to be in band 61B located at the tip of the left arm of chromosome III (Figure 21). Results of the deficiency mapping agree with the *in-situ* data (Figures 3.22, 3.23). Based on this chromosomal location we identified two genomic P1 clones each of which contains at least a portion of the *dip2* gene. Because of technical difficulties in sequencing DNA from large P1 clones (80-100 kb), so far only a 2.7 kb portion of the *Drosophila dip2* gene has been sequenced. There is a continuous open reading frame in this 2.7 kb sequence with a stop codon at nucleotide position 2509 (Figure 24). The predicted amino acid sequence shares a high degree of similarity with that of other DIP2 homologs along its entire length (836 amino acids). These observations suggest the absence of any intronic sequence in this 2.7 kb portion of the *Drosophila dip2* gene.

Search for protein domains in the 'Motif' database (ICR, Kyoto U) failed to detect the presence of any known functional domain in the predicted DIP2 protein. However, a weak similarity to an AMP binding domain consensus (PROSITE database, accession number PDOC00427) was detected. AMP binding

domains are normally found in a variety of enzymes that include insect luciferase, acetyl-CoA ligase, 4-coumarate-CoA ligase as well as others. Sequence analysis in the 'Blocks' database (Henikoff and Henikoff, 1994) revealed weak similarity to a 30 amino acid sequence from members of the adenosine- and AMP-deaminase families. The role this 30 amino acid domain plays in the function of these enzymes has not yet been elucidated. Whether the weak similarities with the AMP binding domain normally found in enzymes for energy-dependent catalysis indicate an enzymatic function for the predicted DIP2 protein is not yet known.

Submission of the C. *elegans* DIP2 sequence in the 'SOSUI' database (Hirokawa *et al.*, 1998) failed to find evidence for the presence of any transmembrane domain in the predicted protein. Analysis of the DIP2 sequence for subcellular localization in the 'PSORT' database (Nakai and Kanehisa, 1992; Horton and Nakai, 1997) predicted the presence of an SV40 large T-antigen type nuclear localization signal (reviewed by Raikhel, 1995). However, the total basic amino acid content of the DIP2 protein is less than 20%, a value lower than that found in most nuclear proteins. Our efforts to express a C-terminal DIP2 protein fragment as GST- or His- fusion proteins in bacteria and as haemaglutinnin-fusion protein in *Drosophila* S2 cells in culture failed. However, fusion of the same DIP2 fragment with a nuclear localization signal allowed expression of the protein in yeast. This observation might indicate that the *dip2* gene codes for a protein that is stable only inside the nucleus.

To assess the role of the *dip2* gene product in the regulation of DISCO function, it is essential to determine the consequence of disruption of *dip2* gene function. In an effort to identify existing mutations that might disrupt *dip2* gene

function, we examined several P-element insertion mutants from the region of the third chromosome where the *dip2* gene is located. Using a probe corresponding to the 3′ end of *dip2* cDNA, available at that time, we were unable to identify any mutant line that carried a P-element insertion inside the *dip2* gene. However, a probe corresponding to the 3′ end of the gene may not be able to detect an insertion at the 5′ end of the gene. Isolation of mutations at the *dip2* locus and also their characterization will shed light on the possible role played by this gene during nervous system development.

The *dip3* gene codes for the ATPase subunit of the *Drosophila* 26S proteasome complex:

The third DISCO interacting protein (DIP3) isolated in the interactor hunt is a putative ATPase, the fourth subunit of the *Drosophila* 26S proteasomal complex (Hoyle and Fisher, 1996. 26S proteasomes are known to regulate a variety of cellular processes through targeted degradation of cytoplasmic and nuclear proteins (reviewed by Goldberg, 1992). It consists of at least two components; a proteolytic core known as the 20S proteasome, and an ATPase complex (Orlowsky, 1990; Goldberg, 1992). 26S proteasomes are responsible for ubiquitin- and ATP-dependent degradation of proteins. The normal functioning of eukaryotic cells depends on these pathways to remove regulatory proteins such as cyclins and signal transduction molecules at appropriate times to ensure normal cell division and development.

Analysis of results from almost 100 hunts has revealed that the proteasomal subunits are often isolated as false positives in interactor hunts using different baits (reviewed in Brent and Finley, 1997). However, the current

literature suggests that functionally relevant interaction between transcription factors and ATPase subunits of 26S proteasomes is not uncommon. For example, the ATPase component of the 26S proteasomal complex has been shown to interact with a variety of transcription factors including Gal4 in yeast and c-FOS is mammalian cells (Swaffield *et al.*, 1992; Wang *et al.*, 1996). Mutation in SUG1, the ATPase subunit of the yeast 26S proteasome suppresses a mutation in the transactivation domain of Gal4 (Swaffield, *et al.*, 1992). To show an *in-vivo* interaction between DISCO and DIP3, it will be necessary to generate mutations in the *dip3* gene. Since *dip3* mRNA has a ubiquitous expression pattern (data not shown), tissue specific modification of *dip3* gene function will be necessary.

How to interpret yeast interaction trap results:

The most difficult problem encountered by investigators using a yeast interaction trap assay is to recognize the interactions that have physiological relevance as opposed to false positives (reviewed in Brent and Finley, 1997). False positive interactions that satisfy all the selection criteria can be of different types. For example, some false interactions never occur in nature, since, the spatial and temporal expression pattern of the interacting proteins do not overlap. These interactions may still be informative in the sense that they may suggest the existence of similar interactions between related molecules. Some false positives may result with "sticky" proteins that activate the reporters in some other ways, for example by interacting with other components of the transcription machinery. Examples of such proteins include heat shock proteins, ribosomal proteins and proteasome subunits. However, the interactions that are clearly false occur fairly infrequently (reviewed by Brent and Finley, 1997).

Interactions that may occur in nature but are not informative include those between baits and members of ubiquitin-dependent proteolytic pathway. Although it may provide a clue as to the degradation process of the bait, it is difficult to follow up the interaction to show its physiological relevance.

Another disadvantage of the interaction trap screening is its inability to detect certain physiologically relevant interactions (reviewed by Brent and Finley, 1997). This system is unable to detect weak interactions with equilibrium dissociation constants weaker than 10-50 μM. Expression of library proteins that are toxic for yeast cells can also lead to false negatives. Furthermore, both interacting proteins in this system contain bulky N-terminal multidomain moieties fused to their N-terminus. These can block interactions that require the N-termini of the partners. Interactions between two proteins also require proper folding of the proteins in the aqueous environment of the yeast nucleus. This is particularly problematic to those proteins that require hydrophobic environment for proper folding, such as, membrane spanning proteins.

The disadvantages of the interaction trap assay suggest that the interactions seen in yeast should be interpreted carefully and reexamined with properly designed follow up experiments to show physiological relevance. The studies presented in this thesis and proposed in the future direction (Chapter 4) outline some of the experiments that can be done to address the above issue.

Materials and methods:

Constructs:

Bait construct with full length *disco* coding region:

In this construct the *disco* coding sequence was cloned in frame with the *lexA* coding sequence located 5′ to the multiple cloning site of the yeast expression vector pEG202. pEG202 (Gyuris *et al.*, 1993) is a yeast-*E. coli* shuttle vector that contains a *E. coli* origin of replication, the ampicillin resistance gene, a yeast origin of replication (2 mm ori) and a yeast selectable marker (HIS3). It also contains the promoter from the yeast alcohol dehydrogenase gene (ADH1), a coding sequence from the bacterial repressor protein LexA, a polylinker and the transcription termination sequence from the yeast ADH1 gene. The *disco* coding region was PCR amplified with primers containing EcoRI (GAATTC) sites. Pfu polymerase (Stratagene) with proof reading activity was used for PCR to eliminate mutations in the amplified product. Absence of any mutation was confirmed through sequence analysis. The amplified product was digested with EcoRI and cloned at EcoRI site of pEG202. The orientation of the *disco* fragment was examined by digesting the construct with XhoI and confirmed through sequence analysis. Sequences of the two primers used for PCR amplification are as follows:

AB6530 (sense primer): 5′ CCC ACC ACA GAA TCC ATG GAG CAC 3′.

AB6531 (antisense primer): 5′ T CGC CAT GGA TCA GAA TTC TGG AC 3′.

Bait construct with 5′ *disco* sequence:

For N-terminal DISCO bait, a 5′ *disco* cDNA fragment corresponding to 186 N-terminal amino acids was PCR amplified with primers containing EcoRI sites and

cloned at EcoRI site of the vector pEG202. The DISCO sequence was cloned in frame with the LexA coding sequence. Sequences of the two primers used for PCR amplification are as follows:

AB6530 (sense primer): 5′ CCC ACC ACA GAA TCC ATG GAG CAC.

AB7045 (antisense primer): 5′ G CAA GCG GAA TTC GTC CGG C 3′.

Bait construct with mutated 5′ *disco* sequence:

For the mutated DISCO bait, a 5′ *disco* cDNA fragment corresponding to 186 N-terminal amino acids of DISCO, but, with a mutation that substitutes Cys at position 127 to Ser (Heilig *et al.*, 1991), was PCR amplified from genomic DNA extracted from *disco1* mutant flies. The primers that were used to amplify the wild type 5′ *disco* fragment were also used to amplify the mutated 5′ *disco* fragment and subcloned into pEG202.

Bait construct with 3′ *disco* sequence:

For the C-terminal DISCO bait, a 3′ *disco* cDNA fragment corresponding to C-terminal 153 amino acids was PCR amplified with primers carrying EcoRI sites and the restriction fragment was cloned at the EcoRI site of pEG202 in frame with the *lexA* coding sequence. Sequences of the two primers used for PCR amplification are as follows:

AB7044 (sense primer): 5′ AGC ATC AAA ATG GAA TCC GAC CCG 3′.

AB6531 (antisense primer): 5′ T CGC CAT GGA TCA GAA TTC TGG AC 3′.

***lacZ* reporter construct:**

The *lacZ* reporter construct pSH18-34 was kindly provided to us by Dr. Roger Brent (Harvard Medical School). The construct contains a TATA box, transcription start site and a small part of the Gal1 coding sequence fused to *lacZ* gene. In this construct, the Gal1 upstream activating sequence was replaced with

four LexA operators (Hanes and Brent, 1989). The reporter construct pJK101 (Brent and Ptashne, 1985) used for the repression assay contains most of the Gal1 upstream activating sequence (UASg), and one LexA operator located between the UASg and the Gal1 TATA box. pSH18-34 and pJK101 are both yeast-*E. coli* shuttle vectors and contain the yeast selectable marker URA3.

GST-DISCO fusion constructs:

The same wild-type and mutated 5′ *disco* fragments that were cloned into the yeast expression vector pEG202 were also used to generate GST-DISCO fusion constructs. These 5′ *disco* fragments were cloned into the EcoRI site of the vector pGEX-1 (Pharmacia). The pGEX-1 vector contains the GST coding sequence upstream of the multiple cloning site.

***In-vitro* expression constructs for *dip1* and *dip2*:**

The *in-vitro* expression vector used for this study was pSPUTK. The pSPUTK is a vector with high expressivity that contains the 5′ untranslated region of *Xenopus* β globin gene and Kozak translation initiation sequence (ANNATGG; Kozak, 1996). It also contains SP6 and T7 promoter sequences. This vector was constructed in Dr. David Andrews's laboratory at McMaster University and was kindly provided to us. Both *dip1* and *dip2* cDNAs with the haemaglutinin epitope tag were PCR amplified from the yeast expression vector pJG4-5 with primers carrying restriction sites. The sense primer had a SalI site, and the antisense primer had a XbaI site. The amplified products were cloned at SalI and XbaI sites of the pSPUTK expression vector. The primers used for this purpose are as follows:

AB10133 (sense): 5′ A GCC TCT TGC TGA GTC GAC ATG CC 3′.

AB10134 (antisense): 5′ GC GAA GAA TCC AAA GCT TCT AGA G 3′.

Strains used:

Yeast strain: The yeast strain *S. cerevisae* EGY48 used in this study was kindly provided by Dr. Roger Brent. The genotype of the strain is *ura3, his3, trp1,* LexAop-*leu2*. The LexAop-*leu2* reporter gene construct is integrated into the genome of EGY48. In this reporter gene construct, regulatory region of the *leu2* gene was replaced with three high-affinity LexA binding sites (LexA operators).

Bacterial strains:

MC1066: The genotype of the strain is *trp1 leu2 ura3*. It was obtained from Dr. Aloke Sil (Pennsylvania State University).

BL21 DE3 : The genotype of the strain is F^- *ompT* $hsdS_b$ ($r^- m^-$) *gal dcm* (DE3). It is a protease negative *E. coli* strain. Is was obtained from Dr. Andre Bedard (York University).

Repression Assay (Brent and Ptashne, 1984):

The *lacZ* reporter construct used for repression assay was pJK101. This assay was performed to verify nuclear localization of different baits used in this study and to check their ability to bind LexA operator (LexAop). The *lacZ* gene expression from this construct is driven by Gal1 promoter. There is one LexAop site located in between a TATA box and the Gal1 promoter in the reporter construct. Binding of the LexAop by the bait represses *lacZ* expression by 2-20 fold.

Procedure:

The yeast strain EGY48 was transformed with three sets of plasmids; (i) pJK101 and a bait construct containing the auxotrophic markers URA3 and HIS3 respectively, (ii) pJK101 and the HIS3 control plasmid pRFHM1 (positive control

for repression of *lacZ* expression), and (iii) pJK101 alone. Double transformants were selected on glucose media lacking Uracil and Histidine, and single transformants were selected on glucose media lacking Uracil.

Four individual colonies from each double transformation were streaked onto galactose/raffinose, X-gal media lacking Uracil and Histidine. Four transformants from single transformation were streaked onto galactose/raffinose, X-gal media lacking Uracil. The blue colour intensities produced by these colonies were compared to each other to determine repression of *lacZ* expression by baits.

Yeast cell transformation:

Except for library transformation, all other yeast cell transformations were done using the protocol described below (Geitz *et al.*, 1992):

Yeast cell cultures were grown in 50ml volume overnight at 30°C in appropriate medium. Overnight cultures were pelleted by centrifugation at 2000g for 5 minutes at 4°C. Cells were washed twice in TE buffer (10 mM Tris.Cl pH 7.5, 1 mM EDTA), resuspended in 2 ml of LA buffer (100 mM LiOAc, 0.5 X TE) and incubated at 30°C for 1 hour with gentle shaking. To 0.2ml of the cells in LA buffer 0.5 mg of transforming DNA was added. To the transformation mixture 0.7ml of PEG solution (100mM LiOAc, 40% PEG-3350, 1 X TE) was added, gently mixed and incubated at 30°C for 1 hour. Cells were then heat shocked at 42°C for 10 minutes, allowed to cool down to room temperature and plated on selective medium. The plates were incubated at 30°C for 3 days to allow generation of yeast colonies of detectable size.

Interaction trap screening:

Library used: A *Drosophila melanogaster* 0-12 hr. embryonic cDNA library constructed in the yeast expression vector pJG4-5 was kindly provided by Dr. Roger Brent. The library was made with unidirectional cDNAs with EcoRI sticky ends at the 5′ end and XhoI sticky ends at the 3′ end. The library plasmid is a 2mm plasmid with the TRP1 auxotrophic marker and the Gal1 promoter. Downstream of the Gal1 promoter there is an ATG codon, followed by 105 codons, encoding 9 amino acids from the SV40 Large T nuclear localization signal, 87 amino acids activation domain called B42 (derived from *E. coli*), and 9 amino acids haemaglutinnin epitope tag.

Amplification of the library: To amplify the *Drosophila* embryonic cDNA library constructed in pJG4-5, the library DNA were transformed into *E. coli* Sure cells using $CaCl_2$ heat shock method. Transformants were plated on LB plates with 50 μg/ml of amphicillin. 2.0×10^7 independent transformants were scraped from the plates with LB, and plasmid DNA was extracted using Qiagen plasmid extraction kit.

Screening procedure:

The screening procedure is essentially as described in Finley and Brent, 1995. EGY48 yeast cells containing the bait and the *lacZ* reporter plasmid were grown overnight in glucose ura^-his^- medium at 30°C in a 5 ml culture volume. It was subcultured starting with 1/1000 th dilution in 80 ml volume. The culture was grown overnight at 30°C to O.D600 =1. The culture was next diluted to O.D600=0.3 in a 200 ml final volume and grown for 3 hours at 30°C to approximately O.D600=0.6. The cells were pelleted at 2500 rpm at room temperature, washed in 125 ml TE (10 mM Tris.Cl pH 7.5, 1 mM EDTA) and

resuspended in 5 ml LA (100 mM LiOAc, 0.5 X TE). To 250µl cells 125 µg of salmon sperm DNA and 5 µg of library DNA were added and mixed gently. To this mixture 1.7 ml of PEG solution (100mM LiOAc, 40% PEG-3350, 1 X TE) was added, and mixed again. The transformation mixture was then incubated at 30°C for 30 minutes without shaking. After 30 minutes 0.22 ml DMSO was added to increase the transformation efficiency and the cells were immediately heat shocked for 10 minutes at 42°C. An aliquot was used to check the transformation efficiency. The remaining transformation mixture was diluted 10 fold with galactose/raffinose media lacking Uracil, Histidine, and Tryptophan. Expression of library cDNAs from the Gal1 promoter was induced by growing the transformants in galactose medium for 4 hours at 30°C. The culture was then pelleted at 2000g for 4 minutes at room temperature. Cell pellet was resuspended in 1ml of galactose/raffinose media lacking Leucine, Uracil, Histidine and Tryptophan to select for colonies that activate *leu2* reporter gene expression. A maximum of 10^6 transformants was plated on one 30mm plate.

Activation of the *lacZ* reporter gene expression:

The transformants that survived on the galactose / raffinose $leu^-ura^-his^-trp^-$ plates, were next plated on galactose / raffinose $leu^-ura^-his^-trp^-$ plates supplemented with 80 µg/ml of X-gal. The colonies were tested for their ability to produce blue color on the X-gal plates.

Isolation of plasmids from yeast cells (Hoffman and Winston, 1987):

Yeast cells containing DISCO interacting protein coding cDNAs were grown overnight at 30°C to saturation in selective medium (glucose medium lacking Uracil, Histidine and Tryptophan). 1.5 ml overnight culture was pelleted and

resuspended in 200µl of solution A (2% triton X-100, 1% SDS, 100 mM NaCl, 10 mM Tris pH 8.0, 1mM EDTA). To the resuspended culture, 200 µl of phenol : chloroform : isoamyl alcohol mixture (25:24:1), and 0.3 g glass beads (acid washed, prebaked) were added. The mixture was vortexed for 2 minutes and then centrifuged at maximum speed for 5 minutes in a bench top centrifuge. Aqueous layer (140 µl) was transferred to a new eppendorf tube. To the aqueous layer 420 µl of ethanol and 4 µl of 1 M $MgCl_2$ were added to precipitate the plasmid DNA. The mixture was incubated on dry ice for 10 minutes to ensure maximum precipitation. The plasmid DNA was collected by centrifugation at maximum speed for 15 minutes at 4°C, washed with 70% ethanol, dried and resuspended in 20 µl of H_2O.

***In-vitro* binding experiment:**

In-vitro expression of DIP1 and DIP2:

The DIP1 and DIP2 proteins were *in-vitro* transcribed and translated from the vector pSPUTK using the expression system from MBI Fermentas. The *dip1* and *dip2* cDNAs were transcribed from the SP6 promoter using SP6 RNA polymerase following manufacturer's protocol. The transcription was done for 30 minutes using non-radiolabeled nucleotides at 37°C in a 20µl reaction volume. Only 2µl of the transcription mixture was used to translate the corresponding protein in rabbit reticulocyte lysate in a 20 µl reaction volume. For translation, [^{35}S] methionine was used to label the translated product. 5 µl of the translated product was analyzed on SDS-polyacrylamide gel for *in-vitro* expressed proteins.

Expression and purification of GST-DISCO fusion proteins:

Both wild-type and mutated GST-N-terminal DISCO fusion constructs, as well as GST alone without a fusion protein were expressed from the pGEX vector (Pharmacia) in the protease negative *E. coli* strain BL21 following manufactures protocol. BL21 cells containing the fusion constructs were grown overnight in LB medium with 100 µg/µl ampicillin. Overnight cultures were diluted 100 fold with fresh LB-ampicillin medium to a final culture volume of 30 ml. The culture was grown to O. D_{600} =0.6. IPTG was added to a final concentration of 0.1 mM to induce expression of the fusion proteins. The induction of the cultures was allowed to proceed for 3 hours at 37°C. The induced cultures were pelleted, washed three times with PBS (sodium phosphate buffer pH 7.4), and resuspended in 10 ml PBS. The resuspended cultures were sonicated 1 ml at a time in polystyrene tubes in a refrigerated cup-horn type sonicator (model XL2020, Heat Systems Inc.). Sonication was done in three cycles of 15 seconds sonication and 30 seconds incubation on ice. The sonicated sample was centrifuged in a microcentrifuge at maximum speed for 15 minutes at 4°C to remove cell debris. The supernatant was carefully transferred to a new tube and Triton was added to a final concentration of 1%. To the supernatant 200 µl of 50% glutathione-agarose beads (Sigma) in PBST (1X phosphate buffer saline with 1% triton) was added. The GST-fusion proteins were allowed to bind to the glutathione-agarose beads for 1 hour at 4°C with gentle shaking. After 1 hour the beads were pelleted by centrifugation for 1 minute. Beads were washed 3 times with 1 ml PBST and one time with 20 mM Hepes buffer pH 7.4.

In-vitro binding experiment:

The protocol for *in-vitro* binding is essentially same as that described in Gekakis *et al.*, 1995. Briefly, 50µl of hydrated glutathione-agarose beads bound to GST-

DISCO fusion proteins, or GST alone, were mixed with 200µl of a binding buffer (20mM Hepes pH 7.4, 100mM KCl, 5mM EDTA, 5mM EGTA, 10% glycerol, 5% Bovine serum albumin (BSA), 0.4% NP40, 1mM dithiothreitol) and 10µl of *in-vitro* expressed DIP1 or DIP2 protein. The mixture was incubated at room temperature for 1 hour, with occasional mixing. After 1 hour, the GST-beads were pelleted by centrifugation, washed twice with 1 ml binding buffer with BSA and twice with 1 ml binding buffer without BSA. Bound proteins were eluted from the beads by boiling with 30 µl of 2 X Laemmli buffer for 5 minutes in a boiling water bath. The eluted samples were electrophoresed on denaturing 12% SDS-polyacrylamide gels. The gels were fixed/destained for 2 hours in 35% methanol and 10% acetic acid to remove unincorporated [^{35}S]methionine. The gels were then dried, exposed to X-ray film overnight and developed after 12 hours.

In-situ expression studies:

Preparation of digoxigenin-labeled probes:

For in-situ expression studies digoxigenin-labeled antisense mRNAs were used as probes. The antisense mRNAs were synthesized *in-vitro* from either T3 or T7 promoter of the SK$^-$ pBluescript vector (depending on the orientation of the cDNA fragments) using respective RNA polymerase.

The *dip1 probe:*

A 900 bp BamHI fragment of the *dip1* cDNA without the repeated region was PCR amplified with Pfu polymerase using primers with BamHI sites and cloned into the BamHI site of the pBluescript vector (Stratagene). The plasmid with the *dip1* cDNA was linearized with XhoI and digoxygenin labeled antisense RNA

probe was transcribed using dig-labeled UTP and T3 RNA polymerase (Boehringer Mannheim). The primers used to generate the BamHI fragment of the *dip1* cDNA were:

AB11916 (sense probe): 5′ T CAT CAA GGA GGA TCC GAT C 3′.

AB 11917 (antisense probe): 5′ GAA GT GGA TCC GAA CAG AGA 3′.

The *dip2* probe:

The digoxygenin labeled antisense *dip2* mRNA was synthesized from a 700 bp EcoRI fragment from the 5′ end of the *dip2* cDNA isolated from the yeast interaction trap vector. The 700 bp EcoRI fragment was cloned at the EcoRI site of the SK⁻ pBluescript vector and the probe was synthesized essentially as described in the previous section.

The *disco* probe:

The 1.7 kb EcoRI *disco* fragment used to construct the full-length *disco* bait was cloned at the EcoRI site of the SK⁻ pBluescript vector for the expression study. The vector containing the *disco* cDNA was linearized and digoxygenin labeled antisense *disco* mRNA was synthesized following the procedure described above.

Preparation and fixation of embryos (Kobayashi et al., 19--):

0-22 hours wild-type (Canton-S) *Drosophila* embryos were collected. Embryos were dechorinated with 50% bleach for five minutes, and then washed with Embryo Wash (7% NaCl, 0.05% Triton X-100). Dechorinated embryos were fixed in a solution containing 5 ml of 40% embryo wash, 4% formaldehyde, 1X fixation buffer mixture, and 5 ml of heptane (5X fixation buffer composition: 800 mM KCl, 200 mM NaCl, 20 mM EGTA, 5 mM spermadine HCl, 2 mM spermine, 150 mM Pipes pH 7.4). Fixation was done for 20 minutes on an orbital shaker. Fixed embryos sank to the interface, that is, the bottom of the top organic phase. The

lower aqueous phase was removed. 5-10 ml of methanol was added and embryos in methanol-heptane mix (1:1) were shaken vigorously for 20-30 seconds to dislodge their vitelline membranes. Devitellinized embryos sank to the bottom of the tube. Embryos were washed several times with methanol and transferred to fresh tube to remove last trace of heptane. Embryos were next rinsed in a 50% ethanol/50% xylene mixture followed by soaking in 100% xylene for 2-3 hours. The xylene soaked embryos were rinsed in a mixture of 50% ethanol/50% xylene, followed by several rinses in 100% ethanol and finally rinsed in a mixture of 50% methanol/50% PBT (0.1 M sodium-phosphate buffer with 0.1% Tween 20). Embryos were transferred to a microcentrifuge tube, post fixed for 10 minutes in 8ml PBT + 2 ml 10% formaldehyde for 10 minutes with constant shaking. Unused fixative was removed from embryos by washing several times with PBT. Embryos were next treated with proteinase-K (50mg/ml of PBT) for precisely 3 minutes with constant mixing. Proteinase-K treatment makes the embryos more permeable to the probe. The proteinase-K reaction was stopped by rinsing 3 times with a solution containing 2 mg glycine/ ml of PBT. Embryos were rinsed twice with PBT and post-fixed again for 10 minutes on a shaker. The fixative was removed by rinsing embryos four times in PBT.

Preparation and fixation of ovaries (Kobayashi *et al.*, 1997):

Ovaries were dissected from 2-3 days old females in PBS and fixed with 4% paraformaldehyde in PBS + 1% DMSO for 20 minutes. The fixative was removed with one PBS and two PBT washes, 5 minutes for each step. Proteinase K treatment was done next for about 20 minutes with 50 µg/ml of the enzyme. The exact timing for this treatment was determined empirically to maintain

integrity of the tissue and to ensure optimal signal intensity. The proteinase K reaction was stopped by rinsing with 2mg/ml of a glycine solution. Ovaries were refixed and washed as before. To improve signal intensity, ovaries were incubated in 90% methanol + 10% DMSO for 1 hour at -20°C, followed by rehydration in PBT. Three PBT washes were done, 5 minutes for each wash.

Prehybridization and hybridization:

Fixed and proteinase-K treated embryos or ovaries were rinsed once in a mixture of 50% PBT/50% prehybridization solution and once in prehybridization solution (50% formamide, 300 mM NaCl, 10 mM Tris. HCl pH 6.8, 10 mM Na-phosphate buffer pH 6.8, 1X Denhardt's solution, 5 mM EDTA and 1 mg/ml of yeast t-RNA), 5 minutes each. These tissue were next prehybridized for 1 hour at 53° C in an orbital rotator. Hybridization was done overnight at 53°C without shaking in hybridization solution (50% formamide, 300 mM NaCl, 10 mM Tris.HCl pH 6.8, Na-phosphate buffer, pH 6.8, 5 mM EDTA, 1X Denhardt's solution, 10% dextran sulfate) containing antisense mRNA probes. For hybridization, a 1/10 th dilution of each probe was denatured at 60°C for 20 minutes. The denatured probe was further diluted to 1/1000 fold in the hybridization solution before adding to the tissue. After overnight hybridization, the embryos/ovaries were washed for 20 minutes each with a series of washing solutions containing a mixture of a post hybridization wash solution (same as prehybridization solution but without t-RNA) and PBT in the ratios 80%/20%, 60%/40%, 40%/60% and 20%/80%, followed by two washes in 100% PBT. The unhybridized probe was removed with RNAse A at a concentration of 20 mg/ml for 25 minutes at 37°C. RNAse A was removed with several PBT washes.

Detection of the in-situ signal:

To detect the hybridized signal, the embryos/ovaries were first incubated for 1 hour with alkaline phosphatase conjugated anti-DIG antibody (1 to 2500 dilutions in PBT, Boehringer Mannheim). Excess antibody was removed with four PBT washes, 20 minutes each. Embryos/ovaries were rinsed once in the detection solution for 20 minutes (100 mM NaCl, 50 mM $MgCl_2$, 100 mM Tris.HCl pH 9.5, 0.1% tween-20). The in-situ signal was detected with the alkaline phosphatase substrates NBT (4-nitro blue tetrazolium chloride) and BCIP (X-phosphate/5-bromo-4-chloro-3-indolyl-phosphate). The alkaline phosphatase enzyme catalyses reaction between NBT and BCIP leading to the production of a purple color complex which is deposited at the site of hybridization. The substrate mixture was made with 45 µl of NBT and 35 µl of BCIP in 10 ml of detection buffer. The enzymatic detection reaction was done in dark. Signal was detected within 4-5 hours of incubation. The reaction was stopped with several PBT washes and embryos/ovaries were stored in 70% glycerol in 1X PBS or cleared in methyl salicylate after dehydration.

Screening of the λgt11 cDNA library:

Amplification of the λgt11 cDNA library:

Amplification of the library was done essentially as described in Stratagene manual. The titre of the λgt11 library was determined through serial dilution of the phage stock in SM buffer (5.8 g NaCl, 2 g MgSO4. 7H2O, 50 ml 1 M Tris- HCl pH 7.5, 5 ml 2% gelatin). Each dilution was used to infect the host strain *E. coli* Y1090r$^-$. The infected culture was plated on 7% agarose and the titre was estimated from the number of plaques obtained on each plate. Based on the titre

value, approximately 10^6 plaques were plated onto twenty large plates (100 cm). Plates were incubated at 37° C for less than 8 hours to prevent overgrowth and merger of individual plaques. Each plate containing approximately 50,000 plaques as covered with 9 ml of SM buffer and stored overnight at 4° C with gentle rocking to allow the phage to diffuse into the buffer. The bacteriophage suspension was recovered from each plate and pooled together. Chloroform was added to this to 5% final concentration and incubated 15 minutes at room temperature to ensure complete lysis of the host cells. Cell debris was removed by centrifugation. The supernatant was stored at 4°C in 0.3% chloroform and/or at -70°C in 7% DMSO.

Screening of the λgt11 library with a *dip1* probe:

The amplified library was screened twice for full-length *dip1* cDNA. About $7.5X10^5$ and 10^6 plaques were screened in each individual trials. The host cells were infected and plated at a density of 30,000-50,000 plaques per plate. Nitrocellulose replica filters were prepared from these plates essentially as described in Stratagene manual (1991). The replica filters were hybridized to [^{32}P]dCTP labeled *dip1* probe synthesized using random primed DNA labeling kit (Boehringer Mannheim). The kit uses random hexanucleotides as primers.

Characterization of the recombinant phage DNA was done following large scale phage DNA isolation procedures of as described in Sambrook *et al.*, 1995. The cDNA fragments from the recombinant phage DNA were subcloned into pBluescript (SK$^-$, Stratagene). The cDNA inserts were sequenced from the plasmid vector using an automated sequencing apparatus PD1 Biosystems of the Mobix core facility of McMaster University.

Screening of λgt11 library and λEXlox cDNA libraries for *dip2* cDNA:

The probe used for the screening was synthesized from the 1.2 kb *dip2* cDNA isolated from the *Drosophila* library used in the yeast interaction trap screening. The λgt11 library was screened twice and a total of about two million plaques were screened. Five positive plaques were isolated, all of which contained approximately a 500 bp fragment corresponding to the 3′ and of the cDNA. Million plaques from the λEXlox library were also screened. DNA from 4 positive plaques were isolated and digested with ApaI and SacI to determine the size of the inserts. All of these plaques had cDNA inserts of size larger than 2 kb. The largest fragment was about 2.5 kb. Restriction mapping showed that all of these fragments correspond to the 3′ end of the *dip2* cDNA.

Northern analysis:

Isolation of total RNA:

Northern analysis was done with 0-22 hour *Drosophila* embryos. Embryos were collected from plates onto a nitex membrane with DEPC treated water, dried on kimwipes, frozen quickly in liquid nitrogen and stored at -80°C. About 1 g of the frozen embryos was homogenized with a sterile plastic rod in 1 ml of SDS-RNA buffer (10 mM Tris pH 7.5, 100 mM NaCl, 1 mM EDTA and 0.5% SDS). To the homogenate an equal volume of phenol/chloroform mixture was added, vortexed well and centrifuged at 3500 rpm for 10 minutes at room temperature. Aqueous phase was transferred to a fresh tube. Phenol/chloroform extraction step was repeated several times until the interface disappeared. The aqueous phase was collected and RNA was precipitated with 1/15 volume of 3 M NaCl

and 2.5 volume of 100% ethanol. Precipitation was done for 40 minutes at -80°C. The precipitate was collected by centrifugation at 6000 rpm for 30 minutes. The pellet was washed with 70% ethanol, dried and resuspended in 500 µl water.

Purification of polyA$^+$ RNA:

Poly A$^+$ RNA was purified from total cellular RNA using an oligo-dT column. A 1 ml oligo-dT column was prepared in a pasteur pipette with DEPC treated water. The column was washed with one column volume of 0.1 N NaOH followed by 2-3 volumes of water or until the pH of the eluant became 7. The column was next equilibrated with TSN (12.5 mM Tris pH 8.0, 250 mM NaCl and 0.125% SDS).

To the total RNA suspended in water an equal volume of TSN was added. RNA was denatured by heated at 65°C for 2 minutes. The solution was cooled on ice and poured into the oligo-dT column. The eluant was collected and ran through the column 3 more times. The column was rinsed with 5 ml of TSN. The polyA$^+$ RNA was eluted with 3 ml of DEPC-treated water. To the eluant 200 ml of 3M NaCl and 7.5 ml of ethanol were added, and incubated for 30 minutes at -80°C to precipitate the polyA$^+$ RNA. The precipitate was collected by centrifugation for 45 minutes at 7000 rpm. The pellet was washed in 70% ethanol and resuspended in 100 µl water. The O.D of the isolated polyA$^+$ RNA was measured at 260nm and 5 µg of the RNA was loaded in each lane of an agarose/formaldehyde gel. The gel electrophoresis, transferring RNA to nitrocellulose membrane and hybridization with *dip1/dip2* probe were done essentially as described in Sambrook (1995).

In situ hybridization to *Drosophila* polytene chromosome (Ashburner, 1989):

Probe used:

For in situ localization of the *dip1* gene on *Drosophila* polytene chromosome, biotin labeled DNA probes were made using biotinylated-dATP. A 1050 bp. EcoRI fragment of the *dip1* cDNA including the repeated region and a 343 bp. Sau3A fragment without the repeated region were used as templates to make probes for the *in situ* hybridization study. The biotin-labeled probes were synthesized using BRL nick translation kit. The reaction was done in a 50 µl volume containing 5 µl of solution A, 7.5 µl of 0.4 mM biotynylated-dATP, 0.5 mg/ml of the template DNA and 5 ml of solution C. The probe was synthesized for 90 minutes at 15° C. The reaction was stopped with 5 µl of 0.5 M EDTA. To inactivate the enzyme the reaction mixture was incubated in a boiling water bath for 10 minutes. The probes were precipitated with 5 µl of 3M Na-acetate and 150 µl of ice cold 100% ethanol. The ethanol precipitation was done for 30 minutes at -80° C. The precipitates were collected by centrifugation for 15 minutes at 4° C. Pellets were washed with 70% ethanol, dried at room temperature and resuspended in the hybridization solution (2X SSC, 0.8 mg/ml salmon sperm DNA, 10% dextran sulphate and 50% formamide) at a concentration of 20 mg/ml. The probes in hybridization solution were denatured by heating for 10 minutes in a boiling water bath, immediately cooled on ice and stored at -20° C for extended period.

Composition of solution A: 0.2 mM of dCTP, dGTP and dTTP; 500 mM Tris-HCl pH 7.8; 50 mM MgCl2; 100 mM 2-mercaptoethanol and 100 mg/ml nuclease free BSA, bovine serum albumin.

Composition of solution C: 0.4 u/ml DNA polymerase I, 40 pg/ml DNaseI, 50 mM Mg-acetate, 1 mM 2-mercaptoethanol, 0.1 mM PMSF, 50% (v/v) glycerol and 100mg/ml nuclease free BSA.

For in-situ localization of the *dip2* gene, a probe was synthesized following the same procedure as described above. The 1.2 kb *dip2* cDNA fragment isolated from the yeast interaction trap vector was used as template.

Pretreatment of microscope slides with SSC-Denhardt's solution:

Microscope slides were incubated for 2.5 hours at 65° C in SSC-Denhardt's solution (20X SSC: 3M NaCl, 0.3 M Na-citrate, 1% polyvinylpyrrolidone, 1% ficoll, 1% nuclease free bovine serum albumin). These were then quickly rinsed in distilled water, and fixed in ethanol-acetic acid fixative (3:1) for 20 minutes at room temperature. After fixation slides were air dried and stored in the refrigerator.

Preparation of chromosomes from salivary glands:

Wild-type (Cantos-S) *Drosophila* third-instar larvae were raised in a less crowded environment in Mother Parkers medium. Salivary glands of these larvae were dissected with fine forceps in 45% acetic acid, removing as much of the fat bodies, salivary gland membrane and salivary ducts from the glands as possible. The glands were transferred to a fresh drop of 45% acetic acid for approximately two minutes. The glands were then transferred to a drop of "1:2:3" solution on a siliconized coverslip and left there for 4-5 minutes. The coverslip containing the salivary glands was picked up with a slide treated in SSC-Denhardt's solution. Chromosomal spreading was done by first tapping the coverslip gently with the rubber end of a pencil, and then pressing it down with thumb. Slides with nicely spread chromosomes were refrigerated overnight to further flatten the salivary

chromosomes. The coverslips were removed from the slides by first dipping the slides in liquid nitrogen for 15 seconds and then popping the coverslip immediately with a razor blade. The slides were immediately placed in 95% ethanol for 15 minutes and then transferred and kept in fresh 95% ethanol for 1.5 hours. The slides were then air dried and stored in the refrigerator until use.

Prehybridization treatment:

The slides with the polytene chromosomes were treated in 2X SSC at 65° C for 30 minutes to remove basic proteins. These were then treated twice with 70% ethanol (for 5 and 10 minutes respectively) and once with 95% ethanol (for 10 minutes). Following ethanol treatment, slides were air dried in the fume hood. The polytene chromosomes on the slides were denatured in 0.07 N NaOH for precisely 2.5 minute, at room temperature. Rinsing was done sequentially in 3 baths of 2X SSC for 5 minutes each at room temperature. Slides were dehydrated again in 2 baths of 70% ethanol (5 minutes each) followed by 2 baths of 95% ethanol (5 minutes and 10 minutes respectively) and air dried in the fume hood.

Hybridization:

The probe was denatured in a boiling water bath for 5 minutes followed by immediate chilling on ice. 15 µl of the probe was applied to a cover slip, and the coverslip was picked up with the slide at the position where the salivary chromosomes were located. Hybridization was done overnight at 37° C in a moist chamber in order to prevent the preparation from drying out.

Washes and detection:

Following overnight hybridization, the slides were washed sequentially in 2 baths of 2X SSC for 10 minutes each at 37° C, followed by 2 baths of 2X SSC for

10 minutes each at room temperature. Slides were next rinsed in PBS for 5 minutes at room temperature. The detection was done using the ABC kit from Boehringer Mannheim and following the manufacturer's protocol. Briefly, the biotin in the probe was allowed to bind streptavidin conjugated to horse radish peroxidase (HRP) enzyme overnight. The biotin-streptavidin complex was detected by using 3,3'diaminobenzidine tetrachloride (DAB), the substrate for the HRP enzyme. HRP catalyzes a reaction between DAB and hydrogen peroxide that generates a brown colored product which is visualized as the *in situ* signal. The ABC kit provides other components that enhance the overall signal intensity. The chromosomes on the slides with the *in situ* signal were stained for 1 minute with a 8% solution of Giemsa (in 0.05 M Tris buffer, pH 7.6) to visualize the polytene chromosome banding pattern.

Deficiency mapping / Southern analysis:

Table 5: Genotypes of the 20A deficiency lines:

Deficiency	flybase ID#	Stock#
Df(1)DCB1-35b/FM6/Dp(1;Y)y[+]mal[106]	Fbab0000370	BL977
Binsn/Df(1)17-137/Dp(1;Y)mal[+]	FBab0000190	UM1800
Df(1)A209/FM7a	FBab0000317	BL3714
Df(1)HM430/FM6/Dp(1;Y)y[+]mal[+]	FBab0000440	UM15810
Binsn/Df(1)16-2-13/Dp(1;Y)mal[+]	FBab0000184	UM1450
C(1)DX,$y^1w^1f^1$/ Df(1)R21/Dp(1;Y)y[+]mal[+]	FBab0000626	UM8100
Df(1)B12/FM6/Dp(1;Y)y[+]mal[106]	FBab0000329	UM14350

Df(1)DCB1-35c/FM7/Dp(1;Y)y[+]mal[126]	FBab0000371	UM14955
Df(1)R22,y^1/FM7a	FBab0000627	UM17700
Df(1)LB6/FM7	FBab0000496	UM16590
Df(1)S54/FM6/Y	FBab0000682	UM18550
Binsn/ Df(1)17-257/Dp(1;Y)y[+]mal[106]	Fbab0000193	UM1955
Df(1)R38,y^1/FM7	FBrf0036523	UM78160
Df(1)R44,$y^1w^1f^1$/C(1)DX,y^1f^1/Dp(1;Y)mal[+]	FBrf0036523	UM8250
Df(1)GA22/FM6	FBab0000397	UM15120

Deficiency lines are maintained in heterozygous conditions over balancer chromosomes. Balancer chromosomes represent special chromosomes that carry multiple inversions (ref). Due to the presence of multiple inversions, recombinations between two heterologous chromosomes are prevented in a heterozygous deficiency line. Absence of recombinations stabilizes the genotype of deficiency chromosomes. The X-chromosome balancers present in the deficiency lines used for this study are; FM6, Binsn, FM7 and FM7a. These balancer chromosomes carry dominant visible markers. As a result a fly with a balancer chromosome is easily recognized. Deficiency lines are lethal under homozygous and hemizygous conditions. X-chromosome deficiencies are maintained in females in heterozygous conditions. Since deficient chromosomes are lethal in homozygous or hemizygous conditions, males do not carry X-chromosome deficiencies. However, there were special strains in which part of the X-chromosome is duplicated on the Y-chromosome. In those lines, males are able to carry X-chromosome deficiencies from the region of duplication. Two such deficiency lines used in our study are D(1)R21 and Df(1)R44. One of the X-

chromosomes in both lines is an attached X-chromosome [C(1)DX], in which two X-chromosomes were attached at the centromere. Since in *Drosophila*, sex type depends on the ratio of X-chromosome to autosomes, in these lines, flies carrying one attached X-chromosome and a Y-chromosome with duplication develop as females, whereas flies with one attached X-chromosome and one deficient X-chromosome die. In these lines, flies that carry a deficient X-chromosome and Y-chromosome with the duplication develop as males. Therefore, in these lines the deficiency chromosome is carried only in males.

For deficiency mapping of the *dip1* gene, females heterozygous for a deficiency chromosome and a balancer chromosome were crossed hemizygous males with a wild-type X-chromosome. From the progeny the female flies heterozygous for the deficiency chromosome and the WT chromosome were selected for southern analysis. The females from the parental line that are heterozygous for the deficiency chromosome and the balancer chromosome were also used for southern analysis. From each of the two lines where a portion of the X-chromosome is duplicated on the Y chromosome, male flies with the deficiency chromosome were used to cross to virgin females with wild-type X-chromosomes. All the female progeny from this cross were heterozygous for the deficiency chromosome and WT chromosome. These females were used for southern analysis.

For southern analysis, the chromosomal DNA from flies of desired genotype were isolated using a rapid small-scale isolation procedure. 50 flies from each line were homogenized with a plastic rod in an eppendorf tube in 500 µl solution A (0.1 M Tris. HCl pH 9.0, 0.1 M EDTA and 1% SDS). The homogenized tissue was incubated at 70°C for 30 minutes for lysis of the cells.

To the homogenate 70 µl of 8 M K-acetate was added and kept on ice for 30 minutes to precipitate cellular proteins. The cell debris and the precipitated proteins were removed by centrifugation at high speed for 15 minutes at 4°C. The supernatant was transferred to a fresh tube and the chromosomal DNA was precipitated with 0.5 volume of isopropanol at room temperature. The precipitate was collected by centrifugation at maximum speed for 5 minutes at room temperature. The pellet was washed with 70% ethanol, dried and dissolved in 100 µl of TE.

The isolated DNA was quantitated in a spectrophotometer at OD_{260} nm. 10 µg of each DNA was digested overnight with EcoRI and BamHI restriction enzymes separately. The digested DNA was electrophoresed on 0.7% agarose gels. After electrophoresis, the gels were used for southern analysis. Southern analysis was done essentially as described in Maniatis *et al.*, 1995. Gels were denatured in 1.5 M NaCl and 0.5 M NaOH for 45 minutes, briefly rinsed in distilled water and then neutralized in 1.5 M NaCl and 0.5 M Tris-HCl pH 7.5 for 45 minutes. DNA from the gels was transferred to nitrocellulose membranes using 10X SSC as transfer buffer. DNA was immobilized by baking the membranes at 80° C for 1 hour. Hybridization was done with [^{32}P]dCTP labeled *dip1* probe made from the non-repetitive region of the *dip1* cDNA using random primed DNA labeling kit.

Table 6: Genotypes of the 61A-F deficiency lines:

deficiency	breakpoint	Flybase ID#	Stock#
Df(3L)emc-E12/TM6B	061A; 061D03	Fbab0002367	BL2577
Df(3L)Ar11	061C3-C4; 61E	Fbab0022342	BL1479
Df(3L)Ar12-1	061C1-C4; 61F3	Fbab0022343	BL1478

Chromosomal DNA from the above three heterozygous deficiency lines (shown below) was isolated. Isolated DNA were digested with EcoRI and BamHI in separate reactions and electrophoresed on 7% agarose gel. The gel was blotted for southern hybridization. The [32P]dCTP labeled probe used for this study was essentially same as that used for northern analysis. The [32P]dCTP labeled *disco* probe used in this study as control probe, was synthesized from a 1.7 kb EcoRI fragment of the *disco* cDNA.

Screening of the genomic clones for *dip1* and *dip2* genes:

The host for the P1 phage is the *E. coli* strain NS3145. Screening of the *Drosophila* genomic P1 clones were done following the colony hybridization procedure described in Sambrook *et al.*, 1989. The kanamycin resistant genomic P1 clones were first allowed to adhere to a nitrocellulose membrane. The cells were then lysed on the membrane with 0.5 N sodium hydroxide and 1.5 M NaCl, followed by neutralization in Tris-HCl buffer. The liberated DNA was immobilized on the membrane by baking the membrane at 80°C for 1 hour. The prehybridization and hybridization steps were done as described in Sambrook *et al.*, 1989, using radiolabeled *dip1* or *dip2* probes. The P1 clones screened are shown in the result section in tables 2 and 4 .

Screening of P-element insertion mutants from the 61 region of the polytene chromosome:

Table 7: Genotype of the P-element insertion mutants screened for mutations at the *dip2* locus:

Stock #	genotype	site of insertion
P1	P{hsneo}102 mwh[1] red[1] e[1], l(3)*[*]/TM3	061A-B
P69	P{hsneo}.fwd[neo1] mwh[1] red[1] e[1]/TM3	061D
P154	y[1]w[1118];P{w[+mC]=lacW}.l(3)L1170[L1170]/ TM3, Ser[1]	061C07-08
P155	y[1]w[1118];P{w[+mC]=lacW}.l(3)L3130[L3130]/ TM3, Ser[1]	061C07-08
P240	P{hsneo}.l(3)neo[1] mwh[1] red[1] e[1]/TM3, Sb[1]	061C
P628	P{ry[+t7.2]=ry11}.l(3)122[1], mwh[1] ry[506] e[1]/ TM3	061A
P1206	P{ry[+t7.2]=lArB}.A55. 1M3 ry[506]	061A
P1235	P{ry[+t7.2]=23.2}T125 ry{506}	061A
P1677	P{ry[+t7.2]=PZ}.l(3)05967[05967] ry[506]/TM3, Sb[1]	061C07-08
P1679	P{ry[+t7.2]=PZ}.l(3)06240[06240] ry[506]/TM3, Sb[1]	061B01-02
P1786	P{ry[+t7.2]=PZ}.ms(3)61CD[03970] ry[506]/TM3, Sb[1]	061CD
P2981	P{ry[+t7.2]=A92}.ptl[1] ry[506]/TM3	061B

Screening procedure: Chromosomal DNA was isolated from P-element insertion lines following the method described previously. These DNA were digested with EcoRI and BamHI in separate digestion reactions. Southern analysis was

done with the digested DNA using standard procedure (Sambrook *et al.*, 1989). The [32P]dCTP labeled probe used for the southern blot was prepared from the 1.2 kb dip2 c-DNA isolated from the yeast interaction trap vector. The probe was synthesized using a random primed DNA labeling kit as described earlier.

Acknowledgement

I thank Dorothy DeSousa, a Ph. D. student of the lab, for her contribution in the in-situ expression studies for the *dip1* gene. I also thank Peter Pelka, a Masters student of the lab for his contribution in cloning of the mouse *dip2* homolog (part of his 4C9 thesis), in sequencing of the *Drosophila dip2* genomic region and in the demonstration of transcription activation ability of the glutamine-rich region of DISCO in yeast. I thank Jhilik De, a former member of the laboratory for her help in screening genomic clones for *dip1* and *dip2* genes.

References:

Altschul, S. F., Gish, W., Miller, W., Myers, E. W and Lipman, D. J. (1990). Basic local alignment search tool. J. Mol. Biol. **215**: 403-410.

Ashburner, M. (1989). *Drosophila*: a laboratory manual. Pp. 37-43. Cold Spring Harbor Laboratory Press, Cold Spring Harbor, New York.

Berg, J. M. (1990). Zinc finger domain: hypothesis and current knowledge. Ann. Rev. Biophys. Biophysical Chem. **19**: 405-421.

Bernstein, B. E., Hoffmann, R. C. and Klevit, R. E. (1994). Sequence-specific DNA recognition by Cys2, His2 Zinc fingers. Ann. N. Y. Acad. Sci. **762**: 92-102.

Bodmer, R. (1993). The gene *tinman* is required for specification of heart and visceral muscles in *Drosophila*. Development **118**, 719-729.

Brent, R. and Ptashne, M. (1984). A bacterial repressor protein or a yeast transcriptional terminator can block upstream activation of a yeast gene. Nature **312**, 612-615.

Brent, R. and Ptashne, M (1985). A eukaryotic transcriptional activator bearing the DNA specificity of a prokaryotic repressor. Cell **43**: 729-736.

Brent, R. and Finley, Jr. R. L. (1997). Understanding gene and allele function with two-hybrid methods. Ann. Rev. Genet. **31**: 663-704.

Campos, A. R., Lee, K. J. and Steller, H. (1995). Establishment of neuronal connectivity during development of the *Drosophila* larval visual system. J. Neurobiol. **28**, 313-329.

Campos-Ortega, J. A. and Hartenstein, V. (1985). The embryonic development of *Drosophila melanogaster* (New York: Springer Verlag).

Cohen, B., Weimer, E. A. and Cohen, S. M. (1991). Early development of leg and wing primordia in the *Drosophila* embryo. Mech. Dev. **33**, 229-240.

Corthesy, B. and Kao, P. N. (1994). Purification by DNA affinity chromatography of two polypeptides that contact the NF-AT DNA binding site in the *interleukin 2* promoter. J. Biol. Chem. **269**: 20682-20690.

Dingwall, C. and Laskey, R. A. (1991). nuclear targeting sequence- a consensus? Trends in Biochem. Sci. 16, 478-481.

Ferrandon, D., Elphick, L., Nusslein-Volhard, C. and Jonston, St. D. (1994). Staufen protein associates with the 3' UTR of *bicoid* mRNA to form particles that move in microtubule-dependent manner. Cell **79**, 1221-1232.

Finley, R. L. Jr. and Brent, R. (1995). Interaction trap cloning with yeast. In *DNA Cloning, Expression Systems: A Practical Approach*, ed. B. D. Hames; D. M. Glover; pp. 169-203. Oxford: Oxford Univ. Press.

Gatignol, A., Buckler, W. A., Berkhout, B. and Jeang, K. T. (1991). Characterization of a human TAR RNA-binding protein that activates the HIV-1 LTR. Science **251**, 1597-1600.

Gavis, E. R., Lunsford, L., Bergsten, S. E. and Lehmann, R. (1996). A conserved 90 nucleotide element mediates translational repression of *nanos* RNA. Development **122**, 2791-2800.

Gekakis, N., Saez, L., Delahaye-Brown, A. -M., Myers, M. P., Sehgal, M., Young, M. W. and Weitz, C. J. (1995). Isolation of *timeless* by PER protein interaction: defective interaction between Timeless protein and long-period mutant *per*. Science **270**, 811-815.

Gietz, D., St. Jean, A., Woods, R. A. and Schiestl, R. H. (1992). Improved method for high efficiency transformation of intact yeast cells. Nuc. Acids Res. **20**: 1425.

Goldberg, A. L. (1992). The mechanism and function of ATP-dependent proteases in bacterial and animal cells. Eup. J. Bio. Chem. **203**, 9-23.

Green, P., Hartenstein, A. Y. and Hartenstein, V. (1993). The embryonic development of the *Drosophila* visual system. Cell. Tissue Res. **273**: 583-598.

Gyuris, J., Golemis, E., Chertkov, H. and Brent, R. (1993). Cdi1, a human G1 and S phase protein phosphatase that associates with Cdk2. Cell **74**, 205-214.

Hallier, M., Lerga, A., Barnache, S., Tavitian, A. and Moreau-Gachelin, F. (1998). The transcription factor Spi-1/PU.1 interacts with the potential splicing factor TLS. J. Biol. Chem. **273**: 4838-4842.

Hanes, S. and Brent, R. (1989). DNA specificity of the *bicoid* activator protein is determined by homeodomain recognition helix residue 9. Cell **57**, 1275-1283.

Hartl, D. L., Nurminsky, D. I., Jones, R. W. and Lozovskaya, E. R. (1994). Genome structure and evolution in *Drosophila*: applications of the flamework P1 maps. Proc. Natl. Acad. Sci. USA **91**: 6824-6829.

Heilig, J. S., Freeman, M., Laverty, T., Lee, K. J., Campos, A. R., Rubin, G. M. and Steller, H. (1991). Isolation and characterization of the *disconnected* gene of *Drosophila melanogaster*. The EMBO journal **10**: 809-815.

Henikoff, S. and Henikoff, J. G. (1994). "Protein family classification based on searching a database blocks". Genomics **19**: 97-107.

Hicks, G. R. and Raikhel, R. V. (1995). Protein import into the nucleus : an integrated view. Ann. Rev. Cell. Dev. Biol. **11**: 155-188.

Higuchi, M., Single, F. N., Kohler, M., Sommer, B., Sprengel, R. and Seeberg, P. H. (1993). RNA editing of AMPA receptor subunit GluR-B: a base-paired intron-exon structure determines position and efficiency. Cell **75**: 1361-1370.

Hirokawa, T., Boon-Chieng, S. and Mitaku, S. SOSUI: Classification and secondary structure prediction system for membrane proteins. Bioinformatics **14**: 378-379.

Hoffman, C. S. and Winston, F. (1987). A ten-minute DNA preparation from yeast efficiently releases autonomous plasmids for transformation of *Escherichia. coli*. Gene **57**: 267-272.

Hoyle, J. and Fisher, E. M. (1996). Genomic organization and mapping of the mouse P26S4 ATPase gene: A member of the remarkably conserved AAA gene family. Genomics **31**: 115-118.

Iino, Y., Sugimoto, A. and Yamamoto, M. (1991). *S. pombe pac1*$^+$, whose overexpression inhibits sexual development, encodes a ribonuclease III-like RNase. The EMBO J. **10**: 221-226.

Jimemez-Garcia, L. F. and Spector, D. L. (1993). In-vivo evidence that transcription and splicing are coordinated by a recruiting mechanism. Cell **73**: 47-59.

Kao, P. N., Chen, L., Brock, G., Ng, J., Kenny, J., Smith, A. J. and Corthesy, B. (1994). Cloning and expression of cyclosporin A- and FK506-sensitive nuclear factor of activated T-cells: NF45 and NF90. J. Biol. Chem. **269**: 20691-20699.

Kim-Ha, J., Smith, J. L. and McDonald, P. M. (1991). *Oscar* mRNA is localized to the posterior pole of the *Drosophila* oocyte. Cell 66, 23-35.

Kobayashi, S., Amikura, R., Nakamura, A. and Lasko, P. (1997). Techniques for analysing protein and RNA distribution in *Drosophila* ovaries and embryos at structural and ultrastructural resolution, In " A Comparative Methods Approach to the Study of Oocytes and Embryos". Ed. J. Richler. Oxford University Press.

Kozak, M. (1996). Interpreting cDNA sequences: some insights from studies on translation. Mamm. Genome **7**: 563-574.

Lai, F., Chen. C. -X., Carter, K. C. and Nishikura, K. (1997). Editing of glutamate receptor B subunit ion channel RNAs by four alternatively spliced DRADA2 double-stranded RNA adenosine deaminases. Mol. Cell. Biol. **17**: 2413-2424.

Lee, K. G., Freeman, M. and Steller, H. (1991). Expression of the *disconnected* gene during development of *Drosophila melanogaster*. The EMBO journal **10**: 817-826.

Liao, H. J., Kobayashi, R. and Mathews, M. B. (1998). Activities of adenovirus virus-associated RNAs: purification and characterization of RNA-binding proteins. Proc. Natl. Acad. Sci. USA **95**: 8514-8519.

Lomeli, H., Mosbacher, J., Melcher, T., Hoger, T., Geiger, J. R., Kuner, T., Monyer, H., Higuchi, H., Bach, A. and Seeberg, P. H. (1994). Control of kinetic properties of AMPA receptor channel by nuclear RNA editing. Science **266**, 1709-1713.

Ma, J. and Ptashne, M. (1988). Converting a eukaryotic transcriptional inhibitor into an activator. Cell **55**: 443-446.

Ma, J. and Ptashne, M (1987). Deletion analysis of GAL4 defines two transcriptional activating segments. Cell **48:** 847-853.

Mackay, J. P. and Crossley, M. (1998). Zinc-fingers are sticking together. Trends Biochem. Sci. **23**: 1-4

Marlor, R. L., Parkhurst, S. M. and Corces, V. G. (1996). The *Drosophila melanogaster* gypsy transposable element encode putative gene products homologous to retroviral proteins. Mol. Cell. Biol. **6**: 1129-1134.

Mehta, A. and Driscoll, D. M. (1998). A sequence-specific RNA-binding protein complements Apobec-1 to edit *apolipoprotein* B mRNA. Mol. Cell. Biol. **18**: 4426-4432.

Melcher, T., Maas, S., Herb, A., Sprengel, R., Seeburg, P. H. and Higuchi, M. (1996). A mammalian RNA editing enzyme. Nature (London) **379**, 460-464.

Merika, M. and Orkin, S. H. (1995). Functional synergy and physical interactions of the erythroid transcription factor GATA-1 with Kruppel family proteins Sp1 and EKLF. Mol. Cell Biol. **15**: 2437-2447.

Miklos, G. L. and Rubin, G. M. (1996). The role of the genome project in determining gene function: insights from model organisms. Cell **86**: 521-529.

Nakai, k. and Kanehisa, M. A. (1992). A knowledge base for predicting protein localization sites in eukaryotic cells. Genomics **14**: 897-911.

Navaratnam, N., Morrison, J. R., Bhattacharya, S., Patel, D., Funahashi, T., Giannoni, F., Teng, B. -B., Davidson, N. O. and Scott, J. (1993). The p27 catalytic subunit of the apolipoprotein B mRNA editing enzyme is a cytidine deaminase. The J. Biol. Chem. **268**: 20709-20712.

Neugebauer, K. M. and Roth, M. B. (1997). Transcription units as RNA processing units. Genes. Dev. **11:** 3279-3285.

Orlowsky, M. (1990). The multicatalytic proteinase complex, a major extralysosomal proteolytic system. Biochem. **29**: 10289-10297.

Ostareck-Lederer, A., Ostareck, D. H., Standart, N. and Thiele, B. J. (1994). Translation of *15-lipoxygenase* mRNA is inhibited by protein that binds to a repeated sequence in the 3' untranslated region. The EMBO J. **13**, 1476-1481.

Padgett, R. A., Grabowski, P. J., Konarska, M. M., Seiler, S. and Sharp, P. A. (1986). Splicing of messenger RNA precursors. Ann. Rev. Biochem. **55**: 1119-1150.

Pelisson, A., Song, S. U., Prud'homme, n., Smith, P. A., Bucheton, A. and Corces, V. G. (1994). Gypsy transposition correlates with the production of a retroviral envelope-like protein under the tissue-specific control of the *Drosophila flamenco* gene. The EMBO J. **13**: 4401-4411.

Pieler, T. and Bellefroid, E. (1994). Perspectives on zinc finger protein function and evolution - an update. Mol. Biol. Reports **20**: 1-8.

Prud'homme, N., Gans, M., Masson, M., Terzian, C. and Bucheton, A. (1995). *Flamenco*, a gene controlling the *gypsy* retrovirus of *Drosophila melanogaster*. Genetics **139**: 697-711.

Rastinejad, F. and Blau, H. M. (1993). Genetic complementation reveals a novel regulatory role for 3' untranslated region in growth and differentiation. Cell **72**: 903-917.

Sachs, A. B. (1993). Messenger RNA degradation in eukaryotes. Cell **74**: 413-421.

Sambrook, J., Fritsch, E. F. and Maniatis, T. (1989). Molecular cloning: a laboratory manual. Cold Spring Harbor Press, Cold Spring Harbor, New York.

Siden-Kiamos, I., Saunders, R. D., Spanos, L., Majerus, T., et al., (1990). Towards a physical map of the *Drosophila melanogaster* genome: mapping of cosmid clones within defined genomic divisions. Nucleic acids Res. **18**: 6261-6270.

Singer, R. H. (1992). The cytoskeleton and mRNA localization. Curr. Opin. Cell. Biol. **4**: 15-19

Song, S. U., Gerasimova, T., Kuckulos, M., Boeke, J. D. and Corces, V. G. (1994). An Env-like protein encoded by a *Drosophila retroelement*: evidence that gypsy is a infectious retrovirus. Genes. Dev. **8**: 2046-2057.

Sorsa, V. (1988). Chromosomes map of *Drosophila* (CRC, Boca Raton, EL) Vols. **1** and **2**.

Spradling, A. C. (1993). Developmental genetics of oogenesis. In the development of *Drosophila melanogaster*, pp. 1-70. Edited by M. Bates and A. Martinez-Arias. Cold Spring Harbor, NY: Cold Spring Harbor Laboratory.

Triezenberg, S. J., Kingsbury, R. and McKnight, S. L. (1988). Functional dissection of VP16, the transactivator of herpes simplex virus immediate early gene expression. Genes. Dev. **2:** 718-729.

Steller, H., Fischbach, K. -F. and Rubin, G. M. (1987). *Disconnected*: A locus required for neuronal pathway formation in the visual system of *Drosophila*. Cell **50**: 1139-1153.

St. Johnston, D., Brown, N. H., Gall, J. G. and Jantsch, M. (1992). Conserved double-stranded RNA-binding domain. Proc. Natl. Acad. Sci. USA **89**: 10979-10983.

Swaffield, J. C., Bromberg, J. F. and Johnston, S. A. (1992). Alterations in a yeast protein resembling HIV Tat-binding protein releive requirement for an acidic activation domain in GAL4. Nature (London) **357**: 698-700.

Tafuri, S. R. and Wolffe, A. P. (1990). *Xenopus* Y-box transcription factors: molecular cloning, functional analysis and the developmental regulation. Proc. Natl. Acad. Sci. USA **87**: 9028-9032.

Tanner, S., StagIgar, I., Georgiev, O., Schafner, W. and Bourquin, J. P. (997). A novel SR-related protein specificallly interacts with the carboxy-terminal domain (CTD) of RNA polymerase II through a conserved interaction domain. Biol. Chem. **378**: 565-571.

Tautz, D. and Pfeifle, C. (1989). A non-radioactive in-situ hybridization method for the localization specific RNAs in *Drosophila* embryos reveals translational control of the segmentation gene *hunchback*. Chromosoma **98**: 81-85.

Tsang, A. P., Visvader, J. E., Turner, C. A., Fuziwara, Y., Yu, C., Weiss, M. J., Crossley, M. and Orkin, S. H. (997). FOG, a multitype zinc finger protein, acts as a cofactor for transcription factor GATA-1 in erythroid and megakaryocytic differentiation. Cell **90**: 109-119.

Tseng, H. and Green, H. (1992). *Basonuclin*: A keratinocyte protein with multiple paired zinc fingers. Proc. Natl. Acad. Sci. USA **89**: 10311-10315.

Walter, A. E., Turner, D. H., Kim, J., Lyttle, M. H., Miller, P., Mathews, D. H. and Zuker, M. (1994). Coaxial stacking of helixes enhances binding of oligonucleotides and improves predictions of RNA folding. Proc. Natl. Acad. Sci. USA **91:** 9218-9222.

Wang, W., Chevray, P. M. and Nathans, D. (1996). Mammalian Sug1 and c-Fos in the nuclear 26S proteasome. Proc. Natl. Acad. Sci. USA **93:** 8236-8240.

Wilson, R. et al. (1994). 2.2 Mb of contiguous nucleotide sequence from chromosome III of C. elegans. Nature **368**: 32-38.

Wilson, R. et al. (1994). 2.2 Mb of contiguous nucleotide sequence from chromosome III of *C. elegans*. Nature **368**: 32-38.

Chapter 4: Conclusion and future direction

Conclusion and future direction

The studies presented in this thesis are aimed at elucidating the mechanisms underlying the establishment of appropriate neuronal connections in the nervous system. To achieve this goal the *Drosophila* larval visual system development was used as a model. The present work shows that not only proper development of neuronal connections in the developing larval visual system is essential for visual system functioning, but, establishment of new neuronal connections at late larval stages may also be important for proper visual response.

The first part of my work shows that a contact between two serotonergic neuronal processes and the LON is established at the larval optic center during third instar larval stage that precedes a change in larval photoresponse from negative phototaxis to neutral (Sawin *et al.*, 1994; Sawin-McCormack *et al.*, 1995). Serotonin plays a role in modulating photosensitivity of eyes in several organisms including *Aplysia*, crayfish and others (Eskin and Maresh, 1982; Arechiga *et al.*, 1990; Barlow *et al.*, 1977). Thus, it seems likely that in *Drosophila*, establishment of connections between the serotonergic processes and the LON may modulate larval photobehavior during late third instar laval stage. However, to conclusively demonstrate such a role for serotonin in *Drosophila*, it will be necessary to examine if the absence of serotonin at the larval optic center has any effect on the change of larval photoresponse during late larval stage. One of the ways to eliminate serotonin from the larval optic center would be to disrupt function of the gene encoding the enzyme Dopadecarboxylase required for serotonin synthesis (Livingstone and Tempel, 1983). Disruption of serotonin

synthesis specifically in the neurons that project to the larval visual center can be achieved through generation of genetic mosaics for the *dopadecarboxylase* gene. This study will allow an opportunity to study the *in vivo* role for serotonin in visual system functioning.

The second part of my thesis addressed the molecular mechanisms of neuronal connectivity formation in the visual system. Since optic lobe specific autoregulatory function of *disco* is important for proper LON connectivity and pathway formation, the study was focused on identifying proteins that regulate *disco* activity in the visual system or act in the *disco* mediated pathway in the optic lobe. Yeast interaction trap screening led to the identification of two previously unknown proteins (DIP1 and DIP2) and a known protein (the ATPase component of the 26S proteasomal complex) that interacted with DISCO in this assay.

The *dip1* cDNA codes for a protein with two putative double stranded RNA-binding domains (dsRBDs). The data presented in this thesis raises the possibility that the DIP1 protein may be the same as that encoded by the *flamenco* gene.

The *dip2* cDNA codes for a highly conserved protein with homologs existing in organisms as divergent as *C. elegans* and humans. Sequence comparison and mRNA expression studies have shown that the *Drosophila* and the mouse *dip2* homologs not only share extensive sequence homology, but also a similar embryonic expression pattern mainly localized to the CNS. These findings may suggest a vital role for the *dip2* homologs in nervous system development.

To determine the *in vivo* significance of the interaction between DISCO and its interacting proteins (DIP1/DIP2), a number of approaches may be taken. The suggested initial approach will be to generate antibodies against the interacting proteins and determine if indeed their spatial and temporal expression pattern overlap with that of DISCO. The cells coexpressing these genes in the visual system may be the ones in which *disco* expression is necessary to direct the formation of LON pathway. Generating antibodies will also be necessary for coimmunoprecipitation studies from embryonic tissue to detect *in vivo* physical associations between DISCO and DIP1/DIP2. However, these studies are often tricky due to low physiological levels of cellular proteins and experimental conditions are often not appropriate to maintain the physical association.

Other approaches, such as ectopic expression studies have been traditionally used as an indirect way to determine the function of a gene, can also be used to study interactions between two proteins. The *disco* gene activity has been shown to cause a severe nervous system connectivity phenotype when expressed ectopically in the nervous system (Kevin Lee, Ph. D thesis, 1993). If DISCO needs a cellular partner (such as DIP1 or DIP2) to exert its effects at ectopic locations, disrupting the expression of its cellular partner (s) may revert the connectivity phenotype produced by *disco* ectopic expression. Since appropriate mutations are presently unavailable, deficiencies can be used to disrupt *dip1* or *dip2* gene functions in such studies. Preferably, two different deficiencies need to be used in transheterozygous conditions to ensure deletion of as small number of genes as possible, thereby eliminating the effect of deletions of other irrelevant genes.

A varity of approaches may be taken to elucidate the function of interacting proteins and their roles as DISCO partners. However, the physiological role of *dip1* and *dip2* genes can be best understood through studies of mutants that disrupt the function of these genes. If suitable existing mutants are unavailable, new mutations may be generated at the *dip1* and *dip2* locus using P-element insertion or chemical mutagenesis. PCR technology has made the P-element mutagenesis easier for genes that have already been cloned. Approximately 50-100 mutant lines can be screened in a single PCR reaction using two primers, one corresponding to the P-element and the other corresponding to the gene to be mutated (Ballinger and Benzer, 1989).

Another effective way to disrupt gene functions is to inject animals with dsRNA corresponding to the gene of interest (Fire *et al.*, 1998). For reasons not clearly understood, dsRNAs are more effective than single stranded antisense RNAs in interrupting endogenous gene functions. Interestingly, only dsRNAs without intronic sequences have the potency to disrupt gene function. The double stranded RNAs cause disappearance of the gene products in the injected organism and in the F1 progeny, but, not in the F2 progeny. These results argue against a nonreversible gene modification. Furthermore, a small amount of the dsRNA can have a profound effect on the gene function, therefore, masking the function of endogenous mRNAs through sense-antisence RNA-hybrid formation is not a likely explanation for dsRNA mediated inactivation of gene functions. A present hypothesis is that the dsRNAs exert their effect by suppressing transcription from the corresponding endogenous genes (Montgomery et al., 1998). The remarkable efficiency of a small amount of dsRNA in silencing gene expression is proposed to be due to either amplification of a gene silencing agent

inside the cells of the injected organism or establishment of a highly catalytic RNA degradation process (Fire *et al.*, 1998; Ngo et al., 1998). The dsRNA-mediated disruption of gene function has been sucessfully used in several organisms including *C. elegans*, *Trypanosoma brucei* and *Drosophila* (Fire, *et al.*, 1998; Ngo *et al.*, 1998; Kennerdell and Carthew, 1998). The two methods described above are examples of a variety of different ways a gene function can be addressed. Once the *in vivo* functional role of *dip1* and *dip2* genes become clear, models explaining the mechanisms of interactions between these proteins and DISCO can be hypothesized and examined.

Information presently available (please refer to the discussion section of chapter 3) suggest several alternative models for DIP1 and DISCO interaction. The first hypothesis is that DIP1 acts as a transcription factor. From the example of NF90, the RNA binding domains of DIP1 can be hypothesized to bind DNA rather than dsRNA substrates. This activity of DIP1 may either stimulate or interfere with the transcriptional regulation function of DISCO. If protein expression studies show coexpression of the DIP1 and DISCO proteins in the optic lobe primordium, the tissue where *disco* autoregulates its own mRNA expression, a negative effect of *dip1* on *disco* function can be ruled out. Previous studies have shown that expression of a nonfunctional DISCO protein is induced in the optic lobe of the *disco1* mutant by restoring wild-type *disco* gene function in this tissue. If DIP1 indeed functions as a transcription factor that promote *disco* autoregulation, in a *disco-dip1* double mutant background, the above induction will be disrupted.

An alternative view is that the DIP1 protein functions as a dsRNA-binding protein with a role in RNA editing. As discussed previously *dip1* may act as a component of an editase complex in which the role of DIP1 is to bind the substrate to be edited, while the catalysis is carried out by a different protein with editase activity. Although a putative editase enzyme that interacts with DIP1 in yeast interaction trap assays has recently been identified, knowledge on the dsRNA substrates for DIP1 is essential in order to further explore its role in mRNA editing. A yeast three-hybrid system that has recently been developed (SenGupta *et al.*, 1996) can be used to identify target mRNAs edited by the hypothetical DIP1 editase complex.

The possible identity of *dip1* and *flamenco* genes may suggest a role for *dip1* in alternative splicing (Pelisson, *et al.*, 1994). To examine this hypothesis, it will be necessary to identify DISCO targets that coexpress with *disco* and *dip1* in the same tissue. The expectation will be that, in a *disco* mutant background expression of the target gene will be completely absent, while in a *dip1* mutant background, only expression of certain alternatively spliced transcripts will be absent. The quickest way to identify a *disco* target will be to screen available enhancer trap lines which show reporter gene expression in the optic lobe region. Absence of the reporter gene expression in any such line, in a *disco* mutant background, may suggest that the gene whose promoter drives the reporter gene expression is a *disco* target. Since *dip1* shares extensive similarity with the glutamate receptor editases, it will be worthwhile to examine if any of the glutamate receptor subtypes act as *in vivo* DISCO target.

These proposed studies will provide further insight that will help elucidate some of the general rules that govern proper neuronal connectivity formation in the nervous system.

References

Arechiga, H., Banuelos, E., Frixione, E., Picones, A. and Rodrigues, S. L. (1990). Modulation of crayfish retinal sensitivity by 5-hydroxytryptamine. J. Exp. Biol. **150**: 123-143.

Barlow, R. B., Chamberlein, S. C. and Kaplan, E. (1977). Efferent inputs and serotonin enhance the sensitivity of the *Limulus* lateral eye. Biol. Bull. **153**: 141.

Eskin, A. and Maresh, R. D. (1982). Serotonin or electrical optic nerve stimulation increases the photosensitivity of the *Aplysia* eye. Comp. Biochem. Physiol. **73**: 27-31.

Fire, A., Xu, S., Montgomery, M. K. Kostas, S. A. Driver, S. E. and Mello, C. C. (1998). Potent and specific genetic interference by double-stranded RNA in *Caenorhabditis elegans*. Nature **391**: 806-811.

Kennerdell, J. R. and Carthew, R. W. (1998). Use of dsRNA-mediated interference to demonstrate that *frizzled* and *frizzled 2* act in the Wingless pathway. Cell **95**: 1017-1026.

Livingstone, M. S. and Tempel, B. L. (1983). Genetic dissection of monamine transmitter synthesis in *Drosophila*. Nature **202**: 67-70.

Montgomery, M. K., Xu, S. and Fire, A. (1998). RNA as a target of dsRNA-mediated genetic interference in *Caenorhabditis elegans*. Proc. Natl. Acad. Sci. USA **95**: 15502-15507.

Ngo, H., Tschudi, C., Gull, K. and Ullu, E. (1998). Double-stranded RNA induces mRNA degradation in *Trypanosoma brucei*. Proc. Natl. Acad. Sci. USA **95**: 14687-14692.

Pelisson, A. Song, S. U., Prud'homme, N., Smith, P. A., Bucheton, A. and Corces, V. G. (1994). Gypsy transposition correlates with the production of a retroviral envelope-like protein under the tissue-specific control of the *Drosophila flamenco* gene. The EMBO J. **13**: 4401-4411.

Sawin, E. P., Harris, L. R., Campos, A. R. and Sokolowski, M. B. (1994). Sensorimotor transformation from light reception to phototactic behavior in *Drosophila* larvae. J. Insect. Behav. **7**: 553-567.

Sawin-McCormack, E. P., Sokolowski, M. B. and Campos, A. R. (1995). Characterization and genetic analysis of *Drosophila melanogaster* photobehavior during larval development. J. Neurogenet. **10**: 119-135.

Sengupta, D. J., Zhang, B., Kraemer, B., Pochart, P., Fields, S. and Wickens, M. (1996). A three-hybrid system to detect RNA-protein interactions in-vivo. Proc. Natl. Acad. Sci. USA **93**: 8496-8501.

APPENDIX

Structural analyses of the repeated region of *dip1* cDNAs.

Figure:

Results of the structural analyses of the repeated region of *dip1* cDNAs:

This Figure shows the results of the structural analyses for *dip1* cDNAs using 'MFOLD' database. Only repeated sequence in the 3' untranslated region (UTR) of the *dip1* cDNAs were used for the structural analyses. These analyses predicted formation of stem-loop structure in the 3' UTR of the corresponding mRNAs. Approximately two repeats are needed to form one stem-loop.
Panel A shows that structural analysis with the four repeats present in the smaller *dip1* cDNA leads to the formation of two stem-loops.
Panel B shows that eight repeats (the approximate number of repeats present in the larger *dip1* cDNA) form four stem-loops.

A

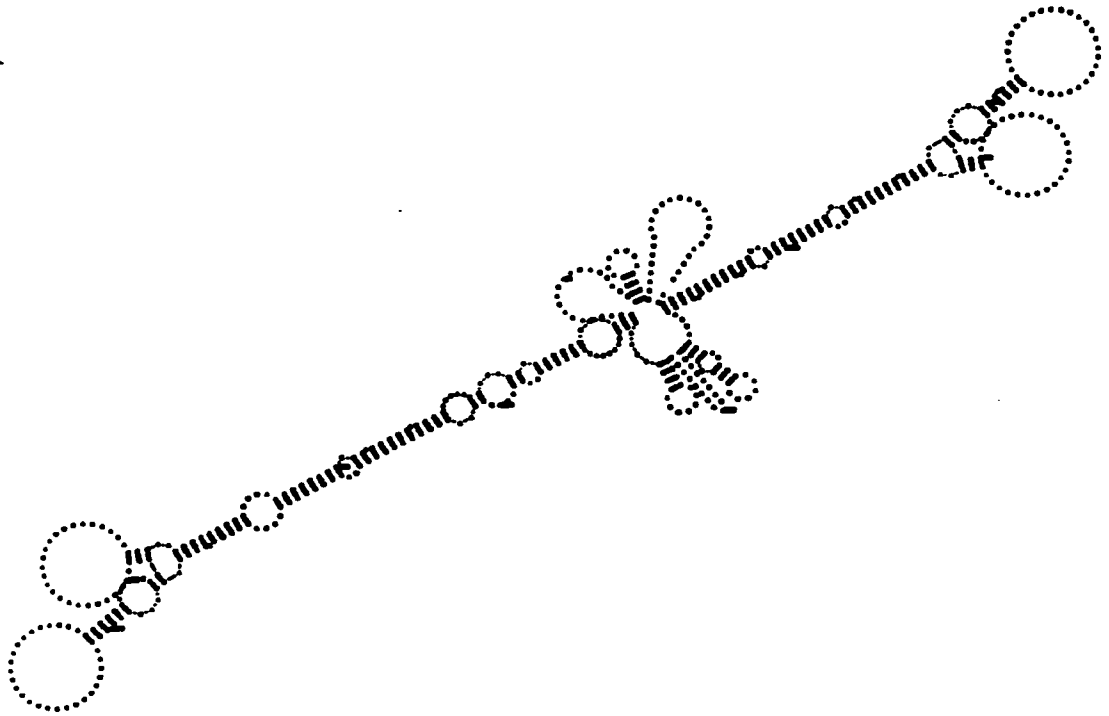

B